Percutaneous absorption in frogs: in vitro and in vivo studies

Developing models for disease treatment and environmental risk management

Victoria Kathleen Llewelyn

BPharm – The University of Sydney

BPharm (Hons) – James Cook University

This thesis submitted in fulfilment of the requirements for the degree of

Doctor of Philosophy

at

James Cook University

Division of Tropical Health and Medicine

College of Medicine and Dentistry

Townsville, QLD

July 2019

Statement of Access

I, Victoria Llewelyn, the author of this thesis, understand that this thesis will be made available for use to others. All users consulting this thesis will have to sign the following statement:

“In consulting this thesis, I agree not to copy or closely paraphrase it in whole or part without the written consent of the author; and to make proper public written acknowledgement for any assistance which I have obtained from it.”

_____ _____

(Victoria K. Llewelyn) (Date)

Declaration

I declare that this thesis is my own work and has not been submitted in any form for another degree or diploma at any university or institution of tertiary education. Information derived from the published or unpublished work of others has been acknowledged in the text and a list of references is given. Every reasonable effort has been made to gain permission and acknowledge the owners of copyright material. I would be pleased to hear from any copyright owner who has been omitted or incorrectly acknowledged.

_____ _____

(Victoria K. Llewelyn) (Date)

Acknowledgements

When I first met Professor Beverley Glass, I told her that I intended to complete a PhD, even though I didn't even have an Honours qualification! Beverley took a chance on me, supervising my Honours, and now, the promised PhD. I would like to thank her for her support, guidance, and unwavering belief that I would "get it done". I would also like to thank my co-supervisor, Dr Lee Berger, who tolerated my frog-naïve questions and showed utmost patience in training me in cardiac puncture procedures. Thank-you Lee for not giving up on me, even when you thought this project might be a lost cause! My thanks to the late Professor Rick Speare, who saw an opportunity for inter-disciplinary collaboration that led to a pharmacist undertaking a PhD on frogs. My gratitude also goes to Emeritus Professor Rhondda Jones, and her tireless enthusiasm for statistics. She would answer my plaintive emails when analyses just wouldn't go right, and was happy to explain the most basic (and complex) of statistical concepts. Dr Sherryl Robertson helped troubleshoot many early HPLC issues, and the feeling of success when I first was able to troubleshoot HPLC method development on my own was exhilarating. Thank-you Sherryl!

My family has supported me through this undertaking, and its ups and downs. Toad-hunting has become an integral part of my boys' childhood, and my husband, John, provided encouragement, laughter, love and support to get me through. When our world came crashing down, John encouraged me to take stock of my life, and to decide what the important things were that made me happy. This PhD made the cut. My parents also deserve mention, not only for their ability to listen patiently to me prattle on even though they have no idea what I'm talking about, but also for child-husbandry when John and I were busy being scientists. Particular mention to dad for his tireless "aren't you finished that PhD **yet**?" — he has no idea how happy I will be to finally answer in the affirmative.

Finally, to my colleagues in Pharmacy at James Cook University, and the members of the One Health Research Group, who have provided support, feedback, and, in the case of my fellow PhD candidates, chocolate, wine, and friendly competition. The road was long, but it would've ended much earlier (and without a PhD) if not for you.

"All models are wrong, but some are useful"

(George E.P. Box)

Statement of the Contribution of Others

Nature of Assistance	Contribution	Names and Affiliations of Co-Contributors
Intellectual support	Supervision	Professor Beverley Glass (JCU) Associate Professor Lee Berger (University of Melbourne)
Intellectual support	Statistical support	Emeritus Professor Rhondda Jones (JCU) Dr Daniel Lindsay (JCU) Dr Michael Meehan (JCU)
Financial support	Research costs: *Analysis of in vivo serum samples, laboratory consumables, travel grant to EAVPT, interstate travel assistance for final polish of thesis*	Discretionary budget allocation account: Staff (JCU) College of Medicine and Dentistry (JCU)
Data collection	Research assistance and infrastructure use: *Assistance with preparation of histology slides*	Rebecca Webb (JCU) Sieara Claytor (JCU) Parasitology lab / histology group (Laboratories and Technical Support (Laboratory Sciences), CPHMVS, JCU)
Data analysis	Research assistance: *Training in HPLC method development and validation*	Dr Sherryl Robertson (JCU)
Data analysis	Research assistance and infrastructure use: *Analysis of in vivo serum samples*	Dr Shane Askew (Advanced Analytical Centre, JCU)

Abstract

Introduction: Frogs are an ecologically-important group of animals that have undergone population declines and extinctions at a significantly increased rate over the past 50 years. While habitat change including habitat contamination with xenobiotics has long been accepted as a primary cause of these declines, more recently the impact of infectious disease, particularly chytridiomycosis, has been acknowledged. Frogs have permeable skin, which is a key contributor to their vulnerability to these environmental hazards. However, while it is known that frogs have permeable skin, little is known about the specifics of percutaneous absorption in frogs, and this has led to a general recommendation that immediate, rapid absorption of any chemical be assumed. Knowledge of percutaneous absorption will therefore advise these beliefs and allow for more targeted risk management practices in frog habitats. Further, owing to their permeable skin, transdermal delivery of therapeutic chemicals presents an ideal way to reduce the impact of disease on frog populations. However, without knowledge of percutaneous absorption in frogs, there is no mechanism to advise selection and formulation of chemicals for treatment of disease via this route. In mammals, in vitro and in vivo percutaneous absorption investigations are well-developed, and the use of mathematical models to predict absorption an area of burgeoning research. These techniques would also be useful in developing understanding of percutaneous absorption in frogs, in order to design effective treatments for disease, and to advise risk management.

Methods: This study aimed to improve understanding of percutaneous absorption in frogs, with view to developing models of absorption that could be used to advise on both risk management and the design of therapeutic treatments for infectious disease. The investigations took place in two stages: 1) model development (in vitro absorption studies), and 2) model refinement (in vivo absorption studies).

In vitro studies utilised diffusion cells to investigate the impact of relative lipophilicity and skin region of application on the absorption of model chemicals caffeine, benzoic acid, and ibuprofen through the skin of two frog species from different primary habitats: the arboreal frog *Litoria caerulea*, and the terrestrial toad *Rhinella marina*. Results of these in vitro studies were then used to design models of absorption in frog skin, which included an interspecies model and of percutaneous absorption and a model of absorption in *Rh. marina* alone. In vitro studies also investigated the impact of co-formulating chemicals with penetration enhancers on absorption kinetics, with these studies concurrently utilising differential scanning calorimetry and histology to determine the impact of these enhancers on the frog skin itself.

In vivo studies sought to determine the utility of the developed in vitro models in predicting in vivo absorption (i.e., in vitro-in vivo, or IVIV, comparison). Firstly, the in vitro studies were replicated in vivo in healthy adult Rh. marina, in order to determine the in vivo absorption kinetics, and a comparison between absorption kinetics predicted from the previously-developed in vitro model provided. Finally, the adjusted model was used to select a drug candidate and dose for potential treatment of infectious disease in frogs, and the results of the in vitro penetration enhancer study used to advise formulation

of the drug for delivery. The absorption and pharmacokinetics of this formulation was then ascertained in healthy *Rh. marina*.

Results and Discussion: In vitro studies found that relative lipophilicity and skin region of application significantly affected flux of chemicals in both *L. caerulea* and *Rh. marina*. In particular, dorsal absorption of all chemicals in *L. caerulea* was significantly lower than ventral absorption, with caffeine, the most hydrophilic chemical, having the highest magnitude of difference between dorsal and ventral surfaces. In *Rh. marina*, absorption was far more consistent between skin regions, however the absorption of caffeine was still significantly higher through the ventral pelvis than through other skin regions. None of the other chemicals exhibited regional variability in absorption in *Rh. marina*. These differences in absorption can be explained by the anatomy and physiology of the skin in these species. Comparing the species, absorption was significantly different between species, logP and between skin regions. Of the penetration enhancers investigated, 20% v/v propylene glycol was effective in enhancing penetration of moderately- and highly-lipophilic chemicals, while having minimal effects on the skin structure. Ethanol at 1% v/v had minimal effects on the skin, however did not increase penetration for any chemical, whereas higher concentrations (10% v/v and 30% v/v) effectively enhanced penetration of moderately- and highly-lipophilic chemicals, however caused significant structural changes to the dermis and epidermis. None of the investigated penetration enhancers were effective in increasing penetration of caffeine.

The IVIV studies found that in vivo absorption rates were lower than those predicted from the in vitro studies for all chemicals. However, the models provided reasonable predictions of serum concentration, with benzoic acid showing the smallest factor of difference between predicted and observed serum concentrations (2.5-fold), and ibuprofen having the highest (10.5-fold). The final study included the selection of chloramphenicol as the chemical for potential treatment of infectious disease. Chloramphenicol dose (250 µg/mL) was selected based on the reported minimum inhibitory concentration (MIC) for the chytrid fungus *Batrachochytrium dendrobatidis (Bd)*, and predictions from the model, and was formulated in 20% v/v propylene glycol. Serum levels of chloramphenicol reached the required MIC for *Bd* within 90-120 min of drug exposure commencing, and remained above MIC for the remaining drug exposure time. The serum levels attained were also well above the MICs for many other common bacterial pathogens in frogs. C_{max} was 17.094 ± 2.813 µg/mL, and T_{max} was reached at 2 h. Elimination was long, with $t_{1/2}$ of 18.676 h.

Conclusions: Models of percutaneous absorption in frog species developed during this work have identified the impacts of relative lipophilicity, skin region of application, and also highlighted interspecies differences in absorption. The development and testing of a model of percutaneous absorption in *Rh. marina* has demonstrated the utility of the developed models in advising selection and design of therapeutics for the treatment of disease in frogs specifically. Such knowledge however is ubiquitous and can be equally applied when advising risk management and mitigation, when percutaneous absorption should be avoided. This study thus makes a significant contribution to the knowledge of percutaneous absorption in frogs, knowledge that will aid in the conservation and preservation of these ecologically-important species for future generations.

Publications in Support of this Thesis

Llewelyn VK, Berger L, Glass BD. Percutaneous absorption of chemicals: developing an understanding for the treatment of disease in frogs. Journal of Veterinary Pharmacology and Therapeutics. 2016;39(2):109-21.

Llewelyn VK, Berger L, Glass BD. Regional variation in percutaneous absorption in the tree frog *Litoria caerulea*. Environmental Toxicology and Pharmacology. 2018;60:5-11.

Llewelyn VK, Berger L, Glass BD. Percutaneous absorption in frog species: variability in skin may influence delivery of therapeutics. Journal of Veterinary Pharmacology and Therapeutics. 2018;41(Suppl. 1):70. [conference abstract]

Llewelyn VK, Berger L, Glass BD. Effects of skin region and relative lipophilicity on percutaneous absorption in the toad *Rhinella marina*. Environmental Toxicology and Chemistry. 2019;38(2):361-7.

Llewelyn VK, Berger L, Glass BD. Permeability of frog skin to chemicals: effect of penetration enhancers. Heliyon. 2019; 5(8):e02127. https://doi.org/10.1016/j.heliyon.2019.e02127.

Conferences and Presentations

Llewelyn VK. “Percutaneous absorption in frog species: variability in skin may influence delivery of therapeutics”. Oral presentation at the 14th International Congress of the European Association for Veterinary Pharmacology and Toxicology (2018)

Llewelyn VK. “Modelling drug absorption in frog skin to treat disease”. Oral presentation at the James Cook University finals of the Three-minute thesis (3MT), September 2017. Townsville, QLD, Australia.

Llewelyn VK, Berger LB, Glass BD. “Giving drugs to frogs: transdermal kinetics in two frog species”. Oral presentation at the Discipline of Pharmacy Research Day, October 2017, Townsville, QLD, Australia

Table of Contents

List of Tables

List of Figures

List of Abbreviations

% v/v	millilitres of solute in 100 millilitres of solution
% w/v	grams of solute in 100 millilitres of solution
∆C	difference in concentration between the outer and inner skin surfaces
µg	microgram
µm	micrometre
ACS	American Chemical Society
API	active pharmaceutical ingredient
ARS	Amphibian Ringer's Solution
AUC_{0-24}	area under the concentration-time curve up to 24 hours
$AUC_{0-\infty}$	area under the concentration-time curve with extrapolation to infinity
Bd	*Batrachochytrium dendrobatidis* (chytrid)
cm	centimetre
C_{max}	maximum peak observed plasma concentration
C_v	concentration of chemical in the donor solution/vehicle
CYP450	Cytochrome P450
D	diffusion coefficient of the chemical in the stratum corneum
Da	Daltons
DMSO	dimethyl sulfoxide
DSC	differential scanning calorimetry
ER	enhancement ratio
FOD	factor of difference
g	grams
h	hour
HPLC	high-performance liquid chromatography
HPβCD	2-hydroxypropyl-beta-cyclodextrin
IS	Internal standard

IV	intravenous
IVIV	in vitro-in vivo
J_{ss}	steady-state flux
k_{el}	terminal elimination rate constant
kg	kilogram
K_p	permeability coefficient
$K_{p\ ARS}$	permeability coefficient (in ARS)
$K_{p\ PE}$	permeability coefficient (in penetration enhancer)
K_{pLC}	Permeability coefficient (in *Litoria caerulea*)
K_{pRM}	Permeability coefficient (in *Rhinella marina*)
l	thickness of the skin / SC
L	litres
LHRH	luteinising hormone releasing hormone
logFlux	logarithm of the flux
logK_p	logarithm of the permeability coefficient
logP	logarithm of the partition coefficient
M	molar
mg	milligram
MGl	mucus gland
MIC	minimum inhibitory concentration
min	minutes
mL	millilitre
mM	millimolar
mm	millimetres
MS-222	tricaine methanesulfonate; tricaine mesylate; ethyl 3-aminobenzoate methanesulfonate
MW	molecular weight

nm	nanometres
NS	not specified
P	apparent partition coefficient of chemical between the vehicle and the skin
PG	propylene glycol
pH	When ≥4, pH is the negative logarithm of hydrogen ion concentration (mol/L). When <4, pH is the negative logarithm of hydrogen ion activity
pKa	negative logarithm of the acid dissociation constant
R	Open-access programming language for statistical analysis and graphics
RCF	relative centrifugal force (or g-force)
SA	surface area of the application site
SC	stratum corneum
SCm	stratum compactum
SD	standard deviation
sec	seconds
SGl	serous gland
SSp	stratum spongiosum
SVL	snout-vent length
T<X>$_{frog}$	transition temperature for transition #<X> in *Rhinella marina*
T<X>$_{mammal}$	transition temperature for transition #<X> in mammals
T_{max}	time to maximum observed plasma concentration
UHPLC	ultra-high-performance liquid chromatography
USP	United States Pharmacopoeia
vEP	“viable” epidermis

Chapter 1: Introduction

1.1 Background

Infectious disease and habitat change, including habitat contamination, habitat loss and climate change, have been identified as the key driving forces behind frog population declines and extinctions over the last 50 years [1-5]. In the wild, frogs are often considered to be indicators of the relative health of the ecosystem they inhabit, as they are highly sensitive to environmental change, in particular habitat contamination with xenobiotics [6, 7]. The sensitivity of frogs to environmental contaminants is due to the increased permeability of their skin compared to other terrestrial vertebrates [8-10]. However, despite the knowledge that frogs' sensitivity to environmental chemicals is due to increased absorption of these contaminants, little is known about the kinetics of percutaneous absorption of chemicals in frog skin.

The catastrophic impact of the amphibian fungal disease chytridiomycosis, caused by the chytrid fungus *Batrachochytrium dendrobatidis* has recently been quantified [3], linking it to population declines in over 500 amphibian species, including an estimated 90 extinctions. Despite many studies investigating potential treatments for this devastating disease [11-20], as yet, no consistently effective treatment has been developed [11, 21], and conservation efforts have largely shifted from disease management in the wild to the collection and maintenance of disease-free captive breeding and insurance colonies of affected species [22, 23]. Unfortunately, holding of captive frogs presents its own inherent challenges. In captivity, frogs are more susceptible to other infectious diseases [24], which have the ability to rapidly spread throughout the colony, jeopardising conservation efforts. Development of improved treatment strategies for infectious disease in frogs is thus central to effective conservation of these animals. Owing to the permeability of frog skin, transdermal treatment modalities provide a simple and effective method to treat disease in large groups of animals. However, without knowledge of percutaneous absorption kinetics in frogs, drug candidates and treatment regimens cannot be optimised.

1.2 Structure and function of frog skin

Frog epidermis is a thin, avascular region comprised of several distinct layers: the relatively lipophilic stratum corneum (SC), and the more aqueous viable epidermis, comprising the

stratum granulosum, stratum spinosum and the stratum germinativum (Figure 1.1). The epidermis, particularly the SC, is much thinner than in mammals, with frog SC often comprising a single cell layer [8] with an average thickness of ~5 µm [25]. The majority of the frog epidermis is composed of keratinocytes, metabolically-active cells which differentiate and migrate from the stratum germinativum towards the outer surface of the epidermis. When these cells reach the SC, they are non-viable corneocytes, suspended in a gelatinous matrix of extracellular lipids. In frogs, this matrix is comprised primarily of triglycerides, nonpolar fatty acids, cholesterol and methyl esters and phospholipids [26].

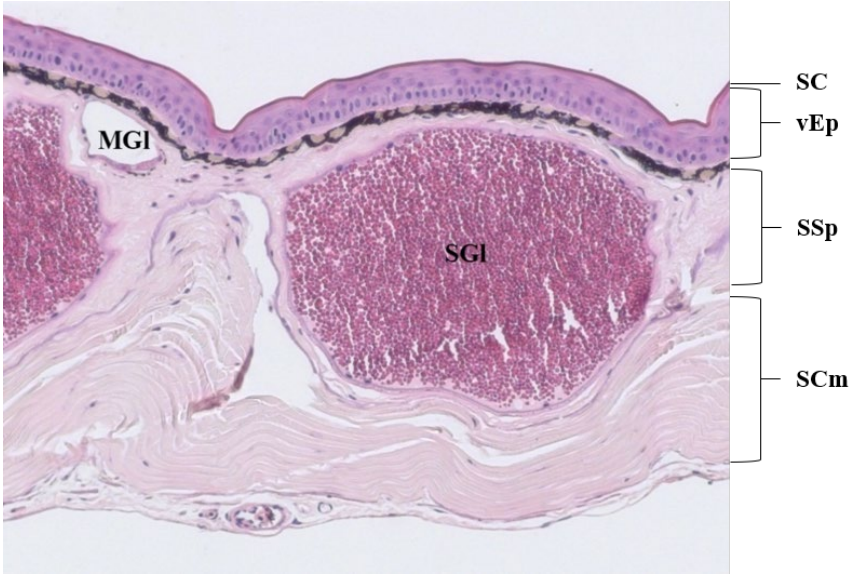

Figure 1.1: Histological section of dorsal *Litoria caerulea* skin
10x magnification. MGl: mucus gland; SGl: serous gland; SC: stratum corneum; vEP: "viable" epidermis; SSp: stratum spongiosum; SCm: stratum compactum

Located directly beneath the epidermis, the dermis is a thick, relatively aqueous region of the skin that provides protection, support and nutrients to the epidermis, while also contributing to the barrier function of the skin. Frog dermis can be further divided into two layers: the stratum spongiosum (SSp) and the stratum compactum (SCm). The SSp contains the sensory nerves and capillaries, and is also where a variety of exocrine glands originate. The SCm is composed of densely-packed connective tissue and provides additional support to the upper layers of skin [25]. As the SC in frogs is thin and so provides only a modest barrier, glandular skin secretions increase protection by providing an additional structural and/or chemical barrier. Frog skin typically contains two types of exocrine gland: serous/poison, and

mucus glands (Figure 1.1). The secretions from these glands differ in terms of viscosity, varying from relatively aqueous, thin secretions to markedly thick and waxy secretions. These secretions are comprised of numerous chemicals, many of which are under investigation for their antimicrobial properties [27]. The density and distribution of glands differ both within and between frog species; more glands occur dorsally in *Lithobates (Rana catesbiana) catesbeianus* [28] and the tree frog *Hyla arborea* [29], whereas in *Rhinella marina* [28] no regional differences were noted, with this species also having a lower overall density of glandular tissue compared to *L. catesbeianus* [28].

The reason for the heightened permeability of frog skin is that, unlike mammalian skin, the skin of frogs has important regulatory functions, including specialised roles in homeostasis and defence. The skin of frogs is responsible for maintenance of fluid and electrolyte levels [8, 30], acid-base balance [25, 31], and a significant proportion of many species' respiration [9]. Further, many species exude a variety of exocrine secretions onto the skin surface, which may provide desiccation resistance, defence and / or protection [32]. Frog skin is the primary site for both water intake and efflux, and so is highly permeable and richly vascularised. Water permeability differs substantially between body regions [33], and is higher on the ventral surface than the dorsum [34, 35], presumably a mechanism to facilitate water uptake from the environment [36]. The ventral skin, particularly the ventral pelvis, is generally thinner and more vascular than the dorsum, with capillary density correlating with relative water permeability [37, 38]. Additionally, owing to the dynamic interface between their skin and the environment, frog species from different habitats have developed different relative skin thicknesses and vascularity as mechanisms to control water balance. For example, frogs from arid environments need to retard general water loss and hence have a more keratinized and condensed outer epidermis [25, 39]; similarly, many arboreal frog species have thicker skin on their dorsum, which is exposed to drying conditions of the sun and wind [40]. Conversely, aquatic frogs typically have a thicker and less-vascularized skin across their entire body surface to reduce water ingress [25].

1.3 Environmental contaminants and frog skin

Owing to their highly permeable skin and reliance on water for at least one part of their lifecycle, frogs have long been accepted as environmental indicators of the wider health of ecosystems. Although some researchers have debated whether the impact of environmental toxicants on frog health has been overemphasised [41], more recent meta-analyses have reiterated the significant impacts of environmental pollutants on amphibians [6, 7]. In early

2018 a scientific opinion was published regarding pesticide risk assessment for amphibians [42], which recommended that dermal absorption of all chemical contaminants in frog habitats be assumed to be 100%. The panel emphasised the urgent need for dermal absorption data in frogs, and highlighted the importance of such data including investigations into the differences in dermal uptake from various skin regions, in order to ensure that potential uptake following exposure, and resultant impacts, can be adequately described.

1.4 Transdermal delivery for treatment of disease in frogs

While there is significant anecdotal evidence of the percutaneous route being used for delivery of therapeutics in frogs, published texts primarily recommend oral or parenteral administration, with only a few drugs recommended to be routinely administered topically or as a bath/soak [43, 44]. These more traditional routes are not ideal in frogs: oral administration to frogs is quite difficult, requiring animal restraint, which may damage their fragile skin or the jaw [45]; similarly, parenteral administration is largely limited to high-care settings as training is required to administer medications via this route. Transdermal dosing avoids many of the problems associated with these more traditional routes of drug administration, whilst providing an easy, non-invasive method of drug delivery. Moreover, the ease of administration when using this route makes it the most appropriate when large numbers of amphibians are held (e.g. in captive insurance colonies or research collections) and for treatment in non-clinical settings, for example in the homes of enthusiasts and collectors [43, 46]. However, as knowledge about percutaneous absorption in frogs is limited, practitioners must select and alter human or other animal formulations to make them appropriate for use in frogs. Unfortunately, this has led to therapies for transdermal delivery being selected based on purported efficacy following administration in mammalian species, with doses that are often simply scaled down for animal size, disregarding differences in kinetics between these physiologically disparate animals. Knowledge of percutaneous absorption in frogs would minimise the inadvertent over- and under-dosing which often occurs when these strategies are employed in drug candidate selection and formulation.

1.5 Mathematical modelling of percutaneous absorption

Mathematical modelling of percutaneous absorption in humans has undergone rapid development over the past thirty years, and now finds use in risk assessment, cosmetology and the selection of therapeutic substances for application to the skin [47]. If only a small

number of chemicals require investigation, it is possible to undertake individual in vitro assessments for each chemical to determine flux across the skin. However, this is not a viable option when investigating a large number of chemicals, for example, when determining which of a group of therapeutic substances would be most likely to be systemically absorbed. Development of a mathematical relationship to estimate the flux and / or permeability of a chemical based on its physicochemical parameters so as to minimise the number of experiments required would be ideal, provided the limitations of the model are known.

Initial attempts to find a mathematical relationship between physicochemical characteristics and permeability through the skin used only a small number of chemicals, often from a group of closely-related chemical compounds. These studies tended to describe a simple linear relationship between lipophilicity and permeability (i.e., the more hydrophobic a compound, the faster its permeation through the skin; [48]), although if the range of chemicals included those of a more extreme lipophilic/hydrophilic character, or a wider range of molecular weights, a parabolic relationship was observed [49, 50]. The collation and publication of the permeability coefficient (K_p) of 94 chemicals across human skin by Flynn [51] provided a large dataset for development of models of absorption, with Flynn also providing algorithms for the dataset, linking relative lipophilicity and molecular weight to flux. However, there has been significant discussion about the reliability of this dataset [52-54]; the data were extracted from no fewer than fifteen different sources, so there is the potential for significant methodological differences in determining the K_p of the different chemicals. Several outliers in the data have been identified and reinvestigated, including a variety of steroid compounds [55, 56], naproxen, nicotine and atropine [57]. Despite these inherent problems, since publication of Flynn's dataset, there has been a rapid increase in the number of mathematical models attempting to quantify the relationship between permeability and the physicochemical properties of chemicals applied to the skin in humans [58]. These models have included quantitative structure-permeability relationship models [55, 59-70], and more recently, machine learning techniques including artificial neural networks [71, 72] and Gaussian processes [73-76]. Despite the wide range of physicochemical characteristics investigated, and large number of models produced, the key characteristics found to be important in predicting permeability remain relatively consistent, and include hydrophobicity, molecular size, and hydrogen bonding ability [77].

1.6 Rationale for this study

Compared to mammals, frogs have very thin, highly-permeable skin [8-10]. However, little is known about how this permeability translates quantitatively into chemical absorption through the skin, as few transdermal kinetic studies in terrestrial frogs have been undertaken [28, 78-84]. Increased permeability of the skin to chemicals can have either positive or detrimental outcomes for frogs; the transdermal route provides an easy, relatively stress-free way to administer drugs for the treatment of disease, however rapid absorption of environmental contaminants is also likely to lead to significant morbidity and/or mortality. While pharmacokinetic studies on individual chemicals will slowly increase the knowledge of percutaneous absorption in frogs, this process is laborious and necessitates significant animal use to obtain sufficient data. Further, such studies provide no mechanism for extrapolating findings to other chemicals or formulations. Mathematical models of absorption in humans, developed from in vitro absorption kinetic data, have been used with some success to predict in vivo percutaneous absorption of chemicals in humans [58]; it is likely that such a model for frogs would have two-fold purpose, being equally able to guide therapeutic chemical selection and formulation, while also advising risk assessment and mitigation in frog habitats.

1.7 Project aims and objectives

The overarching aim of this project is to develop understanding of percutaneous absorption in frogs, through in vitro and in vivo investigations, and the development of mathematical models to describe factors influencing permeability. Before an effective model can be produced, a thorough understanding of skin structure and function in amphibians is paramount, as this will influence the passage of a chemical through the skin. Consideration must also be given to the differences in absorption between regions of a frog's body, and the differences in absorption between frog species from different habitats. Finally, the impact of formulation should be investigated. Knowledge of the factors influencing percutaneous absorption in frogs will facilitate the design of effective models of absorption. These models and formulation knowledge, in turn, will find utility in: 1) optimisation of drug candidate selection and dosing regimen design for treatment of disease, and 2) ecotoxicology, to assist risk mitigation by advising formulation of chemicals that are to be applied in a frog's habitat, and also to advise risk management following contamination of habitats with chemicals.

In order to develop an effective model of percutaneous absorption in frogs, two stages of research are required: 1) model development (in vitro investigations) and 2) model refinement and application (in vivo investigations).

Within the auspices of 1) model development (in vitro investigations), several specific objectives have been defined:

a. Identify anatomical, physicochemical or formulation-based factors that are likely to influence absorption across frog skin
b. Identify which physicochemical properties of chemicals are important in determining rate and extent of percutaneous absorption through frog skin
c. Determine whether the anatomical regional variation in percutaneous absorption within a single frog species significantly influences the rate and / or extent of chemical absorption through the skin
d. Determine whether the anatomical/physiological differences between frog species from different primary habitats significantly influences the rate and / or extent of chemical absorption through the skin
e. Make dosing recommendations from the information gained in 1a–d (re: site of application; different dosing recommendations for different species)
f. Utilise results from objectives 1b–d to inform the development a model of percutaneous absorption in frogs
g. Investigate how altering a formulation through the addition of penetration enhancers influences absorption, with particular focus on changes in the restrictive factors identified in terms of physicochemical properties (1b) and skin region (1c)

Within the auspices of 2) model refinement and application (in vivo investigations), there are two objectives:

a. Compare in vitro model predictions with the in vivo data in frogs, refining the model as needed
b. Use the refined model and results of (1g) to guide selection and formulation of a candidate chemical for transdermal delivery with potential to treat infectious disease in frogs

1.8 Thesis structure and chapter summaries

This thesis is structured to sequentially address the aims and objectives as in Section 1.7, as outlined below:

Chapter	Overview	Objectives addressed
2	Review of percutaneous absorption in frogs, drawn from the extant literature of absorption in mammals and interpreted based on known frog anatomy and physiology. The review also includes reference to the studies that have reported percutaneous absorption in frogs, and seeks to identify factors likely to influence absorption in these animals. A version of this review was published in the *Journal of Veterinary Pharmacology and Therapeutics* [46]. [Llewelyn VK, Berger L, Glass BD. Percutaneous absorption of chemicals: developing an understanding for the treatment of disease in frogs. Journal of Veterinary Pharmacology and Therapeutics. 2016; 39(2):109–21. http://dx.doi.org/10.1111/jvp.12264].	1a, 1b

3	Presents in vitro absorption studies undertaken in two frog species from differing primary habitats, focussing on regional variability in absorption within individual species. The chapter includes a general methodology section, and includes data from two publications, one presenting in vitro absorption data for the arboreal frog *Litoria caerulea* [85], and the other presenting in vitro absorption data in the terrestrial species *Rhinella marina* [86]. Versions of the two papers were published in *Environmental Toxicology and Pharmacology* [85] and *Environmental Toxicology and Chemistry* [86], respectively. [Llewelyn VK, Berger L, Glass BD. Regional variation in percutaneous absorption in the tree frog *Litoria caerulea*. Environmental Toxicology and Pharmacology. 2018; 60:5–11. https://doi.org/10.1016/j.etap.2018.03.019; Llewelyn VK, Berger L, Glass BD. Effects of skin region and relative lipophilicity on percutaneous absorption in the toad *Rhinella marina*. Environmental Toxicology and Chemistry. 2019; 38(2):361–7. http://dx.doi.org/10.1002/etc.4302].	1b, 1c
4	Provides a synthesis and comparison of in vitro absorption in two frog species, and includes a model of absorption that can be used to predict percutaneous absorption in both arboreal and terrestrial frog species. This chapter also provides dosing recommendations for these species, based on the synthesis provided. The abstract of this chapter is based on a conference abstract, published in the *Journal of Veterinary Pharmacology and Therapeutics* [21]. [Llewelyn VK, Berger L, Glass BD. Percutaneous absorption in frog species: variability in skin may influence delivery of therapeutics. Journal of Veterinary Pharmacology and Therapeutics. 2018; 41(Suppl. 1):70. https://doi.org/10.1111/jvp.12639]. The chapter has been prepared as a manuscript for submission to the same journal.	1d, 1e, 1f

5	Presents the impact of penetration enhancers on in vitro absorption kinetics in frog skin, and also provides information about how exposure to these enhancers affects skin structure, through use of differential scanning calorimetry and histology. A version of this chapter has been published in *Heliyon*. [Llewelyn VK, Berger L, Glass BD. Permeability of frog skin to chemicals: effect of penetration enhancers. Heliyon. 2019; 5(8):e02127. https://doi.org/10.1016/j.heliyon.2019.e02127.]	1g
6	Provides an in vitro in vivo comparison of absorption in frog skin. Firstly, a model of in vitro absorption in a terrestrial frog species is presented. The model is then used to predict absorption kinetics for three model chemicals, and the in vivo percutaneous absorption of the same chemicals are determined, and the results compared. This chapter has been formatted as a manuscript for submission to *PLOS ONE*.	1f; 2a
7	Describes how the findings of the previous chapters were used to select and formulate a chemical for the potential treatment of infectious disease in frogs, and reports on the in vivo absorption of this formulation in a healthy terrestrial frog species. This chapter has been formatted as a manuscript for submission to the *Journal of Veterinary Pharmacology and Therapeutics*.	2b
8	A general discussion, highlighting the key findings of each study, limitations of the studies, future directions and overall conclusions.	All objectives

1.9 References

1. Hayes TB, Falso S, Stice GM. The cause of global amphibian declines: a developmental endocrinologist's perspective. Journal of Experimental Biology. 2010; 213:921-33. https://doi.org/10.1242/jeb.040865

2. Collins JP. Amphibian decline and extinction: What we know and what we need to learn. Diseases of Aquatic Organisms. 2010; 92:93–9. http://dx.doi.org/10.3354/dao02307

3. Scheele BC, Pasmans F, Skerratt LF, Berger L, Martel A, Beukema W, et al. Amphibian fungal panzootic causes catastrophic and ongoing loss of biodiversity. Science. 2019; 363:1459-63. http://dx.doi.org/10.1126/science.aav0379

4. Wake DB, Vredenburg VT. Are we in the midst of the sixth mass extinction? A view from the world of amphibians. Proceedings of the National Academy of Sciences of the United States of America. 2008; 105:11466-73. https://doi.org/10.1073/pnas.0801921105

5. Schloegel LM, Daszak P, Cunningham AA, Speare R, Hill B. Two amphibian diseases, chytridiomycosis and ranaviral disease, are now globally notifiable to the World Organization for Animal Health (OIE): an assessment. Diseases of Aquatic Organisms. 2010; 92:101-8. https://doi.org/10.3354/dao02140

6. Egea-Serrano A, Relyea RA, Tejedo M, Torralva M. Understanding of the impact of chemicals on amphibians: a meta-analytic review. Ecology and Evolution. 2012; 2:1382-97. https://doi.org/10.1002/ece3.249

7. Sievers M, Hale R, Parris KM, Swearer SE. Impacts of human-induced environmental change in wetlands on aquatic animals. Biological Reviews. 2018; 93:529-54. https://doi.org/10.1111/brv.12358

8. Helmer P, Whiteside D. Amphibian anatomy and physiology. In: O'Malley B, editor. Clinical Anatomy and Physiology of Exotic Species. Edinburgh: Elsevier Saunders; 2005. p. 3-14.

9. Wright KM. Anatomy for the clinician. In: Wright KM, Whitaker BR, editors. Amphibian medicine and captive husbandry. 1st ed. Malabar, FL: Krieger Publishing Company; 2001. p. 15-30.

10. Haslam IS, Roubos EW, Mangoni ML, Yoshizato K, Vaudry H, Kloepper JE, et al. From frog integument to human skin: dermatological perspectives from frog skin biology. Biological Reviews. 2014; 89:618-655. https://doi.org/10.1111/brv.12072

11. Berger L, Speare R, Pessier A, Voyles J, Skerratt LF. Treatment of chytridiomycosis requires urgent clinical trials. Diseases of Aquatic Organisms. 2010; 92:165–74. http://dx.doi.org/10.3354/dao02238

12. Holden WM, Ebert AR, Canning PF, Rollins-Smith LA. Evaluation of amphotericin b and chloramphenicol as alternative drugs for treatment of chytridiomycosis and their impacts on innate skin defences. Applied and Environmental Microbiology. 2014; 80:4034-41. https://doi.org/10.1128/aem.04171-13

13. Muijsers M, Martel A, Van Rooij P, Baert K, Vercauteren G, Ducatelle R, et al. Antibacterial therapeutics for the treatment of chytrid infection in amphibians: Columbus's egg? BMC Veterinary Research. 2012; 8:175. http://dx.doi.org/10.1186/1746-6148-8-175

14. Brannelly LA, Richards-Zawacki CL, Pessier AP. Clinical trials with itraconazole as a treatment for chytrid fungal infections in amphibians. Diseases of Aquatic Organisms. 2012; 101:95–104. http://dx.doi.org/10.3354/dao02521

15. Woodhams DC, Geiger CC, Reinert LK, Rollins-Smith LA, Lam B, Harris RN, et al. Treatment of amphibians infected with chytrid fungus: learning from failed trials with itraconazole, antimicrobial peptides, bacteria, and heat therapy. Diseases of Aquatic Organisms. 2012; 98:11-25. http://dx.doi.org/10.3354/dao02429

16. Jones MEB, Paddock D, Bender L, Allen JL, Schrenzel MD, Pessier AP. Treatment of chytridiomycosis with reduced-dose itraconazole. Diseases of Aquatic Organisms. 2012; 99:243-9. http://dx.doi.org/10.3354/dao02475

17. Tamukai K, Une Y, Tominaga A, Suzuki K, Goka K. Treatment of spontaneous chytridiomycosis in captive amphibians using itraconazole. Journal of Veterinary Medical Science. 2011; 73:155-9. http://dx.doi.org/10.1292/jvms.10-0261

18. Martel A, Van Rooij P, Vercauteren G, Baert K, Van Waeyenberghe L, Debacker P, et al. Developing a safe antifungal treatment protocol to eliminate *Batrachochytrium dendrobatidis* from amphibians. Medical Mycology. 2011; 49:143-9. http://dx.doi.org/10.3109/13693786.2010.508185

19. Brannelly LA, Skerratt LF, Berger L. Treatment trial of clinically ill corroboree frogs with chytridiomycosis with two triazole antifungals and electrolyte therapy. Veterinary Research Communications. 2015; 39:179–87. https://doi.org/10.1007/s11259-015-9642-5

20. Arellano ML, Velasco MA, Aguirre TM, Zarini O, Belasen AM, James TY, et al. Treatment of adult Valcheta frogs *Pleurodema somuncurense* for chytrid fungus. Conservation Evidence. 2018; 15:37.

21. Llewelyn VK, Berger L, Glass BD. Percutaneous absorption in frog species: variability in skin may influence delivery of therapeutics. Journal of Veterinary Pharmacology and Therapeutics. 2018; 41:70. https://doi.org/10.1111/jvp.12639

22. IUCN SSC Amphibian Specialist Group. Guidelines on the use of ex situ management for species conservation. 2014. Available from: www.iucn.org/about/work/programmes/species/publications/iucn_guidelines_and__policy__statements/

23. IUCN SSC Amphibian Specialist Group. Amphibian conservation action plan. 2015. Available from: https://www.iucn-amphibians.org/resources/acap/

24. Densmore CL, Green DE. Diseases of amphibians. ILAR Journal. 2007; 48:235-54. https://doi.org/10.1093/ilar.48.3.235

25. Toledo RC, Jared C. Cutaneous adaptations to water balance in amphibians. Comparative Biochemistry and Physiology Part A: Physiology. 1993; 105:593-608. http://dx.doi.org/10.1016/0300-9629(93)90259-7

26. Sadowski-Fugitt LM, Tracy CR, Christian KA, Williams JB. Cocoon and epidermis of Australian *Cyclorana* frogs differ in composition of lipid classes that affect water loss. Physiological and Biochemical Zoology. 2012; 85:40-50. http://dx.doi.org/10.1086/663695

27. Rollins-Smith LA, Reinert LK, O'Leary CJ, Houston LE, Woodhams DC. Antimicrobial peptide defenses in amphibian skin. Integrative and Comparative Biology. 2005; 45:137-42. https://doi.org/10.1093/icb/45.1.137

28. Willens S, Stoskopf MK, Baynes RE, Lewbart GA, Taylor SK, Kennedy-Stoskopf S. Percutaneous malathion absorption in the harvested perfused anuran pelvic limb. Environmental Toxicology and Pharmacology. 2006; 22:263-7. https://doi.org/10.1016/j.etap.2006.04.009

29. Goniakowska-Witalińska L, Kubiczek U. The structure of the skin of the tree frog (*Hyla arborea arborea* L.). Annals of Anatomy. 1998; 180:237-46. https://doi.org/10.1016/s0940-9602(98)80080-0

30. Katz U, Nagel W. Biophysics of ion transport across amphibian skin. In: Heatwole H, Barthalmus GT, editors. Amphibian Biology. 1. Chipping Norton: Surrey Beatty & Sons; 1994. p. 98-119.

31. Stiffler DF. The role of cutaneous acid-base-electrolyte exchange in extracellular pH regulation. In: Heatwole H, Barthalmus GT, editors. Amphibian biology. 1. Chipping Norton: Surrey Beatty & Sons; 1994. p. 120-31.

32. Toledo RC, Jared C. Cutaneous granular glands and amphibian venoms. Comparative Biochemistry and Physiology. 1995; 111A:1-29. http://dx.doi.org/10.1016/0300-9629(95)98515-i

33. Bentley PJ, Main AR. Zonal differences in permeability of the skin of some anuran Amphibia. The American Journal of Physiology. 1972; 223:361–3. https://doi.org/10.1152/ajplegacy.1972.223.2.361

34. Bentley PJ, Yorio T. The passive permeability of the skin of anuran amphibia: a comparison of frogs (*Rana pipiens*) and toads (*Bufo marinus*). The Journal of Physiology. 1976; 261:603–15. https://doi.org/10.1113/jphysiol.1976.sp011576

35. Yorio T, Bentley PJ. Asymmetrical permeability of the integument of tree frogs (*hylidae*). Journal of Experimental Biology. 1977; 67:197-204.

36. Pough FH. Amphibian biology and husbandry. Institute for Laboratory Animal Research Journal. 2007; 48:203-13. https://doi.org/10.1093/ilar.48.3.203

37. Christensen CU. Adaptations in the water economy of some anuran amphibia. Comparative Biochemistry and Physiology. 1974; 47A:1035–49. http://dx.doi.org/10.1016/0300-9629(74)90477-0

38. Shoemaker VH, Nagy KA. Osmoregulation in amphibians and reptiles. Annual Reviews in Physiology. 1977; 39:449-71. http://dx.doi.org/10.1146/annurev.ph.39.030177.002313

39. Bani G. Osservazioni sulla ultrastruttura della cute di *Bufo bufo (L.)* e modificazioni a livelli dell'epidermide, in relazione a differenti condizioni ambientali. Monitore Zoologico Italiano Supplemento. 1966; 74:93–124.

40. Amey AP, Grigg GG. Lipid-reduced evaporative water loss in two arboreal hylid frogs. Comparative Biochemistry and Physiology Part A: Physiology. 1995; 111:283–91. https://doi.org/10.1016/0300-9629(94)00213-d

41. Kerby JL, Richards-Hrdlicka KL, Storfer A, Skelly DK. An examination of amphibian sensitivity to environmental contaminants: are amphibians poor canaries? Ecology Letters. 2010; 13:60-7. https://doi.org/10.1111/j.1461-0248.2009.01399.x

42. EFSA PPR Panel (EFSA Panel on Plant Protection Products and their Residues), Ockleford C, Adriaanse P, Berny P, Brock T, Duquesne S, et al. Scientific opinion on the state of the science on pesticide risk assessment for amphibians and reptiles. EFSA Journal. 2018; 16:5125. https://doi.org/10.2903/j.efsa.2018.5125

43. Wright KM, Whitaker BR. Pharmacotherapeutics. In: Wright KM, Whitaker BR, editors. Amphibian medicine and captive husbandry. 1st ed. Malabar, FL: Krieger Publishing Company; 2001. p. 309-32.

44. Wright K, DeVoe RS. Amphibians. In: Carpenter JW, editor. Exotic animal formulary. 4 ed. St Louis: Elsevier Health Sciences; 2013. p. 53-82.

45. Brown C. Restraint and oral administration in frogs. Lab Animal. 2010; 39(9):267–8. https://doi.org/10.1038/laban0910-267

46. Llewelyn VK, Berger L, Glass BD. Percutaneous absorption of chemicals: developing an understanding for the treatment of disease in frogs. Journal of Veterinary Pharmacology and Therapeutics. 2016; 39:109-21. http://dx.doi.org/10.1111/jvp.12264

47. Kielhorn J, Melching-Kollmuss S, Mangelsdorf I. Dermal absorption. Environmental Health Criteria 235. Geneva: WHO; 2006. Available: https://www.who.int/ipcs/publications/ehc/ehc235.pdf?ua=1

48. Lien EJ, Tong GL. Physicochemical properties and percutaneous absorption of drugs. Journal of the Society of Cosmetic Chemists. 1973; 24:371-84.

49. Zhang Q, Grice JE, Li P, Jepps OG, Wang G-J, Roberts MS. Skin solubility determines maximum transepidermal flux for similar size molecules. Pharmaceutical Research. 2009; 26:1974-85. https://doi.org/10.1007/s11095-009-9912-4

50. Flynn GL, Stewart B. Percutaneous drug penetration: Choosing candidates for transdermal development. Drug Development Research. 1988; 13:169-85. http://dx.doi.org/10.1002/ddr.430130209

51. Flynn GL. Physicochemical determinants of skin absorption. In: Gerrity TR, Henry CJ, editors. Principles of Route-to-Route Extrapolation for Risk Assessment. New York: Elsevier; 1990. p. 93-127.

52. Kladt C, Dennerlein K, Göen T, Drexler H, Korinth G. Evaluation on the reliability of the permeability coefficient (Kp) to assess the percutaneous penetration property of chemicals on the basis of Flynn's dataset. International Archives of Occupational and Environmental Health. 2018; 91:467-77. https://doi.org/10.1007/s00420-018-1296-5

53. Korinth G, Schaller KH, Drexler H. Is the permeability coefficient *K*p a reliable tool in percutaneous absorption studies? Archives of Toxicology. 2005; 79:155-9. https://doi.org/10.1007/s00204-004-0618-4

54. Vecchia BE, Bunge AL. Skin absorption databases and predictive equations. In: Hadgraft J, editor. Transdermal drug delivery systems: Revised and expanded. 2 ed. Boca Raton: CRC Press; 2002.

55. Moss GP, Cronin MTD. Quantitative structure-permeability relationships for percutaneous absorption: re-analysis of steroid data. International Journal of Pharmaceutics. 2002; 238:150-09. https://doi.org/10.1016/s0378-5173(02)00057-1

56. Barratt MD. Quantitative structure-activity relationships for skin permeability. Toxicology In Vitro. 1995; 9:27–37. https://doi.org/10.1016/0887-2333(94)00190-6

57. Değim IT, Pugh WJ, Hadgraft J. Skin permeability data: anomalous results. International Journal of Pharmaceutics. 1998; 170:129-33. https://doi.org/10.1016/s0378-5173(98)00113-6

58. Moss GP, Wilkinson SC, Sun Y. Mathematical modelling of percutaneous absorption. Current Opinion in Colloid & Interface Science. 2012; 17:166-72. https://doi.org/10.1016/j.cocis.2012.01.002

59. Baert B, Deconinck E, Van Gele M, Slodicka M, Stoppie P, Bode S, et al. Transdermal penetration behaviour of drugs: CART-clustering, QSPR and selection of model compounds. Bioorganic and Medicinal Chemistry. 2007; 15:6943–55. https://doi.org/10.1016/j.bmc.2007.07.050

60. Moss GP, Dearden JC, Patel H, Cronin MTD. Quantitative structure-permeability relationships (QSPRs) for percutaneous absorption. Toxicology in Vitro. 2002; 16:299-317. https://doi.org/10.1016/s0887-2333(02)00003-6

61. Patel H, ten Berge WF, Cronin MTD. Quantitative structure-activity relationships (QSARs) for the prediction of skin permeation of exogenous chemicals. Chemosphere. 2002; 48:603-13. https://doi.org/10.1016/s0045-6535(02)00114-5

62. Patel H, Cronin M. Determination of the optimal physico-chemical parameters to use in a QSAR-approach to predict skin permeation rate. Liverpool, England: QSAR and Modelling Research Group, School of Pharmacy and Chemistry, John Moores University; 2001. Contract No.: CEFIC-LRI.

63. Cronin MTD, Dearden JC, Moss GP, Murray-Dickson G. Investigation of the mechanism of flux across human skin in vitro by quantitative structure–permeability relationships. European Journal of Pharmaceutical Sciences. 1999; 7:325-30. https://doi.org/10.1016/s0928-0987(98)00041-4

64. Potts RO, Guy RH. A predictive algorithm for skin permeability: The effects of molecular size and hydrogen bond activity. Pharmaceutical Research. 1995; 12:1628-33.

65. Potts RO, Guy RH. Predicting skin permeability. Pharmaceutical Research. 1992; 9:663-9. http://dx.doi.org/10.1023/a:1015810312465

66. Wilschut A, ten Berge WF, Robinson PJ, McKone TE. Estimating skin permeation. The validation of five mathematical skin permeation models. Chemosphere. 1995; 30:1275-96. https://doi.org/10.1016/0045-6535(95)00023-2

67. Abraham MH, Chadha HS, Mitchell RC. The factors that influence skin penetration of solutes. Journal of Pharmacy and Pharmacology. 1995; 47:8–16. https://doi.org/10.1111/j.2042-7158.1995.tb05725.x

68. El Tayar N, Tsai R-S, Testa B, Carrupt P-A, Hansch C, Leo A. Percutaneous penetration of drugs: a quantitative structure-permeability relationship study. Journal of Pharmaceutical Sciences. 1991; 80:744-9. https://doi.org/10.1002/jps.2600800807

69. Pugh WJ, Roberts MS, Hadgraft J. Epidermal permeability - penetrant structure relationships: 3. The effect of hydrogen bonding interactions and molecular size on diffusion across the stratum corneum. International Journal of Pharmaceutics. 1996; 138:149-65. http://dx.doi.org/10.1016/0378-5173(96)04533-4

70. Roberts MS, Pugh WJ, Hadgraft J. Epidermal permeability - penetrant structure relationships: 2. The effect of H-bonding groups in penetrants on their diffusion through the stratum corneum. International Journal of Pharmaceutics. 1996; 132:23-32. http://dx.doi.org/10.1016/0378-5173(95)04278-4

71. Chen L, Guo-ping L, Lu-jia H. Prediction of human skin permeability using artificial neural network (ANN) modeling. Acta Pharmacologica Sinica. 2007; 28:591–600. https://doi.org/10.1111/j.1745-7254.2007.00528.x

72. Değim IT, Hadgraft J, İlbasmiş S, Özkan Y. Prediction of skin penetration using artificial neural network (ANN) modelling. Journal of Pharmaceutical Sciences. 2003; 92:656-64. https://doi.org/10.1002/jps.10312

73. Brown MB, Lau C-H, Lim ST, Davey N, Moss GP, Yoo S-H, et al. An evaluation of the potential of linear and nonlinear skin permeation models for the prediction of experimentally measured percutaneous drug absorption. Journal of Pharmacy and Pharmacology. 2012; 64:566–77. https://doi.org/10.1111/j.2042-7158.2011.01436.x

74. Moss GP, Sun Y, Prapopoulou M, Davey N, Adams R, Pugh WJ, et al. The application of Gaussian processes in the prediction of percutaneous absorption. Journal of Pharmacy and Pharmacology. 2009; 61:1147-53. https://doi.org/10.1211/jpp/61.09.0003

75. Lam LT, Sun Y, Davey N, Adams R, Prapopoulou M, Brown MB, et al. The application of feature selection to the development of Gaussian process models for percutaneous absorption. Journal of Pharmacy and Pharmacology. 2010; 62:738-49. https://doi.org/10.1211/jpp.62.06.0010

76. Sun Y, Brown MB, Prapopoulou M, Davey N, Adams RG, Moss GP. The application of stochastic machine learning methods in the prediction of skin penetration. Applied Soft Computing. 2011; 11:2367-75. https://doi.org/10.1016/j.asoc.2010.08.016

77. Moss GP, Gullick DR, Wilkinson SC. The new breadth of research in the field. predictive methods in percutaneous absorption. Berlin: Springer; 2015. p. 65-89.

78. Roberts AA, Berger L, Robertson SG, Webb RJ, Kosch TA, McFadden M, et al. The efficacy and pharmacokinetics of terbinafine against the frog-killing fungus (*Batrachochytrium dendrobatidis*). Medical Mycology. 2019; 57:204-214. http://dx.doi.org/10.1093/mmy/myy010

79. D'Agostino JJ, West G, Boothe DM, Jayanna PK, Snider T, Hoover JP. Plasma pharmacokinetics of selamectin after a single topical administration in the American bullfrog (*Rana catesbeiana*). Journal of Zoo and Wildlife Medicine. 2007; 38:51-4. http://dx.doi.org/10.1638/06-054.1

80. Balko JA, Watson MK, Papich MG, Posner LP, Chinnadurai SK. Plasma concentrations of ketoprofen and meloxicam after subcutaneous and topical administration in the Smoky Jungle Frog (*Leptodactylus pentadactylus*). The Journal of Herpetological Medicine and Surgery. 2018; 28:89–92. https://doi.org/10.5818/17-10-129.1

81. Valitutto MT, Raphael BL, Calle PP, Papich MG. Tissue concentrations of enrofloxacin and its metabolite ciprofloxacin after a single topical dose in the Coqui frog (*Eleutherodactylus coqui*). Journal of Herpetological Medicine and Surgery. 2013; 23:69-73. https://doi.org/10.5818/1529-9651-23.3.69

82. Ardente AJ, Barlow BM, Burns P, Goldman R, Baynes RE. Vehicle effects on in vitro transdermal absorption of sevoflurane in the bullfrog, *Rana catesbeiana*. Environmental Toxicology and Pharmacology. 2008; 25:373–9. http://dx.doi.org/10.1016/j.etap.2007.12.001

83. Kaufmann K, Dohmen P. Adaption of a dermal in vitro method to investigate the uptake of chemicals across amphibian skin. Environmental Sciences Europe. 2016; 28:10. https://doi.org/10.1186/s12302-016-0080-y

84. Willens S, Stoskopf MK, Baynes RE, Lewbart GA, Taylor SK, Kennedy-Stoskopf S. Percutaneous malathion absorption by anuran skin in flow-through diffusion cells. Environmental Toxicology and Pharmacology. 2006; 22:255-62. https://doi.org/10.1016/j.etap.2006.04.010

85. Llewelyn VK, Berger L, Glass BD. Regional variation in percutaneous absorption in the tree frog *Litoria caerulea*. Environmental Toxicology and Pharmacology. 2018; 60:5-11. https://doi.org/10.1016/j.etap.2018.03.019

86. Llewelyn VK, Berger L, Glass BD. Effects of skin region and relative lipophilicity on percutaneous absorption in the toad *Rhinella marina*. Environmental Toxicology and Chemistry. 2019; 38:361-7. http://dx.doi.org/10.1002/etc.4302

Chapter 2: Percutaneous absorption of chemicals: developing an understanding for the treatment of disease in frogs

Preamble

This chapter provides the literature review compiled for this research. This chapter reviews the chemical-specific, skin-specific, and formulation-specific factors shown to influence absorption in mammalian species, and interprets these in light of known frog anatomy and physiology to identify which of these factors are likely to impact percutaneous absorption in frogs. The manuscript then continues with a specific review of extant studies on transdermal therapeutics in frogs. Implications of percutaneous absorption in view of environmental contamination, including a summary of extant studies investigating percutaneous absorption of agricultural and industrial chemicals in terrestrial frog species is included in Chapter 3 (Section 3.3).

A version of this chapter has been published in the *Journal of Veterinary Pharmacology and Therapeutics* [1] [Percutaneous absorption of chemicals: developing an understanding for the treatment of disease in frogs. Llewelyn VK, Berger L, Glass BD. *Journal of Veterinary Pharmacology and Therapeutics*, 39(2). Copyright © 2015, John Wiley & Sons Ltd]. A copy of the final published version of this manuscript is in Appendix 1.

Statement of Contribution

Llewelyn VK, Berger L, Glass BD. (2016). Percutaneous absorption of chemicals: developing an understanding for the treatment of disease in frogs. Journal of Veterinary Pharmacology and Therapeutics, 39(2):109-121. http://dx.doi.org/10.1111/jvp.12264

Authors' contributions

Llewelyn collected, reviewed and synthesised the literature and wrote the first draft of the paper. This draft was critically reviewed and revised by Berger and Glass. Llewelyn handled submission and revision of the manuscript.

Victoria K. Llewelyn

Beverley D. Glass

Lee Berger

Chapter embargoed

Chapter embargoed

Chapter embargoed

Chapter embargoed

Chapter embargoed

Chapter embargoed

Chapter embargoed

Chapter embargoed

Chapter embargoed

Chapter embargoed

Chapter embargoed

Chapter embargoed

Chapter embargoed

Chapter embargoed

Chapter embargoed

Chapter embargoed

Chapter embargoed

Chapter embargoed

Chapter embargoed

Chapter embargoed

Chapter embargoed

Chapter embargoed

Chapter embargoed

Chapter embargoed

Chapter embargoed

Chapter embargoed

Chapter embargoed

Chapter embargoed

Chapter embargoed

Chapter embargoed

Chapter 3: Determining baseline in vitro percutaneous absorption kinetics in two frog species

Preamble

As identified in Chapter 2, the relative lipophilicity of the applied chemical is likely to be a primary influence percutaneous absorption in frogs, and so it is important to ensure the absorption kinetics of chemicals covering a range of logP values are investigated. Additionally, skin structure, specifically thickness and vascularisation, are likely to influence the percutaneous absorption of chemicals in frog skin. These skin characteristics are known to vary both within and between frog species, being particularly disparate in species from different primary habitats. However, it is unknown whether these distinct morphological differences result in significant differences in percutaneous absorption.

This chapter therefore presents research undertaken in determining baseline in vitro absorption kinetics for three model chemicals — caffeine, benzoic acid, and ibuprofen — through the skin of two frog species: the arboreal frog *Litoria caerulea*, and the terrestrial toad *Rhinella marina*. These model chemicals were selected for use in these studies as they are commonly-used model chemicals for percutaneous absorption studies, and cover a wide range of relative lipophilicities (logP between –0.07 and 3.97) and aqueous solubilities.

This chapter is comprised of versions of two published studies, one for each frog species [1, 2]. As the methodology is shared for these studies, this chapter is presented in three subsections: (3.1) General Methodology, including the development and validation for high-performance liquid chromatography (HPLC) analyses used in these studies and methodology for the diffusion cell experiments including data analysis; (3.2) Introduction, results and discussion specific to *Litoria caerulea*; and (3.3) Introduction, results and discussion specific to *Rhinella marina*. Final published versions of these manuscripts are in Appendices 2a and 2b.

Statement of Contribution

Llewelyn VK, Berger L, Glass BD. (2018). Regional variation in percutaneous absorption in the tree frog *Litoria caerulea*. Environmental Toxicology and Pharmacology, 60:5–11. http://doi.org/10.1016/j.etap.2018.03.019

Llewelyn VK, Berger L, Glass BD. Effects of skin region and relative lipophilicity on percutaneous absorption in the toad *Rhinella marina*. Environmental Toxicology and Chemistry. 2019; 38(2):361–7. http://doi.org/10.1002/etc.4302

Authors' contributions

Llewelyn designed the experiments, developed and validated the methods, collected the data and performed the data analysis. Llewelyn wrote the first draft of the papers, which were critically reviewed and revised by Berger and Glass. Llewelyn handled submission and revision of the manuscripts.

Victoria K. Llewelyn

Beverley D. Glass

Lee Berger

Chapter embargoed

Chapter embargoed

Chapter embargoed

Chapter embargoed

Chapter embargoed

Chapter embargoed

Chapter embargoed

3.2 Percutaneous absorption in the green tree frog *Litoria caerulea*

This section is a version of the following publication:

Regional variation in percutaneous absorption in the tree frog *Litoria caerulea*. Llewelyn VK, Berger L, Glass BD. *Environmental Toxicology and Pharmacology*, 60. Copyright © 2018 Elsevier B.V.
https://doi.org/10.1016/j.etap.2018.03.019

A copy of the published version of this paper is in Appendix 2a. Methodology for this publication has been provided in Section 3.1.

Chapter embargoed

Chapter embargoed

Chapter embargoed

Chapter embargoed

Chapter embargoed

Chapter embargoed

Chapter embargoed

Chapter embargoed

3.3 Percutaneous absorption in the cane toad *Rhinella marina*

This section is a version of the following publication:

Effects of skin region and relative lipophilicity on percutaneous absorption in the toad *Rhinella marina*. Llewelyn VK, Berger L, Glass BD. *Environmental Toxicology and Chemistry*, 38(2). Copyright © 2018 SETAC.
http://dx.doi.org/10.1002/etc.4302

A copy of the published version of this paper is in Appendix 2b. Methodology for this publication has been provided in Section 3.1.

Chapter embargoed

Chapter embargoed

Chapter embargoed

Chapter embargoed

Chapter embargoed

Chapter embargoed

Chapter embargoed

Chapter embargoed

Chapter embargoed

Chapter embargoed

Chapter embargoed

Chapter embargoed

Chapter embargoed

Chapter embargoed

Chapter embargoed

Chapter embargoed

Chapter embargoed

Chapter 4: Interspecific variability in percutaneous absorption in frogs

Preamble

Chapter 3 presented the in vitro absorption findings for three model chemicals in different skin regions for two frog species (*Litoria caerulea* and *Rhinella marina)*, with the discussion focussed on the impact of skin region on absorption in each species individually. However, the structure of the skin between frog species is reported to differ based on the primary habitat of the species, and this is likely to impact on absorption kinetics through the skin (Chapter 2). It is therefore of import to provide a direct comparison of in vitro absorption kinetics between these species. Further, while information about absorption in species from a single habitat-type is valuable as it can likely be extrapolated to other species from the same habitat, specific guidance of how absorption differs between species from different primary habitats would have wider utilisation in advising development of effective treatment strategies for disease, and also in risk mitigation and management.

This chapter therefore presents a comparison of in vitro absorption kinetics between the arboreal frog *L. caerulea* and the terrestrial toad *Rh. marina*, synthesised from data collected and presented in Chapter 3, and interpreted in light of histological sections of skin produced from both species. The in vitro absorption data was then used to create the first model of absorption between frog species, which is also presented in this chapter. Finally, considerations for the clinician, when designing transdermal treatments in these species are presented, in light of the findings.

The in vitro comparison and histology work (i.e., all work except for the model) was presented at the 14th International Congress of the European Association for Veterinary Pharmacology and Toxicology, and the abstract presented is based on the published abstract for this conference. [Percutaneous absorption in frog species: variability in skin may influence delivery of therapeutics. Llewelyn VK, Berger L, Glass BD. *Journal of Veterinary Pharmacology and Therapeutics*, 41(Suppl. 1). Copyright © Journal of Veterinary Pharmacology and Therapeutics © 2018 John Wiley & Sons, Ltd. https://doi.org/10.1111/jvp.12639]. A copy of the final published version of this abstract is in Appendix 5.

This chapter has been prepared for publication in the *Journal of Veterinary Pharmacology and Therapeutics*, and is currently under review.

Statement of Contribution

Llewelyn VK, Berger L, Glass BD. (2018a). Percutaneous absorption in frog species: variability in skin may influence delivery of therapeutics. *Journal of Veterinary Pharmacology and Therapeutics, 41*(Suppl. 1), 70. [conference abstract]. https://doi.org/10.1111/jvp.12639

Llewelyn VK, Berger L, Glass BD. (To be submitted). Interspecific variability in percutaneous absorption in frogs: potential therapeutic issues. *For submission to the Journal of Veterinary Pharmacology and Therapeutics*.

Authors' contributions

Llewelyn wrote the conference abstract with editorial input from Berger and Glass. Llewelyn presented this work.

Llewelyn analysed data previously collected (Chapter 3, [1, 2]) to create models of absorption. Llewelyn performed data analysis, figure production, and model creation. Llewelyn reviewed histological slides with input from Berger. Llewelyn wrote the first draft of the paper, which was critically reviewed and revised by Berger and Glass. Llewelyn will handle submission and revision of the manuscript.

Victoria K. Llewelyn

Beverley D. Glass

Lee Berger

Chapter embargoed

Chapter embargoed

Chapter embargoed

Chapter embargoed

Chapter embargoed

Chapter embargoed

Chapter embargoed

Chapter embargoed

Chapter embargoed

Chapter embargoed

Chapter embargoed

Chapter embargoed

Chapter embargoed

Chapter embargoed

Chapter 5: Investigating the impact of penetration enhancers on percutaneous absorption in frogs

Preamble

The literature review and synthesis provided (Chapter 2) identified three key issues likely to impact on percutaneous absorption in frogs: 1) physicochemical parameters of the applied chemical (particularly logP), 2) skin differences (both between skin regions in individuals and also between species from different habitats), and 3) formulation changes, especially the addition of penetration enhancers. To this end, Chapter 3 systematically investigated the impact of logP and skin region of application on percutaneous absorption in two frog species: *Litoria caerulea* and *Rhinella marina*. As these species are from different primary habitats, Chapter 4 presented a direct comparison of absorption between these species, and then provided a mathematical model of percutaneous absorption for chemicals in these species. Finally, specific recommendations for clinicians when selecting chemicals for transdermal delivery in frogs were provided. However, thus far all absorption kinetics reported have been for chemicals formulated in Amphibian Ringer's solution, a simple aqueous electrolyte solution. It is therefore unknown how formulation with penetration enhancers will impact on the absorption kinetics reported.

This chapter presents the effect of penetration enhancers: 1 / 10 / 30% v/v ethanol and 20% v/v propylene glycol on the in vitro absorption kinetics of three model chemicals – caffeine, benzoic acid, and ibuprofen – through *Rh. marina* skin. These enhancers are commonly included in therapeutic formulations used in frogs, and may also be present in agrichemicals and as environmental contaminants, and so investigations as to their impact on absorption in frog skin are judicious. Further, the concentrations investigated were selected based on their previous use in therapeutic transdermal formulations in frogs, with no ill-effects reported. Additionally, as penetration enhancers may affect the barrier properties of the skin, the effect of exposure to enhancers on skin structure was also were also determined. This included exposing skin samples to the different enhancers, and then using differential scanning calorimetry and histology to investigate changes in the skin following exposure.

A version of this chapter has been published in the Heliyon [(1)] [Permeability of frog skin to chemicals: effect of penetration enhancers. Llewelyn VK, Berger L, Glass BD. Heliyon, 5(8):e02127. 2019. https://doi.org/10.1016/j.heliyon.2019.e02127]. A copy of the final published version of this manuscript is in Appendix 8.

Statement of Contribution

Llewelyn VK, Berger L, Glass BD. (2019). Permeability of frog skin to chemicals: effect of penetration enhancers. *Heliyon,* 5(8): e02127*.* https://doi.org/10.1016/j.heliyon.2019.e02127

Authors' contributions

Llewelyn designed the experiments, developed and validated the methods, collected the data and performed the data analysis. Llewelyn wrote the first draft of the paper, which was critically reviewed and revised by Berger and Glass. Llewelyn handled submission and revision of the manuscript.

Victoria K. Llewelyn

Beverley D. Glass

Lee Berger

Chapter embargoed

Chapter embargoed

Chapter embargoed

Chapter embargoed

Chapter embargoed

Chapter embargoed

Chapter embargoed

Chapter embargoed

Chapter embargoed

Chapter embargoed

Chapter embargoed

Chapter embargoed

Chapter embargoed

Chapter embargoed

Chapter embargoed

Chapter embargoed

Chapter embargoed

Chapter embargoed

Chapter embargoed

Chapter embargoed

Chapter embargoed

Chapter embargoed

Chapter embargoed

Chapter embargoed

Chapter embargoed

Chapter embargoed

Chapter embargoed

Chapter embargoed

Chapter embargoed

Chapter embargoed

Chapter embargoed

Chapter embargoed

Chapter 6: Developing a model of percutaneous absorption in frogs: in vitro in vivo comparison

Preamble

Chapters 3 and 4 presented data from in vitro studies of percutaneous absorption in frogs, finding that absorption was significantly different between species from primary habitat, and also between skin regions within species. However, these differences could largely be explained through consideration of differences in skin anatomy and physiology. While the use of diffusion cell data to predict in vivo absorption in humans is accepted, it is currently unknown how whether such an in vitro-in vivo correlation exists for frogs. Therefore, this chapter presents the in vivo absorption data for the same model chemicals— caffeine, benzoic acid, and ibuprofen — in the cane toad *Rhinella marina.*

Firstly, a model of in vitro absorption in *Rh. marina* was produced from data collected and presented in Section 3.3. The larger size of *Rh. Marina* compared to *Litoria caerulea* allowed collection of absorption data from both ventral pelvic and ventral thoracic skin, and so the individual species model included an additional factor level for skin region (compared to the interspecies model of presented in Chapter 4, which could only discriminate between ventral and dorsal skin regions, with ventral data representing a hybrid of both ventral pelvic and ventral thoracic absorption). Following model creation, the in vitro experiments were replicated in vivo in healthy adult male *Rh. marina.* The resultant absorption kinetics were then compared to the in vitro predictions to determine the model's success in predicting percutaneous absorption in vivo.

This work is prepared for publication in *PLOS ONE*, and is currently under review.

Statement of Contribution

Llewelyn VK, Berger L, Glass BD. (To be submitted). Developing a model of percutaneous absorption in frogs: in vitro in vivo comparison. *For submission to PLOS One.*

Authors' contributions

Llewelyn analysed data previously collected (Chapter 3, [1, 2]) to create a series of models. Llewelyn performed data analysis and model creation. Berger and Llewelyn co-developed the experimental methodology for the in vivo study. Llewelyn ran the experiments and performed sample extraction; extracted samples were analysed by an external contractor. Llewelyn performed the data analysis on in vivo results. Llewelyn wrote the first draft of the paper, which was critically reviewed and revised by Berger and Glass. Llewelyn will handle submission and revision of the manuscript.

Victoria K. Llewelyn

Beverley D. Glass

Lee Berger

Chapter embargoed

Chapter embargoed

Chapter embargoed

Chapter embargoed

Chapter embargoed

Chapter embargoed

Chapter embargoed

Chapter embargoed

Chapter embargoed

Chapter embargoed

Chapter embargoed

Chapter embargoed

Chapter embargoed

Chapter embargoed

Chapter embargoed

Chapter embargoed

Chapter embargoed

Chapter embargoed

Chapter embargoed

Chapter embargoed

Chapter embargoed

Chapter 7: Formulation and testing of a novel treatment for chytridiomycosis in frogs

Preamble

This penultimate chapter provides a synthesis of findings thus presented in this thesis, by using the model developed from in vitro data (Chapter 3) and refined following in vivo studies (Chapter 6) to select a candidate chemical — chloramphenicol — for treatment of infectious disease in frogs. Information collected on the impacts of penetration enhancers on absorption kinetics (Chapter 5) was then used to formulate the chemical in a suitable vehicle for optimal absorption. This novel formulation was then administered to healthy adult *Rhinella marina*, and some preliminary pharmacokinetic parameters of chloramphenicol in vivo ascertained.

This work is prepared for publication in *Diseases of Aquatic Organisms*, but has yet to be submitted.

Statement of Contribution

Llewelyn VK, Berger L, Glass BD. (To be submitted). Can in vitro transdermal absorption data predict in vivo outcomes? The case of chloramphenicol in frogs. *For submission to the Journal of Veterinary Pharmacology and Therapeutics*.

Authors' contributions

Llewelyn designed and ran the experiment, including design of the formulation used and extraction of the samples. Extracted samples were analysed by an external contractor. Llewelyn performed the data analysis and developed the figures and tables. Llewelyn wrote the first draft of the paper, which was critically reviewed and revised by Berger and Glass. Llewelyn will handle submission and revision of the manuscript.

Victoria K. Llewelyn

Beverley D. Glass

Lee Berger

Chapter embargoed

Chapter embargoed

Chapter embargoed

Chapter embargoed

Chapter embargoed

Chapter embargoed

Chapter embargoed

Chapter embargoed

Chapter embargoed

Chapter embargoed

Chapter embargoed

Chapter embargoed

Chapter embargoed

Chapter embargoed

Chapter embargoed

Chapter embargoed

Chapter embargoed

Chapter embargoed

Chapter embargoed

Chapter embargoed

Chapter embargoed

Chapter embargoed

Chapter embargoed

Chapter embargoed

Chapter embargoed

Chapter embargoed

Chapter embargoed

Chapter embargoed

Chapter 8: General discussion and Conclusions

Preamble

This final chapter provides the key findings of both the in vitro and in vivo studies of percutaneous absorption in frogs, and considers the utility of these findings in terms of both the therapeutic management of frogs and also in risk assessment and mitigation in frog habitats. The in vitro studies conducted, which utilised methods previously validated for use in mammals, provide the experimental methodology for researchers to continue to investigate percutaneous absorption in frog species. The models of absorption developed highlight the most important determinants of percutaneous absorption in frog skin, both within a single terrestrial species and between species from different primary habitats. Finally, the in vivo studies provide evidence for the use of these models in predicting in vivo absorption, whether for risk assessment or in designing a treatment for an infectious disease in terrestrial frogs.

Contributions to the existing knowledge of percutaneous absorption in frogs have been made throughout this thesis. Prior to design of the individual experiments, a review of the extant literature on percutaneous absorption in mammals and in frogs was made (Chapter 2), and this information synthesised considering known frog skin anatomy and physiology to identify factors likely to influence percutaneous absorption in frogs. These findings were then used to both inform and refine the experimental designs for the in vitro experiments.

The in vitro investigations determined how regional variation in the skin within a frog species influences absorption (Chapter 3) and provided comparison of absorption kinetics in frog species from terrestrial and arboreal habitats (Chapter 4), allowing development of the first in vitro percutaneous absorption models for frogs (Chapters 4 and 6). Finally, as chemicals are rarely formulated in water alone, the effect on absorption of formulation of chemicals with commonly-used penetration enhancers, and the impact of these enhancers on frog skin itself, was investigated (Chapter 5).

The initial in vivo investigations sought to refine the developed in vitro absorption model, and so the ability of the in vitro model to predict the in vivo situation was determined (Chapter 6). Finally, the refined model (Chapter 6), and data collected and synthesised in Chapters 2, 3, 5 were used to select, formulate and test the in vivo absorption of a chemical for the potential treatment of infectious disease in frogs (Chapter 7).

Chapter embargoed

Chapter embargoed

Chapter embargoed

Chapter embargoed

Chapter embargoed

Chapter embargoed

Chapter embargoed

Chapter embargoed

Chapter embargoed

Chapter embargoed

Chapter embargoed

Chapter embargoed

Chapter embargoed

Chapter embargoed

Chapter embargoed

Chapter embargoed

Chapter embargoed

Chapter embargoed

Chapter embargoed

Chapter embargoed

Chapter embargoed

Chapter embargoed

Chapter embargoed

Bibliography

Abraham MH, Chadha HS, Mitchell RC. The factors that influence skin penetration of solutes. Journal of Pharmacy and Pharmacology. 1995; 47:8–16. https://doi.org/10.1111/j.2042-7158.1995.tb05725.x

Adami C, Spadavecchia C, Angeli G, d'Ovidio D. Alfaxalone anesthesia by immersion in oriental fire-bellied toads (*Bombina orientalis*). Veterinary Anaesthesia and Analgesia. 2015; 42:547-51. http://dx.doi.org/10.1111/vaa.12252

Aguilar NG, Palcios CAM, Ross LG. Controlled anaesthesia of *Rana catesbeiana* (Shaw) and *Rana pipiens* (Schreber 1792) using xylocaine delivered by spray. Aquaculture Research. 1999; 30:309-11. http://dx.doi.org/10.1046/j.1365-2109.1999.00328.x

Akomeah FK, Martin GP, Brown MB. Variability in human skin permeability in vitro: comparing penetrants with different physicochemical properties. Journal of Pharmaceutical Sciences. 2007; 96:824-34. https://doi.org/10.1002/jps.20773

ALOGPS 2.1 [Internet]. Virtual computational chemistry laboratory. 2005. Available from: http://www.vcclab.org

American Veterinary Medical Association. AVMA guidelines for the euthanasia of animals: 2013 edition2013 02-04-2015. Available from: https://www.avma.org/KB/Policies/Documents/euthanasia.pdf

Amey AP, Grigg GG. Lipid-reduced evaporative water loss in two arboreal hylid frogs. Comparative Biochemistry and Physiology Part A: Physiology. 1995; 111:283–91. https://doi.org/10.1016/0300-9629(94)00213-d

Andrews JM. Determination of minimum inhibitory concentrations. Journal of Antimicrobial Chemotherapy. 2001; 48:5-16. https://doi.org/10.1093/jac/dkf083

Ardente AJ, Barlow BM, Burns P, Goldman R, Baynes RE. Vehicle effects on in vitro transdermal absorption of sevoflurane in the bullfrog, *Rana catesbeiana*. Environmental Toxicology and Pharmacology. 2008; 25:373–9. http://dx.doi.org/10.1016/j.etap.2007.12.001

Arellano ML, Velasco MA, Aguirre TM, Zarini O, Belasen AM, James TY, et al. Treatment of adult Valcheta frogs *Pleurodema somuncurense* for chytrid fungus. Conservation Evidence. 2018; 15:37.

Babita K, Kiumar V, Rana V, Jain S, Tiwary AK. Thermotropic and spectroscopic behaviour of the skin: Relationship with percutaneous permeation enhancement. Current Drug Delivery. 2006; 3:95-113. https://doi.org/10.2174/156720106775197466

Baert B, Deconinck E, Van Gele M, Slodicka M, Stoppie P, Bode S, et al. Transdermal penetration behaviour of drugs: CART-clustering, QSPR and selection of model compounds. Bioorganic and Medicinal Chemistry. 2007; 15:6943–55. https://doi.org/10.1016/j.bmc.2007.07.050

Baggot JD, Giguère S. Principles of antimicrobial drug bioavailability and disposition. In: Giguère S, Prescott JF, Dowling PM, editors. Antimicrobial Therapy in Veterinary Medicine. Ames, Iowa: John Wiley & Sons; 2013. p. 41-77.

Baldwin RA. The water balance response of the pelvic “patch” of *Bufo punctatus* and *Bufo boreas*. Comparative Biochemistry and Physiology Part A: Physiology. 1974; 47:1285-95. http://dx.doi.org/10.1016/0300-9629(74)90103-0

Balko JA, Watson MK, Papich MG, Posner LP, Chinnadurai SK. Plasma concentrations of ketoprofen and meloxicam after subcutaneous and topical administration in the Smoky Jungle Frog (*Leptodactylus pentadactylus*). The Journal of Herpetological Medicine and Surgery. 2018; 28:89–92. https://doi.org/10.5818/17-10-129.1

Bani G. Osservazioni sulla ultrastruttura della cute di *Bufo bufo (L.)* e modificazioni a livelli dell'epidermide, in relazione a differenti condizioni ambientali. Monitore Zoologico Italiano Supplemento. 1966; 74:93–124.

Barratt MD. Quantitative structure-activity relationships for skin permeability. Toxicology In Vitro. 1995; 9:27–37. https://doi.org/10.1016/0887-2333(94)00190-6

Baustian M. The contribution of lymphatic pathways during recovery from hemorrhage in the toad *Bufo marinus*. Physiological Zoology. 1988; 61:555-63. https://doi.org/10.1086/physzool.61.6.30156164

Belden J, McMurray S, Smith L, Reilley P. Acute toxicity of fungicide formulations to amphibians at environmentally relevant concentrations. Environmental Toxicology and Chemistry. 2010; 29:2477-80. https://doi.org/10.1002/etc.297

Benech-Kieffer F, Meuling WJA, Leclerc C, Roza L, Leclaire J, Nohynek G. Percutaneous absorption of Mexoryl SX® in human volunteers: comparison with in vitro data. Skin Pharmacology and Applied Skin Physiology. 2003; 16:343-55. https://doi.org/10.1159/000072929

Bentley PJ, Main AR. Zonal differences in permeability of the skin of some anuran Amphibia. The American Journal of Physiology. 1972; 223:361–3. https://doi.org/10.1152/ajplegacy.1972.223.2.361

Bentley PJ, Yorio T. The passive permeability of the skin of anuran amphibia: a comparison of frogs (*Rana pipiens*) and toads (*Bufo marinus*). The Journal of Physiology. 1976; 261:603–15. https://doi.org/10.1113/jphysiol.1976.sp011576

Bentley PJ. Adaptations of amphibia to arid environments. Science. 1966; 152:619-23. https://doi.org/10.1126/science.152.3722.619

Berger L, Speare R, Marantelli G, Skerratt LF. A zoospore inhibition technique to evaluate the activity of antifungal compounds against *Batrachochytrium dendrobatidis* and unsuccessful treatment of experimentally infected green tree frogs (*Litoria caerulea*) by fluconazole and benzalkonium chloride. Research in Veterinary Science. 2009; 87:106-10. http://dx.doi.org/10.1016/j.rvsc.2008.11.005

Berger L, Speare R, Pessier A, Voyles J, Skerratt LF. Treatment of chytridiomycosis requires urgent clinical trials. Diseases of Aquatic Organisms. 2010; 92:165–74. http://dx.doi.org/10.3354/dao02238

Berger L, Speare R, Skerratt LF. Distribution of *Batrachochytrium dendrobatidis* and pathology in the skin of green tree frogs *Litoria caerulea* with severe chytridiomycosis. Diseases of Aquatic Organisms. 2005; 68:65-70. http://dx.doi.org/10.3354/dao068065

Bernal MH, Solomon KR, Carrasquilla G. Toxicity of formulated glyphosate (Glyphos) and Cosmo-Flux to larval and juvenile Colombian frogs 2. Field and laboratory microcosm acute toxicity. Journal of Toxicology and Environmental Health. 2009; 72:966-73. https://doi.org/10.1080/15287390902929717

Bishop PJ, Speare R, Poulter R, Butler M, Speare BJ, Hyatt A, et al. Elimination of the amphibian chytrid fungus *Batrachochytrium dendrobatidis* by Archey's frog *Leiopelma archeyi*. Diseases of Aquatic Organisms. 2009; 84:9-15. http://dx.doi.org/10.3354/dao02028

Blaylock LA, Ruibal R, Platt-Aloia K. Skin structure and wiping behavior of Phyllomedusine frogs. Copeia. 1976; 1976:283-95. https://doi.org/10.2307/1443948

Bonate PL. Pharmacokinetic-pharmacodynamic modeling and simulation. 2 ed. New York: Springer; 2011.

Bos JD. The 500 Dalton rule for the skin penetration of chemical compounds and drugs. Experimental Dermatology. 2000; 9:165-9. http://dx.doi.org/10.1034/j.1600-0625.2000.009003165.x

Bowerman J, Rombough C, Weinstock SR. Terbinafine hydrochloride in ethanol effectively clears *Batrachochytrium dendrobatidis* in amphibians. Journal of Herpetological Medicine and Sugery. 2010; 20:24-8. http://dx.doi.org/10.5818/1529-9651-20.1.24

Brannelly LA, Martin G, Llewelyn J, Skerratt LF, Berger L. Age- and size-dependent resistance to chytridiomycosis in the invasive cane toad *Rhinella marina*. Diseases of Aquatic Organisms. 2018; 131:107-20. https://doi.org/10.3354/dao03278

Brannelly LA, Richards-Zawacki CL, Pessier AP. Clinical trials with itraconazole as a treatment for chytrid fungal infections in amphibians. Diseases of Aquatic Organisms. 2012; 101:95–104. http://dx.doi.org/10.3354/dao02521

Brannelly LA, Skerratt LF, Berger L. Treatment trial of clinically ill corroboree frogs with chytridiomycosis with two triazole antifungals and electrolyte therapy. Veterinary Research Communications. 2015; 39:179–87. https://doi.org/10.1007/s11259-015-9642-5

Brinkmann I, Müller-Goymann CC. An attempt to clarify the influence of glycerol, propylene glycol, isopropyl myristate and a combination of propylene glycol and isopropyl myristate on human stratum corneum. Pharmazie. 2005; 60:215-20.

Bronaugh RL, Stewart RF. Methods for in vitro percutaneous absorption studies V: Permeation through damaged skin. Journal of Pharmaceutical Sciences. 1985; 74:1062-6. http://dx.doi.org/10.1002/jps.2600741008

Brown C. Restraint and oral administration in frogs. Lab Animal. 2010; 39:267–8. https://doi.org/10.1038/laban0910-267

Brown D, Grosso A, de Sousa RC. The amphibian epidermis: Distribution of mitochondria-rich cells and the effect of oxytocin. Journal of Cell Science. 1981; 52:197-213.

Brown MB, Lau C-H, Lim ST, Davey N, Moss GP, Yoo S-H, et al. An evaluation of the potential of linear and nonlinear skin permeation models for the prediction of experimentally measured percutaneous drug absorption. Journal of Pharmacy and Pharmacology. 2012; 64:566–77. https://doi.org/10.1111/j.2042-7158.2011.01436.x

Brühl CA, Pieper S, Weber B. Amphibians at risk? Susceptibility of terrestrial amphibian life stages to pesticides. Environmental Toxicology and Chemistry. 2011; 30:2465-72. https://doi.org/10.1002/etc.650

Brühl CA, Schmidt T, Pieper S, Alscher A. Terrestrial pesticide exposure of amphibians: An underestimated cause of global decline? Scientific Reports. 2013; 3:1135. http://dx.doi.org/10.1038/srep01135

Buttemer WA, Thomas C. Influence of temperature on evaporative water loss and cutaneous resistance to water vapour diffusion in the orange-thighed frog (*Litoria xanthomera*). Australian Journal of Zoology. 2003; 51:111-8. https://doi.org/10.1071/zo02057

Cakir Y, Strauch SM. Tricaine (MS-222) is a safe anesthetic compound compared to benzocaine and pentobarbital to induce anesthesia in leopard frogs (*Rana pipiens*). Pharmacological Reports. 2005; 57:467-74.

Capello C, Fischer U, Hungerbühler K. What is a green solvent? A comprehensive framework for the environmental assessment of solvents. Green Chemistry. 2007; 9:927-34. https://doi.org/10.1039/B617536H

Carey C, Bryant CJ. Possible interrelations among environmental toxicants, amphibian development, and decline of amphibian populations. Environmental Health Perspectives. 1995; 103:13-7. http://dx.doi.org/10.2307/3432406

Carver S, Bell BD, Waldman B. Does chytridiomycosis disrupt amphibian skin function? Copeia. 2010; 2010:487-95. http://dx.doi.org/10.1643/ch-09-128

Cecala KK, Price SJ, Dorcas ME. A comparison of the effectiveness of recommended doses of MS-222 (tricaine methanesulfonate) and Orajel® (benzocaine) for amphibian anaesthesia. Herpetological Review. 2007; 38:63-6.

Ceschel GC, Maffei P, Lombardi Borgia S. Correlation between the transdermal permeation of ketoprofen and its solubility in mixtures of a pH 6.5 phosphate buffer and various solvents. Drug Delivery. 2002; 9:39-45. https://doi.org/10.1080/107175402753413163

Chen L, Guo-ping L, Lu-jia H. Prediction of human skin permeability using artificial neural network (ANN) modeling. Acta Pharmacologica Sinica. 2007; 28:591–600. https://doi.org/10.1111/j.1745-7254.2007.00528.x

Christensen CU. Adaptations in the water economy of some anuran amphibia. Comparative Biochemistry and Physiology. 1974; 47A:1035–49. http://dx.doi.org/10.1016/0300-9629(74)90477-0

Christian K, Parry D, Green B. Water loss and an extraepidermal lipid barrier in the Australian treefrog *Litoria caerulea*. Annual Meeting of the American Society of Zoologists, American Microscopical Society, Animal Behaviour Society, The Crustacean Society, International Association of Astacology, Society of Systematic Zoology and the Western Society of Naturalists; San Francisco: American Zoologist; 1988. p. 17A.

Christian K, Parry D. Reduced rates of water loss and chemical properties of skin secretions of the frogs *Litoria caerulea* and *Cyclorana australis*. Australian Journal of Zoology. 1997; 45:13-20. https://doi.org/10.1071/zo96046

Civan MM, Peterson-Yantorno K. Intracellular pH regulation in frog skin: a ^{31}P-nuclear magnetic resonance study. American Journal of Physiology. 1986; 251:F831-F8. https://doi.org/10.1152/ajprenal.1986.251.5.f831

Clarke BT. The natural history of amphibian skin secretions, their normal functioning and potential medical applications. Biological Reviews. 1997; 72:365-79. http://dx.doi.org/10.1017/s0006323197005045

Clendenning WE, Stoughton RB. Importance of the aqueous/lipid partition coefficient for percutaneous absorption of weak electrolytes. Journal of Investigative Dermatology. 1962; 39:47-9. http://dx.doi.org/10.1038/jid.1962.7

Collins JP. Amphibian decline and extinction: What we know and what we need to learn. Diseases of Aquatic Organisms. 2010; 92:93–9. http://dx.doi.org/10.3354/dao02307

Court MH. Feline drug metabolism and disposition: pharmacokinetic evidence for species differences and molecular mechanisms. Veterinary Clinics of North America: Small Animal Practice. 2013; 43:1039-54. https://doi.org/10.1016/j.cvsm.2013.05.002

Cronin MTD, Dearden JC, Moss GP, Murray-Dickson G. Investigation of the mechanism of flux across human skin in vitro by quantitative structure–permeability relationships. European Journal of Pharmaceutical Sciences. 1999; 7:325-30. https://doi.org/10.1016/s0928-0987(98)00041-4

Cross SE, Magnusson BM, Winckle G, Anissimov YG, Roberts MS. Determination of the effect of lipophilicity on the in vitro permeability and tissue reservoir characteristics of topically applied solutes in human skin layers. Journal of Investigative Dermatology 2003; 120:759-64. https://doi.org/10.1046/j.1523-1747.2003.12131.x

Cunningham AA, Langton TES, Bennett PM, Lewin JF, Drury SEN, Gough RE, et al. Pathological and microbiological findings from incidents of unusual mortality of the common frog (*Rana temporaria*). Philosophical Transactions: Biological Sciences. 1996; 351:1539-57. https://doi.org/10.1098/rstb.1996.0140

D'Agostino JJ, West G, Boothe DM, Jayanna PK, Snider T, Hoover JP. Plasma pharmacokinetics of selamectin after a single topical administration in the American bullfrog (*Rana catesbeiana*). Journal of Zoo and Wildlife Medicine. 2007; 38:51-4. http://dx.doi.org/10.1638/06-054.1

Dal Pozzo A, Pastori N. Percutaneous absorption of parabens from cosmetic formulations. International Journal of Cosmetic Science. 1996; 18:54-66.

Davis LE, Neff CA, Baggot JD, Powers TE. Pharmacokinetics of chloramphenicol in domesticated animals. American Journal of Veterinary Research. 1972; 33:2259-66.

de Brito-Gitirana L, Azevedo RA. Morphology of *Bufo ictericus* integument (Amphibia, Bufonidae). Micron. 2005; 36:532-8. https://doi.org/10.1016/j.micron.2005.03.013

Değim IT, Hadgraft J, İlbasmiş S, Özkan Y. Prediction of skin penetration using artificial neural network (ANN) modelling. Journal of Pharmaceutical Sciences. 2003; 92:656-64. https://doi.org/10.1002/jps.10312

Değim IT, Pugh WJ, Hadgraft J. Skin permeability data: anomalous results. International Journal of Pharmaceutics. 1998; 170:129-33. https://doi.org/10.1016/s0378-5173(98)00113-6

Denda M, Sato J, Masuda Y, Tsuchiya T, Koyama J, Kuramoto M, et al. Exposure to a dry environment enhances epidermal permeability barrier function. The Journal of Investigative Dermatology. 1998; 111:858-63. http://dx.doi.org/10.1046/j.1523-1747.1998.00333.x

Denney W, Duvvuri S, Buckeridge C. Simple, automatic noncompartmental analysis: The PKNCA R package. Journal of Pharmacokinetics and Pharmacodynamics. 2015; 42:11. http://dx.doi.org/10.1007/s10928-015-9432-2 Available from: https://github.com/billdenney/pknca

Densmore CL, Green DE. Diseases of amphibians. ILAR Journal. 2007; 48:235-54. https://doi.org/10.1093/ilar.48.3.235

Dinehart SK, Smith LM, McMurray ST, Anderson TA, Smith PN, Haukos DA. Toxicity of a glufosinate- and several glyphosate-based herbicides to juvenille amphibians from the Southern High Plains, USA. Science of the Total Environment. 2009; 407:1065-71. https://doi.org/10.1016/j.scitotenv.2008.10.010

Doss GA, Nevarez JG, da Cunha F. Evaluation of metomidate hydrochloride as an anesthetic in leopard frogs (*Rana pipiens*). Journal of Zoo and Wildlife Medicine. 2014; 45:53-9. http://dx.doi.org/10.1638/2013-0056r1.1

d'Ovidio D, Spadavecchia C, Angeli G, Adami C. Etomidate anaesthesia by immersion in oriental fire-bellied toads (*Bombina orientalis*). Laboratory Animals. 2015; 49:319-26. http://dx.doi.org/10.1177/0023677215571655

Downes H. Relative metabolic rate as a basis for extrapolation of drug-elimination times from mammals to frogs. Journal of Herpetological Medicine and Surgery. 2002; 12:4-11. https://doi.org/10.5818/1529-9651.12.4.4

Dragicevic N, Atkinson JP, Maibach HI. Chemical penetration enhancers: Classification and mode of action. In: Dragicevic N, Maibach HI, editors. Percutaneous penetration enhancers chemical methods in penetration enhancement: Modification of the stratum corneum. Berlin: Springer; 2015. p. 11-28.

Easteal S. The history of introductions of *Bufo marina* (Amphibia: Anura); a natural experiment in evolution. Biological Journal of the Linnean Society. 1981; 16:93-113. https://doi.org/10.1111/j.1095-8312.1981.tb01645.x

EFSA PPR Panel (EFSA Panel on Plant Protection Products and their Residues), Ockleford C, Adriaanse P, Berny P, Brock T, Duquesne S, et al. Scientific opinion on the state of the science on pesticide risk assessment for amphibians and reptiles. EFSA Journal. 2018; 16:5125. https://doi.org/10.2903/j.efsa.2018.5125

Egea-Serrano A, Relyea RA, Tejedo M, Torralva M. Understanding of the impact of chemicals on amphibians: a meta-analytic review. Ecology and Evolution. 2012; 2:1382-97. https://doi.org/10.1002/ece3.249

El Tayar N, Tsai R-S, Testa B, Carrupt P-A, Hansch C, Leo A. Percutaneous penetration of drugs: a quantitative structure-permeability relationship study. Journal of Pharmaceutical Sciences. 1991; 80:744-9. https://doi.org/10.1002/jps.2600800807

Elias PM. Epidermal lipids, barrier function, and desquamation. Journal of Investigative Dermatology. 1983; 80:44s-9s. http://dx.doi.org/10.1111/1523-1747.ep12537108

Elkan E. Ground substance: An anuran defense against desiccation. In: Lofts B, editor. Physiology of the amphibia. 3. New York: Academic press, Inc; 1976. p. 101-10.

El-Mofty MM. Induction of leukaemia in chloramphenicol-treated toads. Eastern Mediterranean Health Journal [Internet]. 2000; 6:1026-34. Available from: https://apps.who.int/iris/bitstream/handle/10665/118961/EMHJ_2000_6_5-6_1026_1034.pdf?sequence=1&isAllowed=y

Ertl RP, Winston GW. The microsomal mixed function oxidase system of amphibians and reptiles: components, activities and induction. Comparative Biochemistry and Physiology - C Toxicology and Pharmacology. 1998; 121:85-105. https://doi.org/10.1016/s0742-8413(98)10032-4

European Medicines Agency Committee for Human Medicinal Products. Propylene glycol used as an excipient. 2017 9 October 2017. Contract No.: EMA/CHMP/334655/2013.

European Medicines Agency Committee for Human Medicinal Products. Draft guideline on quality and equivalence of topical products. 2018. Contract No.: CHMP/QWP/708282/2018.

Felsemburgh FA, de Almeida PG, de Carvalho-e-Silva SP, de Brito-Gitirana L. Microscopical methods promote the understanding of the integument biology of *Rhinella ornata*. Micron. 2009; 40:198-205. https://doi.org/10.1016/j.micron.2008.09.003

Finizio A, Vighi M, Sandroni D. Determination of n-octanol/water partition coefficient (Kow) of pesticide critical review and comparison of methods. Chemosphere. 1997; 34:131-61. https://doi.org/10.1016/s0045-6535(96)00355-4

Flynn GL, Stewart B. Percutaneous drug penetration: Choosing candidates for transdermal development. Drug Development Research. 1988; 13:169-85. http://dx.doi.org/10.1002/ddr.430130209

Flynn GL. Physicochemical determinants of skin absorption. In: Gerrity TR, Henry CJ, editors. Principles of Route-to-Route Extrapolation for Risk Assessment. New York: Elsevier; 1990. p. 93-127.

Fox H. The structure of the integument. In: Heatwole H, Barthalmus GT, editors. Amphibian biology. 1. Chipping Norton: Surrey Beatty & Sons; 1994. p. 1-32.

Francoeur ML, Golden GM, Potts RO. Oleic acid: Its effects on stratum corneum in relation to (trans)dermal drug delivery. Pharmaceutical Research. 1990; 7:621-7.

Franz TJ. Percutaneous absorption. On the relevance of in vitro data. Journal of Investigative Dermatology. 1975; 64:190-5. https://doi.org/10.1111/1523-1747.ep12533356

Fryday S, Thompson H. Toxicity of pesticides to aquatic and terrestrial life stages of amphibians and occurrence, habitat use and exposure of amphibian species in agricultural environments. EFSA Supporting Publications. 2012; 9:343. https://doi.org/10.2903/sp.efsa.2012.EN-343

Garner TWJ, Garcia G, Carroll B, Fisher MC. Using itraconazole to clear *Batrachochytrium dendrobatidis* infection, and subsequent depigmentation of *Alytes muletensis* tadpoles. Diseases of Aquatic Organisms. 2009; 83:257-60. http://dx.doi.org/10.3354/dao02008

Gentz EJ. Medicine and surgery of amphibians. ILAR Journal. 2007; 48:255-9. http://dx.doi.org/10.1093/ilar.48.3.255

Gleason FH, Marano AV. The effects of antifungal substances on some zoosporic fungi (Kingdom Fungi). Hydrobiologia. 2011; 659:81-92. https://doi.org/10.1007/s10750-010-0117-y

Godin B, Touitou E. Transdermal skin delivery: Predictions for humans from *in vivo*, *ex vivo* and animal models. Advanced Drug Delivery Reviews. 2007; 59:1152-61. https://doi.org/10.1016/j.addr.2007.07.004

Goniakowska-Witalińska L, Kubiczek U. The structure of the skin of the tree frog (*Hyla arborea arborea* L.). Annals of Anatomy. 1998; 180:237-46. https://doi.org/10.1016/s0940-9602(98)80080-0

Goulet F, Hélie P, Vachon P. Eugenol anesthesia in African clawed frogs (*Xenopus laevis*) of different body weights. Journal of the American Association for Laboratory Animal Science. 2010; 49:460-3.

Goulet F, Vachon P, Hélie P. Evaluation of the toxicity of eugenol at anaesthetic doses in African Clawed Frogs (*Xenopus laevis*). Toxicologic Pathology. 2011; 39:471-7. https://doi.org/10.1177/0192623311399785

Graczyk TK, Canfield MR, Bicknese EJ, Wisnieski AP. Progressive ulcerative dermatitis in a captive wold-caught South American giant tree frog (*Phyllomedusa bicolor*) with microsporidial septicemia. Journal of Zoo and Wildlife Medicine. 1996; 27:522-7. Available from: https://www.jstor.org/stable/20095617

Grasso P, Lansdown ABG. Methods of measuring, and factors affecting, percutaneous absorption. Journal of the Society of Cosmetic Chemists. 1972; 23:481-521.

Greenwald L, Munford J. Insulin transport across intact frog skin. General and Comparative Endocrinology. 1976; 29:426-9. http://dx.doi.org/10.1016/0016-6480(76)90058-7

Greiner-Sosanko E, Lower DR, Virji MA, Krasowski MD. Simultaneous determination of lamotrigine, zonisamide, and carbamazepine in human plasma by high-performance liquid chromatography. Biomedical Chromatography. 2007; 21:225-8. https://doi.org/10.1002/bmc.753

Greven H, Zanger K, Schwinger G. Mechanical properties of the skin of *Xenopus laevis*. Journal of Morphology. 1995; 244:15-22. http://dx.doi.org/10.1002/jmor.1052240103

Groff JM, Mughannam A, McDowell TS, Wong A, Dykstra MJ, Frye FL, et al. An epizootic of cutaneous zygomycosis in cultured dwarf African clawed frogs (*Hymenochirus curtipes*) due to *Basidiobolus ranarum*. Journal of Medical and Veterinary Mycology. 1991; 29:215-23. http://dx.doi.org/10.1080/02681219180000331

Guénette SA, Beaudry F, Vachon P. Anaesthetic properties of propofol in African Clawed Frogs (*Xenopus laevis*). Journal of the American Association for Laboratory Animal Science. 2008; 47:35-8.

Guénette SA, Hélie P, Beaudry F, Vachon P. Eugenol for anaesthesia of African clawed frogs (*Xenopus laevis*). Veterinary Anaesthesia and Analgesia. 2007; 34:164-70. http://dx.doi.org/10.1111/j.1467-2995.2006.00316.x

Guénette SA, Lair S. Anaesthesia of the Leopard frog, *Rana pipiens*: A comparative study between four different agents. Journal of Herpetological Medicine and Surgery. 2006; 16:38-44. https://doi.org/10.5818/1529-9651.16.3.38

Hadgraft J, Valenta C. pH, pKa and dermal delivery. International Journal of Pharmaceutics. 2000; 200:243-7. http://dx.doi.org/10.1016/s0378-5173(00)00402-6

Hafeez F, Maibach HI. Occlusion effect on in vivo percutaneous penetration of chemicals in man and monkey: partition coefficient effects. Skin Pharmacology and Physiology. 2013; 26:85-91. http://dx.doi.org/10.1159/000346273

Haslam IS, Roubos EW, Mangoni ML, Yoshizato K, Vaudry H, Kloepper JE, et al. From frog integument to human skin: dermatological perspectives from frog skin biology. Biological Reviews. 2013. https://doi.org/10.1111/brv.12072

Hayes TB, Falso S, Stice GM. The cause of global amphibian declines: a developmental endocrinologist's perspective. Journal of Experimental Biology. 2010; 213:921-33. https://doi.org/10.1242/jeb.040865

Helmer P, Whiteside D. Amphibian anatomy and physiology. In: O'Malley B, editor. Clinical Anatomy and Physiology of Exotic Species. Edinburgh: Elsevier Saunders; 2005. p. 3-14.

Hernández SE, Sernia C, Bradley AJ. The effect of three anaesthetic protocols on the stress response in cane toads (*Rhinella marina*). Veterinary Anaesthesia and Analgesia. 2012; 39:584-90. http://dx.doi.org/10.1111/j.1467-2995.2012.00753.x

Hill WA, Newman SJ, Craig L, Carter C, Czarra J, Brown JP. Diagnosis of *Aeromonas hydrophila*, Mycobacterium species, and *Batrachochytrium dendrobatidis* in an African Clawed Frog (*Xenopus laevis*). Journal of the American Association for Laboratory Animal Science. 2010; 49:215-20.

Holden WM, Ebert AR, Canning PF, Rollins-Smith LA. Evaluation of amphotericin b and chloramphenicol as alternative drugs for treatment of chytridiomycosis and their impacts on innate skin defenses. Applied and Environmental Microbiology. 2014; 80:4034-41. https://doi.org/10.1128/aem.04171-13

Hothorn T, Bretz F, Westfall P. Simultaneous inference in general parametric models. Biometrical Journal. 2008; 50:346-63. https://doi.org/10.1002/bimj.200810425

Howe CM, Berrill M, Pauli BD, Helbing CC, Werry K, Veldhoen N. Toxicity of glyphosate-based pesticides to four North American frog species. Environmental Toxicology and Chemistry. 2004; 23:1928-38. https://doi.org/10.1897/03-71

Hunter RP, Isaza R. Concepts and issues with interspecies scaling in zoological pharmacology. Journal of Zoo and Wildlife Medicine. 2008; 39:517-26. http://dx.doi.org/10.1638/2008-0041.1

Hunter RP. Interspecies allometric scaling. Hanbook of Experimental Pharmacology. 2010; 199:139-57. https://doi.org/10.1007/978-3-642-10324-7_6

Iglauer F, Willmann F, Hilken G, Huisinga E, Dimigen J. Antithelmintic treatment to eradicate cutaneous capillariasis in a colony of South African Clawed Frogs (*Xenopus laevis*). Laboratory Animal Science. 1997; 47:477-82.

International Conference on Harmonization (ICH). Guidance for industry: Q2B: Validation of analytical procedures: methodology. Geneva: ICH; 1996.

IUCN Red List of Threatened Species [Internet]. 2014 [cited 29 January 2014]. Available from: https://www.iucnredlist.org

IUCN Red List of Threatened Species [Internet]. 2019 [cited 18 June 2019]. Available from: https://www.iucnredlist.org

IUCN SSC Amphibian Specialist Group. Amphibian conservation action plan. 2015. Available from: https://www.iucn-amphibians.org/resources/acap/

IUCN SSC Amphibian Specialist Group. Guidelines on the use of ex situ management for species conservation. 2014. Available from: www.iucn.org/about/work/programmes/species/publications/iucn_guidelines_and__policy__statements/

Jacobi U, Kaiser M, Richter H, Audring H, Sterry W, Lademann J. The number of stratum corneum cell layers correlates with the pseudo-absorption of the corneocytes. Skin Pharmacology and Physiology. 2005; 18:175-9. http://dx.doi.org/10.1159/000085862

Jakasa I, Kezic S. Evaluation of *in-vivo* animal and *in-vitro* models for prediction of dermal absorption in man. Human and Experimental Toxicology. 2008; 27:281-8. https://doi.org/10.1177/0960327107085826

Jones MEB, Paddock D, Bender L, Allen JL, Schrenzel MD, Pessier AP. Treatment of chytridiomycosis with reduced-dose itraconazole. Diseases of Aquatic Organisms. 2012; 99:243-9. http://dx.doi.org/10.3354/dao02475

Judd FW. Toxicity of monosodium methanearsonate herbicide to Couch's Spadefoot Toad, *Scaphiopus couchi*. Herpetologica. 1977; 33:44-6.

Kasim NA, Whitehouse M, Ramachandran C, Bermejo M, Lennernäs H, Hussain AS, et al. Molecular properties of WHO essential drugs and provisional biopharmaceutical classification. Molecular Pharmaceutics. 2004; 1:85-96. https://doi.org/10.1021/mp034006h

Katz U, Nagel W. Biophysics of ion transport across amphibian skin. In: Heatwole H, Barthalmus GT, editors. Amphibian Biology. 1. Chipping Norton: Surrey Beatty & Sons; 1994. p. 98-119.

Kaufmann K, Dohmen P. Adaption of a dermal in vitro method to investigate the uptake of chemicals across amphibian skin. Environmental Sciences Europe. 2016; 28:10. https://doi.org/10.1186/s12302-016-0080-y

Kearns GL, Wilson JT. Determination of ibuprofen in serum by high-performance liquid chromatography and application to ibuprofen disposition. Journal of Chromatography. 1981; 226:183-90. https://doi.org/10.1016/s0378-4347(00)84219-x

Kerby JL, Richards-Hrdlicka KL, Storfer A, Skelly DK. An examination of amphibian sensitivity to environmental contaminants: are amphibians poor canaries? Ecology Letters. 2010; 13:60-7. https://doi.org/10.1111/j.1461-0248.2009.01399.x

Kielhorn J, Melching-Kollmuss S, Mangelsdorf I. Dermal absorption. Environmental Health Criteria 235. Geneva: WHO; 2006. Available: https://www.who.int/ipcs/publications/ehc/ehc235.pdf?ua=1

Kladt C, Dennerlein K, Göen T, Drexler H, Korinth G. Evaluation on the reliability of the permeability coefficient (Kp) to assess the percutaneous penetration property of chemicals on the basis of Flynn's dataset. International Archives of Occupational and Environmental Health. 2018; 91:467-77. https://doi.org/10.1007/s00420-018-1296-5

Korinth G, Schaller KH, Drexler H. Is the permeability coefficient *K*p a reliable tool in percutaneous absorption studies? Archives of Toxicology. 2005; 79:155-9. https://doi.org/10.1007/s00204-004-0618-4

Kouchak M, Handali S. Effects of various penetration enhancers on penetration of aminophylline through shed snake skin. Jundishapur Journal of Natural Pharmaceutical Products. 2014; 9:24-9. https://doi.org/10.17795/jjnpp-12904

Krause K, Reaville D, Weldy S, editors. Fatal ivermectin toxicity in a collection of frogs. Annual conference of the Association of Reptilian and Amphibian Veterinarians; 2012; Oakland, California.

Lalonde-Robert V, Beaudry F, Vachon P. Pharmacologic parameters of MS222 and physiologic changes in frogs (*Xenopus laevis*) after immersion at anesthetic doses. Journal of the American Association for Laboratory Animal Science. 2012; 51:464-8.

Lam LT, Sun Y, Davey N, Adams R, Prapopoulou M, Brown MB, et al. The application of feature selection to the development of Gaussian process models for percutaneous absorption. Journal of Pharmacy and Pharmacology. 2010; 62:738-49. https://doi.org/10.1211/jpp.62.06.0010

Lampe MA, Burlingame AL, Whitney J, Williams ML, Brown BE, Roitman E, et al. Human stratum corneum lipids: characterization and regional variations. Journal of Lipid Research. 1983; 24:120-30.

Lane ME. Skin penetration enhancers. International Journal of Pharmaceutics. 2013; 447:12-21. https://doi.org/10.1016/j.ijpharm.2013.02.040

Lehman PA, Raney SG, Franz TJ. Percutaneous absorption in man: In vitro-in vivo correlation. Skin Pharmacology and Physiology. 2011; 24:224-30. https://doi.org/10.1159/000324884

Letcher J, Glade M. Efficacy of ivermectin as an anthelmintic in leopard frogs. Journal of the American Veterinary Medical Association. 1992; 200:537-8.

Letcher J. Intracelomic use of tricaine methanesulfonate for anaesthesia of bullfrogs (*Rana catesbeiana*) and leopard frogs (*Rana pipiens*). Zoo Biology. 1992; 11:243-51. https://doi.org/10.1002/zoo.1430110404

Lien EJ, Tong GL. Physicochemical properties and percutaneous absorption of drugs. Journal of the Society of Cosmetic Chemists. 1973; 24:371-84.

Lillywhite HB, Licht P. Movement of water over toad skin: Functional role of epidermal sculpturing. Copeia. 1974; 1974:165-71. http://dx.doi.org/10.2307/1443019

Lin SY, Hou SJ, Hsu THS, Yeh FL. Comparisons of different animal skins with human skin in drug percutaneous penetration studies. Methods and Findings in Experimental and Clinical Pharmacology. 1992; 14:645-54.

Liu L, Lan R, Liu L, Wang Y, Zhang Y, Wang Y, et al. Antimicrobial resistance and cytotoxicity of *Citrobacter* spp. in Maanshan Anhui Province, China. Frontiers in Microbiology. 2017; 8. http://dx.doi.org/10.3389/fmicb.2017.01357

Llewelyn VK, Berger L, Glass BD. Effects of skin region and relative lipophilicity on percutaneous absorption in the toad *Rhinella marina*. Environmental Toxicology and Chemistry. 2019; 38:361-7. http://dx.doi.org/10.1002/etc.4302

Llewelyn VK, Berger L, Glass BD. Percutaneous absorption in frog species: variability in skin may influence delivery of therapeutics. Journal of Veterinary Pharmacology and Therapeutics. 2018; 41:70. https://doi.org/10.1111/jvp.12639

Llewelyn VK, Berger L, Glass BD. Percutaneous absorption of chemicals: developing an understanding for the treatment of disease in frogs. Journal of Veterinary Pharmacology and Therapeutics. 2016; 39:109-21. http://dx.doi.org/10.1111/jvp.12264

Llewelyn VK, Berger L, Glass BD. Permeability of frog skin to chemicals: effect of penetration enhancers. Heliyon. 2019; 5(8):e02127. https://doi.org/10.1016/j.heliyon.2019.e02127.

Llewelyn VK, Berger L, Glass BD. Regional variation in percutaneous absorption in the tree frog *Litoria caerulea*. Environmental Toxicology and Pharmacology. 2018; 60:5-11. https://doi.org/10.1016/j.etap.2018.03.019

Longphre M, Gatten Jr R. Individual variability in sustained performance, aerobic metabolism, oxygen transport, and enzyme activity in toads (*Bufo marinus*). Copeia. 1994; 4:887-96.

Magnusson BM, Pugh WJ, Roberts MS. Simple rules for defining the potential of compounds for trandermal delivery or toxicity. Pharmaceutical Research. 2004; 21:1047-54. http://dx.doi.org/10.1023/b:pham.0000029295.38564.e1

Mangione S, Garcia G, Cardozo O. The Eberth-Katschenko layer in three species of ceratophryines anurans (Anura: Caratophrydae). Acta Zool-Stockholm. 2011; 92:21-6.

Mann R, Hyne R, Choung C, Wilson S. Amphibians and agricultural chemicals: review of the risks in a complex environment. Environmental Pollution. 2009; 157:2903-27. http://dx.doi.org/10.1016/j.envpol.2009.05.015

Martel A, Van Rooij P, Vercauteren G, Baert K, Van Waeyenberghe L, Debacker P, et al. Developing a safe antifungal treatment protocol to eliminate *Batrachochytrium dendrobatidis* from amphibians. Medical Mycology. 2011; 49:143-9. http://dx.doi.org/10.3109/13693786.2010.508185

Mauel MJ, Miller DL, Frazier KS, Hines II ME. Bacterial pathogens isolated from cultured bullfrogs (*Rana castesbeiana*). Journal of Veterinary Diagnostic Investigation. 2002; 14:431-3. https://doi.org/10.1177/104063870201400515

McClanahan Jr. L, Baldwin R. Rate of water uptake through the integument of the desert toad, *Bufo punctatus*. Comparative Biochemistry and Physiology. 1969; 28:381-9. http://dx.doi.org/10.1016/0010-406x(69)91351-6

Menard MR. External application of antibiotic to improve survival of adult laboratory frogs (*Rana pipiens)*. Laboratory Animal Science. 1984; 34:94-6.

Miller D, Rajeev S, Brookins M, Cook J, Whittington L, Baldwin C. Concurrent infection with Ranavirus, *Batrachochytrium dendrobatidis*, and Aeromonas in a captive anuran colony. Journal of Zoo and Wildlife Medicine. 2008; 39:445-9. https://doi.org/10.1638/2008-0012.1

Mills PC, Cross SE. Transdermal drug delivery: Basic principles for the veterinarian. The Veterinary Journal. 2006; 172:218-33. http://dx.doi.org/10.1016/j.tvjl.2005.09.006

Mitchell MA. Anesthetic considerations for amphibians. Journal of Exotic Pet Medicine. 2009; 18:40-9. http://dx.doi.org/10.1053/j.jepm.2008.11.006

Mombarg M, Claessen H, Lambrechts L, Zwart P. Quantification of percutaneous absorption of metronidazole and levamisole in the fire-bellied toad (*Bombina orientalis*). Journal of Veterinary Pharmacology and Therapeutics. 1992; 15:433-6. http://dx.doi.org/10.1111/j.1365-2885.1992.tb01035.x

Moss GP, Cronin MTD. Quantitative structure-permeability relationships for percutaneous absorption: re-analysis of steroid data. International Journal of Pharmaceutics. 2002; 238:150-09. https://doi.org/10.1016/s0378-5173(02)00057-1

Moss GP, Dearden JC, Patel H, Cronin MTD. Quantitative structure-permeability relationships (QSPRs) for percutaneous absorption. Toxicology in Vitro. 2002; 16:299-317. https://doi.org/10.1016/s0887-2333(02)00003-6

Moss GP, Gullick DR, Wilkinson SC. The new breadth of research in the field. predictive methods in percutaneous absorption. Berlin: Springer; 2015. p. 65-89.

Moss GP, Sun Y, Prapopoulou M, Davey N, Adams R, Pugh WJ, et al. The application of Gaussian processes in the prediction of percutaneous absorption. Journal of Pharmacy and Pharmacology. 2009; 61:1147-53. https://doi.org/10.1211/jpp/61.09.0003

Moss GP, Wilkinson SC, Sun Y. Mathematical modelling of percutaneous absorption. Current Opinion in Colloid & Interface Science. 2012; 17:166-72. https://doi.org/10.1016/j.cocis.2012.01.002

Muijsers M, Martel A, Van Rooij P, Baert K, Vercauteren G, Ducatelle R, et al. Antibacterial therapeutics for the treatment of chytrid infection in amphibians: Columbus's egg? BMC Veterinary Research. 2012; 8:175. http://dx.doi.org/10.1186/1746-6148-8-175

Naik A, Kalia YN, Guy RH. Transdermal drug delivery: overcoming the skin's barrier function. Pharmaceutical Science and Technology Today. 2000; 3:318-26. http://dx.doi.org/10.1016/s1461-5347(00)00295-9

Nerurkar J, Beach JW, Park MO, Jun HW. Solubility of (+/-)-ibuprofen and S (+)-ibuprofen in the presence of cosolvents and cyclodextrins. Pharmaceutical Development and Technology. 2005; 10:413-21. https://doi.org/10.1081/pdt-200054446

Nichols DK, Lamirande EW, Pessier AP, Longcore JE, editors. Experimental transmission and treatment of cutaneous chytridiomycosis in poison dart frogs (*Dendrobates auratus* and *Dendrobates tinctorius*). American Association of Zoo Veterinarians and International Association of Aquatic Animals Medical Joint Conference; 2000 September 17-21; New Orleans, LA.

Ohmer MEB, Cramp RL, White CR, Harlow PS, McFadden MS, Merino-Viteri A, et al. Phylogenetic investigation of skin sloughing rates in frogs: relationships with skin characteristics and disease-driven declines. Proceedings of the Royal Society B: Biological Sciences. 2019; 286. https://doi.org/10.1098/rspb.2018.2378

Organisation for Economic Co-operation and Development. Guidance document for the conduct of skin absorption studies. Paris: OECD Environmental Health and Safety Publications; 2004.

Organisation for Economic Co-operation and Development. Guidance notes on dermal absorption. 156 ed. Paris: OECD Environment, Health and Safety Publications; 2011.

Organisation for Economic Co-operation and Development. Skin absorption: in vitro method. OECD guidance for the testing of chemicals 2004.

Osborne DW, Musakhanian J. Skin penetration and permeation properties of Transcutol®—neat or diluted mixtures. AAPS PharmSciTech. 2018; 19:3512-33. https://doi.org/10.1208/s12249-018-1196-8

Overman TL. Antimicrobial susceptibility of *Aeromonas hydrophila*. Antimicrobial Agents and Chemotherapy. 1980; 17:612-4. https://doi.org/10.1128/aac.17.4.612

Page A, Kirkpatrick W, Massam M. Risk Assessments for exotic reptiles and amphibians introduced to Australia – African clawed frog (*Xenopus laevis*). Department of Agriculture and Food, Government of Western Australia; 2010.

Papich MG. Chloramphenicol and derivatives, macrolides, lincosamides, and miscellaneous antimicrobials. In: Riviere JE, Papich MG, editors. Veterinary Pharmacology and Therapeutics. 10 ed. Hoboken, NJ: John Wiley & Sons, Incorporated; 2018. p. 903-52.

Parker JM, Mikaelian I, Hahn N, Diggs HE. Clinical diagnosis and treatment of epidermal chytridiomycosis in African clawed frogs (*Xenopus tropicalis*). Comparative Medicine. 2002; 52:265-8.

Pasteris SE, Bühler MI, Nader-Macías ME. Microbiological and histological studies of farmed-bullfrog (*Rana catesbeiana*) tissues displaying red-leg syndrome. Aquaculture. 2006; 251:11-8. https://doi.org/10.1016/j.aquaculture.2005.05.007

Patel H, Cronin M. Determination of the optimal physico-chemical parameters to use in a QSAR-approach to predict skin permeation rate. Liverpool, England: QSAR and Modelling Research Group, School of Pharmacy and Chemistry, John Moores University; 2001. Contract No.: CEFIC-LRI.

Patel H, ten Berge WF, Cronin MTD. Quantitative structure-activity relationships (QSARs) for the prediction of skin permeation of exogenous chemicals. Chemosphere. 2002; 48:603-13. https://doi.org/10.1016/s0045-6535(02)00114-5

Pessier AP. Management of disease as a threat to amphibian conservation. International Zoo Yearbook. 2008; 42:30-9. http://dx.doi.org/10.1111/j.1748-1090.2008.00047.x

Pinheiro J, Bates D, DebRoy S, Team RC. nlme: Linear and nonlinear mixed effects models. R package version 31-1312017.

Posner LP, Bailey KM, Richardson EY, Motsinger-Reif AA, Harms CA. Alfaxolone anesthesia in bullfrogs (*Lithobates catesbeiana*) by injection or immersion. Journal of Zoo and Wildlife Medicine. 2013; 44:965-71. http://dx.doi.org/10.1638/2013-0090r.1

Potts RO, Guy RH. A predictive algorithm for skin permeability: The effects of molecular size and hydrogen bond activity. Pharmaceutical Research. 1995; 12:1628-33.

Potts RO, Guy RH. Predicting skin permeability. Pharmaceutical Research. 1992; 9:663-9. http://dx.doi.org/10.1023/a:1015810312465

Pough FH. Amphibian biology and husbandry. Institute for Laboratory Animal Research Journal. 2007; 48:203-13. https://doi.org/10.1093/ilar.48.3.203

Poulter R, Bishop P, Speare R. A protocol for treating chytrid (*Batrachochytrium dendrobatidis*)-infected frogs. Available online: www.nzfrogs.org/site/nzfrog/files/Treatment%20Protocol.pdf

Preblud SR, Gill CJ, Campos JM. Bactericidal activities of chloramphenicol and eleven other antibiotics against *Salmonella* spp. Antimicrobial Agents and Chemotherapy. 1984; 25:327-30. https://doi.org/10.1128/aac.25.3.327

Pugh WJ, Roberts MS, Hadgraft J. Epidermal permeability - penetrant structure relationships: 3. The effect of hydrogen bonding interactions and molecular size on diffusion across the stratum corneum. International Journal of Pharmaceutics. 1996; 138:149-65. http://dx.doi.org/10.1016/0378-5173(96)04533-4

Pulcini C, Bush K, Craig WA, Frimodt-Møller N, Grayson ML, Mouton JW, et al. Forgotten antibiotics: An inventory in Europe, the United States, Canada, and Australia. Clinical Infectious Diseases. 2012; 54:268-74. https://doi.org/10.1093/cid/cir838

Quaranta A, Bellantuono V, Cassano G, Lippe C. Why amphibians are more sensitive than mammals to xenobiotics. PLoS ONE. 2009; 4:e7699. http://dx.doi.org/10.1371/journal.pone.0007699.

R Core Team. R: A language and environment for statistical computing. In: R Foundation for Statistical Computing, editor. Vienna, Austria 2016.

Ranade VV. Drug delivery systems: 6. Transdermal drug delivery. The Journal of Clinical Pharmacology. 1991; 31:401-18. http://dx.doi.org/10.1002/j.1552-4604.1991.tb01895.x

Relyea RA. The lethal impact of roundup on aquatic and terrestrial amphibians. Ecological Applications. 2005; 15:1118-24. https://doi.org/10.1890/04-1291

Riviere JE, Papich MG. Potential problems of developing trandermal patches for veterinary applications. Advanced Drug Delivery Reviews. 2001; 50:175-203. http://dx.doi.org/10.1016/s0169-409x(01)00157-0

Riviere JE, Shapiro DP, Coppoc GI. Percutaneous absorption of gentamicin by the leopard frog, *Rana pipiens*. Journal of Veterinary Pharmacology and Therapeutics. 1979; 2:235-9. http://dx.doi.org/10.1111/j.1365-2885.1979.tb00381.x

Roberts AA, Berger L, Robertson SG, Webb RJ, Kosch TA, McFadden M, et al. The efficacy and pharmacokinetics of terbinafine against the frog-killing fungus (*Batrachochytrium dendrobatidis*). Medical Mycology. 2019; 57:204-214. http://dx.doi.org/10.1093/mmy/myy010

Roberts MS, Cross SE, Pellett MA. Skin transport. In: Walters KA, editor. Dermatological and transdermal formulations. Drugs and the pharmaceutical sciences. New York: CRC Press; 2002. p. 89–195.

Roberts MS, Pugh WJ, Hadgraft J. Epidermal permeability - penetrant structure relationships: 2. The effect of H-bonding groups in penetrants on their diffusion through the stratum corneum. International Journal of Pharmaceutics. 1996; 132:23-32. http://dx.doi.org/10.1016/0378-5173(95)04278-4

Roberts MS. Targeted drug delivery to the skin and deeper tissues: Role of physiology, solute structure and disease. Clinical and Experimental Pharmacology and Physiology. 1997; 24:874-9. http://dx.doi.org/10.1111/j.1440-1681.1997.tb02708.x

Rollins-Smith LA, Reinert LK, O'Leary CJ, Houston LE, Woodhams DC. Antimicrobial peptide defenses in amphibian skin. Integrative and Comparative Biology. 2005; 45:137-42. https://doi.org/10.1093/icb/45.1.137

Roth JJ. Vascular supply to the ventral pelvic region of anurans as related to water balance. Journal of Morphology. 1973; 140:443-60. https://doi.org/10.1002/jmor.1051400405

Roussel L, Abdayem R, Gilbert E, Pirot F, Haftek M. Influence of excipients on two elements of the stratum corneum barrier: intercellular lipids and epidermal tight junctions. In: Dragicevic N, Maibach HI, editors. Percutaneous penetration enhancers chemical methods in penetration enhancement: Drug manipulation strategies and vehicle effects. Berlin, Heidelberg: Springer Berlin Heidelberg; 2015. p. 69-90.

Rowson AD, Obringer AR, Roth TL. Non-invasive treatments of luteinizing hormone-releasing hormone for inducing spermiation in American (*Bufo americanus*) and Gulf Coast (*Bufo valliceps*) toads. Zoo Biology. 2001; 20:63-74. http://dx.doi.org/10.1002/zoo.1007

Ryuzak M, Kojima H, Tamai Y. Study on amphibian lipids II. Characteristic constituents of monoglycosylceramides from the skin of three frog species. Comparative Biochemistry and Physiology. 1975; 52:81-4. https://doi.org/10.1016/0306-4492(75)90017-9

Sadowski-Fugitt LM, Tracy CR, Christian KA, Williams JB. Cocoon and epidermis of Australian *Cyclorana* frogs differ in composition of lipid classes that affect water loss. Physiological and Biochemical Zoology. 2012; 85:40-50. http://dx.doi.org/10.1086/663695

Saunte DM, Simmel F, Frimodt-Moller N, Stolle LB, Svejgaard EL, Haedersdal M, et al. In vivo efficacy and pharmacokinetics of voriconazole in an animal model of dermatophytosis. Antimicrobial Agents and Chemotherapy. 2007; 51:3317-21. https://doi.org/10.1128/aac.01185-06

Scheele BC, Hunter DA, Grogan L, Berger L, Kolby J, McFadden M, et al. Interventions for reducing extinction risk in chytridiomycosis-threatened amphibians. Conservation Biology. 2014; 28:1195-205. http://dx.doi.org/10.1111/cobi.12322

Scheele BC, Pasmans F, Skerratt LF, Berger L, Martel A, Beukema W, et al. Amphibian fungal panzootic causes catastrophic and ongoing loss of biodiversity. Science. 2019; 363:1459-63. http://dx.doi.org/10.1126/science.aav0379

Scheuplein RJ, Blank IH. Permeability of the skin. Physiological Reviews. 1971; 51:702-47. https://doi.org/10.1152/physrev.1971.51.4.702

Schloegel LM, Daszak P, Cunningham AA, Speare R, Hill B. Two amphibian diseases, chytridiomycosis and ranaviral disease, are now globally notifiable to the World Organization for Animal Health (OIE): an assessment. Diseases of Aquatic Organisms. 2010; 92:101-8. https://doi.org/10.3354/dao02140

Schwinger G, Zanger K, Greven H. Structural and mechanical aspects of the skin of *Bufo marinus* (Anura, Amphibia). Tissue and Cell. 2001; 33:541-7. https://doi.org/10.1054/tice.2001.0208

Shoemaker VH, Nagy KA. Osmoregulation in amphibians and reptiles. Annual Reviews in Physiology. 1977; 39:449-71. http://dx.doi.org/10.1146/annurev.ph.39.030177.002313

Shoemaker VH. The stimulus for the water-balance response to dehydration in toads. Comparative Biochemistry and Physiology. 1965; 15:81-8. https://doi.org/10.1016/0010-406X(65)90336-1

Sievers M, Hale R, Parris KM, Swearer SE. Impacts of human-induced environmental change in wetlands on aquatic animals. Biological Reviews. 2018; 93:529-54. https://doi.org/10.1111/brv.12358

Siimer E, Kurvits M. Calorimetric studies of benzoic acid-cyclodextrin inclusion complexes. Thermochimica Acta. 1989; 140:161-8. https://doi.org/10.1016/0040-6031(89)87295-8

Sim RR, Sullivan KE, Valdes EV, Fleming GJ, Terrell SP. A comparison of oral and topical vitamin A supplementation in African foam-nesting frogs (*Chiromantis xerampelina*). Journal of Zoo and Wildlife Medicine. 2010; 41:456-60. http://dx.doi.org/10.1638/2009-0208.1

Skerratt LF, Berger L, Speare R, Cashins S, McDonald KR, Phillott AD, et al. Spread of chytridiomycosis has caused the rapid global decline and extinction of frogs. EcoHealth. 2007; 4:125-34. http://dx.doi.org/10.1007/s10393-007-0093-5

Smith JM, Stump KC. Isoflurane anesthesia in the African Clawed Frog (*Xenopus laevis*). Contemporary Topics in Laboratory Animal Science. 2000; 39:39-42.

Smith SW. Chloromycetin in the treatment of "red leg". Science. 1950; 112:274-5. https://doi.org/10.1126/science.112.2906.274

Stiffler DF. The role of cutaneous acid-base-electrolyte exchange in extracellular pH regulation. In: Heatwole H, Barthalmus GT, editors. Amphibian biology. 1. Chipping Norton: Surrey Beatty & Sons; 1994. p. 120-31.

Stock I. Natural antibiotic susceptibility of *Proteus* spp., with special reference to *P. mirabilis* and *P. penneri* strains. Journal of Chemotherapy. 2003; 15:12-26. https://doi.org/10.1179/joc.2003.15.1.12

Stone SM, Clark-Price SC, Boesch JM, Mitchell MA. Evaluation of righting reflex in cane toads (*Bufo marinus*) after topical application of sevoflurane jelly. American Journal of Veterinary Research. 2013; 74:823-7. http://dx.doi.org/10.2460/ajvr.74.6.823

Storrs Méndez SI, Tillitt DE, Rittenhouse TAG, Semlitsch RD. Behavioral response and kinetics of terrestrial atrazine exposure in American toads (*Bufo americanus*). Archives of Environmental Contamination and Toxicology. 2009; 57:590-7. https://doi.org/10.1007/s00244-009-9292-0

Sun Y, Brown MB, Prapopoulou M, Davey N, Adams RG, Moss GP. The application of stochastic machine learning methods in the prediction of skin penetration. Applied Soft Computing. 2011; 11:2367-75. https://doi.org/10.1016/j.asoc.2010.08.016

Switzenbaum MS, Veltman S, Mericas D, Wagoner B, Schoenberg T. Best management practices for airport deicing stormwater. Chemosphere. 2001; 43:1051-62. https://doi.org/10.1016/S0045-6535(00)00199-5

Talbot CR. Regional variation and control of cutaneous gas exchange in bullfrogs. Respiration Physiology. 1992; 89:261-72. https://doi.org/10.1016/0034-5687(92)90085-b

Tamukai K, Une Y, Tominaga A, Suzuki K, Goka K. Treatment of spontaneous chytridiomycosis in captive amphibians using itraconazole. Journal of Veterinary Medical Science. 2011; 73:155-9. http://dx.doi.org/10.1292/jvms.10-0261

Taylor SK, Williams ES, Mills KW. Effects of malathion on disease susceptibility in Woodhouse's toads. Journal of Wildlife Diseases. 1999; 35:536-41. https://doi.org/10.7589/0090-3558-35.3.536

Toledo RC, Jared C. Cutaneous adaptations to water balance in amphibians. Comparative Biochemistry and Physiology Part A: Physiology. 1993; 105:593-608. http://dx.doi.org/10.1016/0300-9629(93)90259-7

Toledo RC, Jared C. Cutaneous granular glands and amphibian venoms. Comparative Biochemistry and Physiology. 1995; 111A:1-29. http://dx.doi.org/10.1016/0300-9629(95)98515-i

Tracy CR. A model of the dynamic exchanges of water and energy between a terrestrial amphibian and its environment. Ecological Monographs. 1976; 46:293–326. https://doi.org/10.2307/1942256

Trommer H, Neubert RHH. Overcoming the stratum corneum: The modulation of skin penetration. Skin Pharmacology and Physiology. 2006; 19:106-21. https://doi.org/10.1159/000091978

Tur E, Maibach HI, Guy RH. Percutaneous penetration of methyl nicotinate at three anatomic sites: evidence for an appendageal contribution to transport? Skin Pharmacology. 1991; 4:230-4. http://dx.doi.org/10.1159/000210956

Valitutto MT, Raphael BL, Calle PP, Papich MG. Tissue concentrations of enrofloxacin and its metabolite ciprofloxacin after a single topical dose in the Coqui frog (*Eleutherodactylus coqui*). Journal of Herpetological Medicine and Surgery. 2013; 23:69-73. https://doi.org/10.5818/1529-9651-23.3.69

Vanburen CS, Norman DB, Fröbisch NB. Examining the relationship between sexual dimorphism in skin anatomy and body size in the white-lipped treefrog, *Litoria infrafrenata* (Anura: Hylidae) Zoological Journal of the Linnean Society. 2018; zly070. http://dx.doi.org/10.1093/zoolinnean/zly070

Vecchia BE, Bunge AL. Skin absorption databases and predictive equations. In: Hadgraft J, editor. Transdermal drug delivery systems: Revised and expanded. 2 ed. Boca Raton: CRC Press; 2002.

Viborg AL, Rosenkilde P. Water potential receptors in the skin regulate blood perfusion in the ventral pelvic patch of toads. Physiological and Biochemical Zoology. 2004; 77:39-49. http://dx.doi.org/10.1086/380212

Vickaryous MK, Sire J-Y. The integumentary skeleton of tetrapods: origin, evolution and development. Journal of Anatomy. 2009; 214:441-64. https://doi.org/10.1111/j.1469-7580.2008.01043.x

Voyles J, Young S, Berger L, Campbell C, Voyles WF, Dinudom A, et al. Pathogenesis of chytridiomycosis, a cause of catastrophic amphibian declines. Science. 2009; 326:582-5. https://doi.org/10.1126/science.1176765

Wack CL, Lovern MB, Woodley SK. Trandermal delivery of corticosterone in terrestrial amphibians. General and Comparative Endocrinology. 2010; 169:269-75. http://dx.doi.org/10.1016/j.ygcen.2010.09.004

Wagner N, Reichenbecher W, Teichmann H, Tappeser B, Lötters S. Questions concerning the potential impact of glyphosate-based herbicides on amphibians. Environmental Toxicology and Chemistry. 2013; 32:1688-700. https://doi.org/10.1002/etc.2268

Wake DB, Vredenburg VT. Are we in the midst of the sixth mass extinction? A view from the world of amphibians. Proceedings of the National Academy of Sciences of the United States of America. 2008; 105:11466-73. https://doi.org/10.1073/pnas.0801921105

Walker IDF, Whitaker BR. Amphibian therapeutics. Veterinary Clinics of North America - Exotic Animal Practice. 2000; 3:239-55. https://doi.org/10.1016/s1094-9194(17)30103-2

Watkinson RM, Herkenne C, Guy RH, Hadgraft J, Oliveira G, Lane ME. Influence of ethanol on the solubility, ionization and permeation characteristics of ibuprofen in silicone and human skin. Skin Pharmacology and Physiology. 2009; 22:15-21. https://doi.org/10.1159/000183922

Waxman DJ, Holloway MG. Sex differences in the expression of hepatic drug metabolizing enzymes. Molecular Pharmacology. 2009; 76:215-28. https://doi.org/10.1124/mol.109.056705

Wayson KA, Downes H, Lynn RK, Gerber N. Anesthetic effects and elimination of tricaine methanesulphonate (MS-222) in terrestial vertebrates. Comparative Biochemistry and Physiology. 1976; 55:37-41. https://doi.org/10.1016/0306-4492(76)90009-5

Wayson KA, Downes H, Lynn RK, Gerber N. Studies on the comparative pharmacology and selective toxicity of tricaine methanesulfonate: Metabolism as a basis of the selective toxicity in poikilotherms. The Journal of Pharmacology and Experimental Therapeutics. 1976; 198:695-708.

Wei Y-L, Ding L-H, Dong C, Niu W-P, Shuang S-M. Study on inclusion complex of cyclodextrin with methyl xanthine derivatives by fluorimetry. Spectrochimica Acta Part A: Molecular and Biomolecular Spectroscopy. 2003; 59:2697-703.

Weltje L, Ufer A, Hamer M, Sowig P, Demmig S, Dechet F. Risk assessment considerations for plant protection products and terrestrial life-stages of amphibians. Science of the Total Environment. 2018; 636:500-11.

Wilcox MH. Chloramphenicol and thiamphenicol. In: Finch RG, Greenwood D, Whitley RJ, Norrby SR, editors. Antibiotic and chemotherapy: anti-infective agents and their use in therapy. 9 ed2010. p. 245-9.

Wildlife Disease Association. WDA allometric scaling [Mobile application software] 2017 [Version 1.0]: Available from: https://play.google.com/store/apps/details?id=appinventor.ai_WDAAllometricScaling.AllometricScaling

Willens S, Stoskopf MK, Baynes RE, Lewbart GA, Taylor SK, Kennedy-Stoskopf S. Percutaneous malathion absorption in the harvested perfused anuran pelvic limb. Environmental Toxicology and Pharmacology. 2006; 22:263-7. https://doi.org/10.1016/j.etap.2006.04.009

Willens S, Stoskopf MK, Baynes RE, Lewbart GA, Taylor SK, Kennedy-Stoskopf S. Percutaneous malathion absorption by anuran skin in flow-through diffusion cells. Environmental Toxicology and Pharmacology. 2006; 22:255-62. https://doi.org/10.1016/j.etap.2006.04.010

Willens S. Effects of percutaneous malathion absorption in anurans [dissertation on the Internet]. Raleigh, NC: North Carolina State University; 2005. Available from: https://www.lib.ncsu.edu/resolver/1840.16/5611

Williams AC, Barry BW. Penetration enhancers. Advanced Drug Delivery Reviews. 2012; 64:128-37. http://dx.doi.org/10.1016/j.addr.2012.09.032

Williams AC. Transdermal and topical drug delivery. London: Pharmaceutical Press; 2003.

Wilschut A, ten Berge WF, Robinson PJ, McKone TE. Estimating skin permeation. The validation of five mathematical skin permeation models. Chemosphere. 1995; 30:1275-96. https://doi.org/10.1016/0045-6535(95)00023-2

Withers PC, Hillman SS, Drewes RC. Evaporative water loss and skin lipids of anuran amphibians. The Journal of Experimental Zoology. 1984; 232:11-7. https://doi.org/10.1002/jez.1402320103

Woodhams DC, Geiger CC, Reinert LK, Rollins-Smith LA, Lam B, Harris RN, et al. Treatment of amphibians infected with chytrid fungus: learning from failed trials with itraconazole, antimicrobial peptides, bacteria, and heat therapy. Diseases of Aquatic Organisms. 2012; 98:11-25. http://dx.doi.org/10.3354/dao02429

Woodward AP, Berger L, Skerratt LF. In vitro sensitivity of the amphibian pathogen *Batrachochytrium dendrobatidis* to antifungal therapeutics. Research in Veterinary Science. 2014; 97:364-6. http://dx.doi.org/10.1016/j.rvsc.2014.06.013

Wright K, DeVoe RS. Amphibians. In: Carpenter JW, editor. Exotic animal formulary. 4 ed. St Louis: Elsevier Health Sciences; 2013. p. 53-82.

Wright KM, Whitaker BR. Pharmacotherapeutics. In: Wright KM, Whitaker BR, editors. Amphibian medicine and captive husbandry. 1st ed. Malabar, FL: Krieger Publishing Company; 2001. p. 309-32.

Wright KM. Anatomy for the clinician. In: Wright KM, Whitaker BR, editors. Amphibian medicine and captive husbandry. 1st ed. Malabar, FL: Krieger Publishing Company; 2001. p. 15-30.

Wright KM. Restraint techniques and euthanasia. In: Wright KM, Whitaker BR, editors. Amphibian medicine and captive husbandry. 1st ed. Malabar, FL: Krieger Publishing Company; 2001. p. 111-22.

Wygoda M. Low cutaneous evaporative water loss in arboreal frogs. Physiological Zoology. 1984; 57:329-37. https://doi.org/10.1086/physzool.57.3.30163722

Yorio T, Bentley PJ. Asymmetrical permeability of the integument of tree frogs (*hylidae*). Journal of Experimental Biology. 1977; 67:197-204.

Young JE, Christian KA, Donnellan S, Tracy CR, Parry D. Comparative analysis of cutaneous evaporative water loss in frogs demonstrated correlation with ecological habitats. Physiological and Biochemical Zoology. 2005; 78:847-56. https://doi.org/10.1086/432152

Young S, Speare R, Berger L, Skerratt LF. Chloramphenicol with fluid and electrolyte therapy cures terminally ill green tree frogs (*Litoria caerulea*) with chytridiomycosis. Journal of Zoo and Wildlife Medicine. 2012; 43:330-7. http://dx.doi.org/10.1638/2011-0231.1

Zhang Q, Grice JE, Li P, Jepps OG, Wang G-J, Roberts MS. Skin solubility determines maximum transepidermal flux for similar size molecules. Pharmaceutical Research. 2009; 26:1974-85. https://doi.org/10.1007/s11095-009-9912-4

Zhong HA, Mashinson V, Woolman TA, Zha M. Understanding the molecular properties and metabolism of top prescribed drugs. Current Topics in Medicinal Chemistry. 2013; 13:1290-307. http://dx.doi.org/10.2174/15680266113139990034

Chapter 9: Appendices

Appendix 1

Percutaneous absorption of chemicals: developing an understanding for the treatment of disease. Llewelyn VK, Berger L, Glass BD. *Journal of Veterinary Pharmacology and Therapeutics*, 39(2). Copyright © 2015, John Wiley & Sons Ltd. http://dx.doi.org/10.1111/jvp.12264.

JOURNAL OF
Veterinary Pharmacology and Therapeutics

J. vet. Pharmacol. Therap. doi: 10.1111/jvp.12264 REVIEW ARTICLE

Percutaneous absorption of chemicals: developing an understanding for the treatment of disease in frogs

V. K. LLEWELYN*

L. BERGER† &

B. D. GLASS*

*Pharmacy, College of Medicine and Dentistry, James Cook University, Townsville, Qld, Australia; †One Health Research Group, College of Public Health, Medical and Veterinary Sciences, James Cook University, Townsville, Qld, Australia

Llewelyn, V. K., Berger L., Glass B. D. Percutaneous absorption of chemicals: developing an understanding for the treatment of disease in frogs. *J. vet. Pharmacol. Therap.* doi: 10.1111/jvp.12264.

The permeable nature of frog skin presents an alternative route for the delivery of therapeutic chemicals to treat disease in frogs. However, although therapeutic chemicals are often topically applied to the skin of frogs, their pharmacokinetics have rarely been reported. To provide evidence to guide both candidate drug and formulation selection, we highlight factors expected to influence percutaneous absorption through frog skin, including the anatomy and physiology of the skin and the physicochemical properties of applied therapeutic chemicals. Importantly, we also highlight the effects of the formulation on percutaneous absorption, especially the inclusion of potential penetration enhancers as excipients. Finally, we collate empirical data on the topical application of various therapeutic chemicals in postmetamorphic frogs and show that, in contrast to mammalian species, even large chemicals (i.e. >500 Da) and those with a wide range of log *P* values (−4 through +6) are likely to be absorbed percutaneously. Topical application in frogs thus promises a convenient and effective method for delivering systemic treatments of a diverse range of chemicals; however, further experimental quantification is required to ensure optimal outcomes.

(Paper received 25 November 2014; accepted for publication 27 July 2015)

Victoria K. Llewelyn, Pharmacy, College of Medicine and Dentistry, James Cook University, Townsville, Qld 4811, Australia. E-mail: tori.llewelyn@jcu.edu.au

Appendix 2a

Regional variation in percutaneous absorption in the tree frog *Litoria caerulea*. Llewelyn VK, Berger L, Glass BD. *Environmental Toxicology and Pharmacology*, 60. https://doi.org/10.1016/j.etap.2018.03.019

Environmental Toxicology and Pharmacology 60 (2018) 5–11

Contents lists available at ScienceDirect

Environmental Toxicology and Pharmacology

journal homepage: www.elsevier.com/locate/etap

Regional variation in percutaneous absorption in the tree frog *Litoria caerulea*

Victoria K. Llewelyn[a,*], Lee Berger[b], Beverley D. Glass[a]

[a] Pharmacy, College of Medicine and Dentistry, James Cook University, Townsville, 4811, Australia
[b] One Health Research Group, College of Public Health, Medical and Veterinary Sciences, James Cook University, Townsville, 4811, Australia

ARTICLE INFO

Keywords:
Skin Absorption
Anura
Skin
Administration, Cutaneous

ABSTRACT

Frog skin structure and physiology differs between skin regions, however little is known about how these differences affect transdermal absorption of chemicals. Further, no information is available regarding how the relative lipophilicity of a chemical influences its transdermal pharmacokinetics in frog skin. This study investigated the *in vitro* percutaneous absorption of three model chemicals - benzoic acid, caffeine, and ibuprofen - through dorsal and ventral skin of the tree frog *Litoria caerulea*. Flux was significantly higher through the ventral skin for all chemicals. Relative lipophilicity affected flux differently in different skin regions. These differences are likely due to significantly thicker dorsal skin increasing absorption path length, and also possibly owing to lipoid secretions on the dorsum providing an additional diffusional barrier. This knowledge can advise risk mitigation of xenobiotics in agricultural and industrial settings, and also guide selection of chemicals and doses when considering transdermal drug therapy in captive frogs.

1. Introduction

The permeability of frogs' skin is likely to influence 1) their risk of absorbing environmental xenobiotics, and 2) development of topical therapeutics for treatment of disease. However, although many studies report systemic effects in frogs following topical exposure to a variety of environmental pesticides (Brühl et al., 2011) and therapeutic chemicals (Llewelyn et al., 2016), the transdermal pharmacokinetics through frog skin is relatively unknown.

With the identification of infectious chytridiomycosis and its devastating effects on frog populations worldwide (Skerratt et al., 2007), therapeutic treatment of frogs utilizing the transdermal route has become more commonplace (for review of these studies, see Llewelyn et al. (2016)). However, the majority of these studies do not provide true pharmacokinetic data for the chemicals investigated, instead focusing on clinical endpoints (cure or death). While data on the pharmacological outcomes for the treatment of individual disease states for individual chemicals is useful, these investigative methods do not provide generalizable findings, and there has been difficulty replicating the results in other frog species (Roberts et al., 2018). It is possible that this difficulty is due to regional differences in frog skin morphology and physiology (Bentley and Main, 1972; Talbot, 1992; Toledo and Jared, 1993) impacting the transdermal kinetics of the chemicals being applied to the skin. In particular, epidermal thickness and vascularization of the skin can differ significantly between dorsal and ventral skin regions (Fox, 1994; Toledo and Jared, 1993) in some frog species. The magnitude of difference between skin regions can also differ substantially between species, and is often related to the primary habitat of the species (Young et al., 2005). For example, aquatic species often have a relatively uniform skin thickness and reduced vascularization across all skin regions, whereas the ventral skin of arboreal species is often significantly thinner and more vascularized than their dorsum (Roth, 1973; Toledo and Jared, 1993). It is likely that these differences in skin permeability will also impact on the transdermal pharmacokinetics of chemicals applied to frog skin, however the impact of these differences on transdermal pharmacokinetics has not been studied in depth, with studies largely limited to investigations on the movement of water and electrolytes across the skin (Yorio and Bentley, 1977).

Guidelines exist to advise investigations of transdermal penetration in mammalian species for exposure-prevention and risk analysis purposes, and for therapeutic delivery of chemicals (Organisation for Economic Co-operation and Development, 2004, 2011). These guidelines recommend that the transdermal kinetics of a series of model compounds – chemicals of similar molecular weight, but with varying lipophilicity – be determined in order to establish baseline absorption kinetics for topically-administered agents within a species

Abbreviations: ARS, Amphibian Ringer's Solution; HPβCD, 2-hydroxypropyl-beta-cyclodextrin; logFlux, log 10 logarithm of the calculated flux for a chemical

* Corresponding author.
E-mail address: tori.llewelyn@jcu.edu.au (V.K. Llewelyn).

https://doi.org/10.1016/j.etap.2018.03.019
Received 13 December 2017; Received in revised form 23 March 2018; Accepted 26 March 2018
Available online 28 March 2018
1382-6689/

(Organisation for Economic Co-operation and Development, 2004, 2011). An adaptation of these guidelines has been trialed by Kaufmann and Dohmen (2016), who used a static diffusion (Franz) cell to determine the transdermal pharmacokinetics of a finite dose of two model chemicals, caffeine and testosterone, through the skin of the aquatic frog *Xenopus laevis*. However, as aquatic frog species have often negligible differences in skin thickness and vascularization between dorsal and ventral skin regions (Roth, 1973; Toledo and Jared, 1993), it is essential to establish baseline transdermal pharmacokinetic parameters for a frog species with known regional differences in skin structure. To this end, this study investigated the transdermal penetration of three model drugs in the arboreal frog species *Litoria caerulea*, to provide quantitative evidence of the differences in permeability between skin regions in this species. This will go some way to inform both future environmental xenobiotic exposure prevention, and development of therapeutics for serious disease in frogs - including evidence for drug choice and treatment delivery.

2. Material and methods

2.1. Study animals

Adult *Litoria caerulea* (Green Tree Frog, or White's tree frog), part of a larger captive research population held by the One Health Research Group (James Cook University, Australia), were used for the study. *L. caerulea* is an Australian native frog with a wide distribution, and is one of the most common amphibian pets worldwide. This species is easy to breed, maintain, and handle – and so provides a convenient model species for this study. Twenty-two frogs (12 female, 10 male), ranging from 12.55 to 55.15 g body weight (median = 19.28 g) were used, with frogs being randomly allocated to one of three chemical treatments.

2.2. Chemicals and apparatus

2.2.1. Chemicals and solutions

Reagent grade caffeine, ACS reagent grade benzoic acid (Sigma-Aldrich) and ≥ 98% ibuprofen (Sigma) were used in separate experiments as model chemicals. Amphibian Ringer's solution (ARS) was prepared according to published methods (Wright and Whitaker et al., 2001); 113 mM sodium chloride, 2 mM potassium chloride, 1.35 mM calcium chloride, 2.4 mM sodium bicarbonate), spiked with 2.75 mg/ml 2-hydroxypropyl-beta-cyclodextrin (HPβCD; Aldrich Chemistry) for ibuprofen experiments to assist solubilization. 0.2% w/v ethyl 3-aminobenzoate methanesulfonate solution (MS-222; Aldrich Chemistry) was buffered to pH 7.3 with sodium bicarbonate. Methanol and acetonitrile were high-performance liquid chromatography (HPLC) grade (Fisher Chemicals, Trinidad and Thermo Fisher Scientific, Australia), formic acid was analytical grade (Thermo Fisher Scientific, Australia) and water used in HPLC was ultrapure (Milli-Q Integral, Millipore Australia). All solutions were freshly prepared.

2.2.2. Diffusion cells

Diffusion cells used were a static Franz cell (Permegear, USA), consisting of a 1 ml donor chamber with a 9 mm orifice, and a 5 ml receptor chamber. The donor chamber was filled with a saturated solution of one of the model chemicals (benzoic acid, caffeine, or ibuprofen) in ARS ± HPβCD ("infinite dose"). The receptor fluid was ARS, with added HPβCD for the ibuprofen experiments. Receptor fluid was continually stirred with a magnetized stirrer bar, and allowed to equilibrate in the diffusion cell for 30 min prior to skin mounting.

2.2.3. HPLC

The HPLC system comprised a Shimadzu Nexera-i LC-2040C 3D with photodiode-array detector. Post-run analysis was performed using Labsolutions 5.82 (Shimadzu). All HPLC methods were validated, with samples run in triplicate. Quantification of benzoic acid was performed on a Sunfire™ C18 column (250 × 4.6 mm, 5 µm; Waters), using a mobile phase containing acetonitrile and water (50:50) plus 0.1% v/v formic acid, at 30 °C with a flow rate of 1 ml.min^{-1}. Detection was at 229 nm. Quantification of caffeine was performed on a Kinetex® 5 µm C18 column (250 mm × 4.6 mm; Phenomenex), using a mobile phase containing methanol and water (35:65) at 40 °C with a flow rate of 1 ml.min^{-1}. Detection was at 275 nm. Quantification of ibuprofen was performed on a Kinetex® 5 µm C18 column (250 mm × 4.6 mm; Phenomenex), using a mobile phase containing acetonitrile and water (75:25) plus 0.1% v/v formic acid at 40 °C with a flow rate of 1 ml.min^{-1}. Detection was at 262 nm.

2.2.3.1. HPLC method validation. HPLC methods for each of the three chemicals were validated in accordance with the International Conference on Harmonization (ICH) guidelines for analytical method validation (International Conference on Harmonization (ICH), 1996). This included confirmation of specificity, linearity, range, precision and accuracy. Stability studies of the solutions for HPLC analysis were also performed.

For each of the three chemicals, separate standard solutions were prepared as needed from a freshly-prepared stock solution. Receptor fluid (ARS ± HPβCD) was used as the solvent for all chemical solutions prepared.

2.2.3.2. Specificity. Specificity of the method was investigated by comparing the chromatogram produced by a known concentration of a standard solution for each chemical with the chromatogram produced following injection of receptor fluid alone. Comparison of these chromatograms is essential to ensure complete resolution of the chemical peak from any potential interference produced by components of the mobile phase and receptor fluid.

2.2.3.3. Linearity and range. Standard solutions for each chemical were prepared by serial dilution of the stock solution, with six standard solutions prepared for caffeine and ibuprofen, and eight prepared for benzoic acid. A standard calibration curve was produced for each chemical over their respective concentration ranges (benzoic acid: 0.25–200 µg/ml; caffeine 1 – 500 µg/ml; ibuprofen 1 – 75 µg/ml). Each sample was analyzed in triplicate, and peak area versus analyte concentration plotted.

2.2.3.4. Precision. The precision of the method was assessed by injecting ten individual samples of a mid-range standard solution for each chemical. Relative standard deviation (RSD) was calculated.

2.2.3.5. Accuracy. Accuracy can be concluded provided specificity, linearity and precision are demonstrated.

2.2.3.6. Solution stability. Recovery of each chemical in receptor fluid was determined by storing a series of three standard solutions at 15 °C for 48 h, to confirm the stability of all three chemicals during Franz cell experiments and analyses. The standard solution concentrations for each comprised a low-, mid- and high-range standard concentration as follows: benzoic acid: 0.25, 50 and 200 µg/ml, caffeine: 1, 50 and 500 µg/ml, ibuprofen: 1, 25 and 75 µg/ml. Samples were analyzed by HPLC against freshly prepared calibration standards to determine chemical content at t = 0, 24 and 48 h.

2.3. Skin preparation

Animals were minimally handled to prevent damage to the skin. Euthanasia was carried out by bathing in buffered 0.2% w/v MS-222. Immediately following euthanasia, full-thickness ventral and dorsal skin samples were excised, rinsed in ARS, and mounted on a diffusion cell, with the skin surface facing the donor chamber. In the smaller frogs, one skin sample was taken from each of the dorsal and ventral

Table 1
Physicochemical properties (molecular weight and logP) and method validation results for range, linearity and precision for the three model chemicals used in this study. *: logP values are experimental values as per VCCLAB (2005).

Chemical	Molecular weight	LogP*	Range (μg/ml)	Correlation coefficient (R^2)	Precision – RSD of peak area (%)
Benzoic acid	122.13	1.87	0.25 – 200	0.999	0.272
Caffeine	194.22	−0.07	1 – 500	0.999	0.029
Ibuprofen	206.28	3.97	1 – 75	1	0.315

Table 2
Percentage recovery from low, mid- and high-range standard solutions of each model chemical following 24 and 48 h storage at 15 °C.

	LOW		MID		HIGH	
	Recovery (%)		Recovery (%)		Recovery (%)	
	24 hr	48 hr	24 hr	48 hr	24 hr	48 hr
Benzoic acid	100.7	99.6	100.3	99.4	100.4	99.6
Caffeine	101.2	100.8	99.2	98.1	99.6	100.0
Ibuprofen	101.1	98.9	100.0	98.2	100.1	99.7

sides. In larger frogs, two dorsal samples and one ventral sample was taken. Samples were taken from the truncal midline in smaller individuals and bilaterally along the truncal midline for dorsal samples in larger frogs. The number of skin samples yielded per treatment were as follows: benzoic acid – 5 dorsal and 8 ventral; caffeine – 6 dorsal and 7 ventral; ibuprofen – 6 dorsal and 6 ventral.

2.4. Absorption kinetics

The cutaneous absorption kinetics of three model chemicals with similar molecular weights but differing relative lipophilicities (Table 1) was determined. Each chemical was dissolved in ARS (spiked with 2.75 mg/ml HPβCD for ibuprofen) to achieve an infinite dose for application to the donor chamber. Following mounting of skin samples on the Franz cells, 1 ml of saturated donor solution was applied to the donor chamber, and 1 ml samples were collected from the receptor chamber at t = 0, 30, 60, 90, 120, 150, 180, 240, 300, 360 min for caffeine and benzoic acid, and at t = 0, 30, 60, 90, 120, 180, 240, 300, 360, 1440 min for ibuprofen. The receptor volume was replenished with fresh receptor fluid following each sample collection. Samples were then analyzed for chemical content using the validated HPLC method described.

Flux (μg/cm^2/hr) was calculated for each sample from the steady-state slope of the cumulative absorption versus time plot. Data were examined and analyzed using R (R Core Team, 2016). The influence of chemical and region on chemical flux through the skin was determined by fitting a linear mixed effects model using the nlme package (Pinheiro et al., 2017), allowing for heteroscedasticity in the data. The model initially utilized flux, chemical, skin region, sex and frog weight as fixed factors, with each individual animal as a random effect. As sex and weight did not influence flux they were removed from the model. For each combination of chemical / region, multiple pairwise comparisons of mean flux were then performed using Tukey's post hoc test (Hothorn et al., 2008).

3. Results

3.1. HPLC method validation

Comparison of the chromatograms produced by standard solutions containing the chemical and solutions containing receptor fluid only demonstrated no interference with the chemical peak, and so specificity of the method was confirmed. Linearity of each method was confirmed, with the regression coefficient being > 0.995 for each chemical over their investigated ranges (Table 1). Precision is indicated if the relative standard deviation of the ten samples is $< 1\%$, and the values for each chemical investigated were below this value (Table 1). As specificity, linearity and precision have been confirmed, accuracy can be inferred (International Conference on Harmonization (ICH), 1996).

Recovery of each model chemical following 48 hour s storage at 15 °C was in the acceptable range of 100 + / − 2% permitted by the USP for all standard concentrations examined (Table 2), confirming stability for each chemical throughout the diffusion cell experiments and associated analyses.

3.2. Skin absorption kinetics

The cumulative absorption versus time plots showed that ibuprofen had the lowest absorption through both skin regions (Figs. 1 and 2). However, the relative absorption of caffeine and benzoic acid differed between skin regions – with benzoic acid showing the highest absorption through dorsal skin, while caffeine had the highest absorption through the ventral skin. To further investigate these differences, flux for each chemical was calculated from the slope of the cumulative absorption versus time plots. There were significant differences ($p < 0.001$) between ventral and dorsal absorption rates for all chemicals studied, with ventral flux being higher for each of the chemicals compared to dorsal flux (Fig. 3). Further, for a specified skin region, the flux of each chemical was significantly different from each other ($p < 0.001$).

As absorption through the skin is likely to be influenced by the relative lipophilicity of the chemical, the logarithm of flux (logFlux) versus the logarithm of partition coefficient (logP) for ventral and dorsal skin regions (Fig. 4) was plotted. Interestingly, a linear reduction in flux with increasing lipophilicity was found for ventral absorption of chemicals, whereas for the dorsal skin samples, a parabolic relationship was observed.

4. Discussion

This study investigated the transdermal absorption of three model chemicals of differing lipophilicity through the skin of the green tree frog, *Litoria caerulea*. Flux through the ventral skin was higher than through the dorsal skin for all chemicals, although the magnitude of difference changed depending on the chemical involved. Caffeine, the most hydrophilic chemical, exhibited the highest and most variable flux through the ventral skin, and ibuprofen, the most lipophilic chemical, exhibited the lowest flux. Interestingly, the relationship between relative lipophilicity and flux differed between skin regions, with a linear reduction in flux as lipophilicity increased through ventral skin and a parabolic relationship when flux was measured in dorsal skin. This may be explained by regional variations in thickness of lipoid and hydrophilic skin layers.

Despite the potential impact of environmental xenobiotic absorption in frogs, little information is available regarding the effect of site of application/exposure on transdermal pharmacokinetics in frogs. As many frog species demonstrate significant differences in skin thickness and cutaneous vascularization in different skin regions, it is likely that the application site will significantly impact on absorption kinetics in these species. *L. caerulea* is a member of the hylid frog family, which consists mainly of arboreal species. Tree-dwelling hylid frogs demonstrate regional differences in skin structure, having significantly thicker skin on their dorsum – mainly due to a thicker dermis containing a high density of glands and more connective tissue. As arboreal habitats are quite drying, it is unsurprising that studies have found significantly reduced evaporative water loss from the dorsal skin in many hylid frog

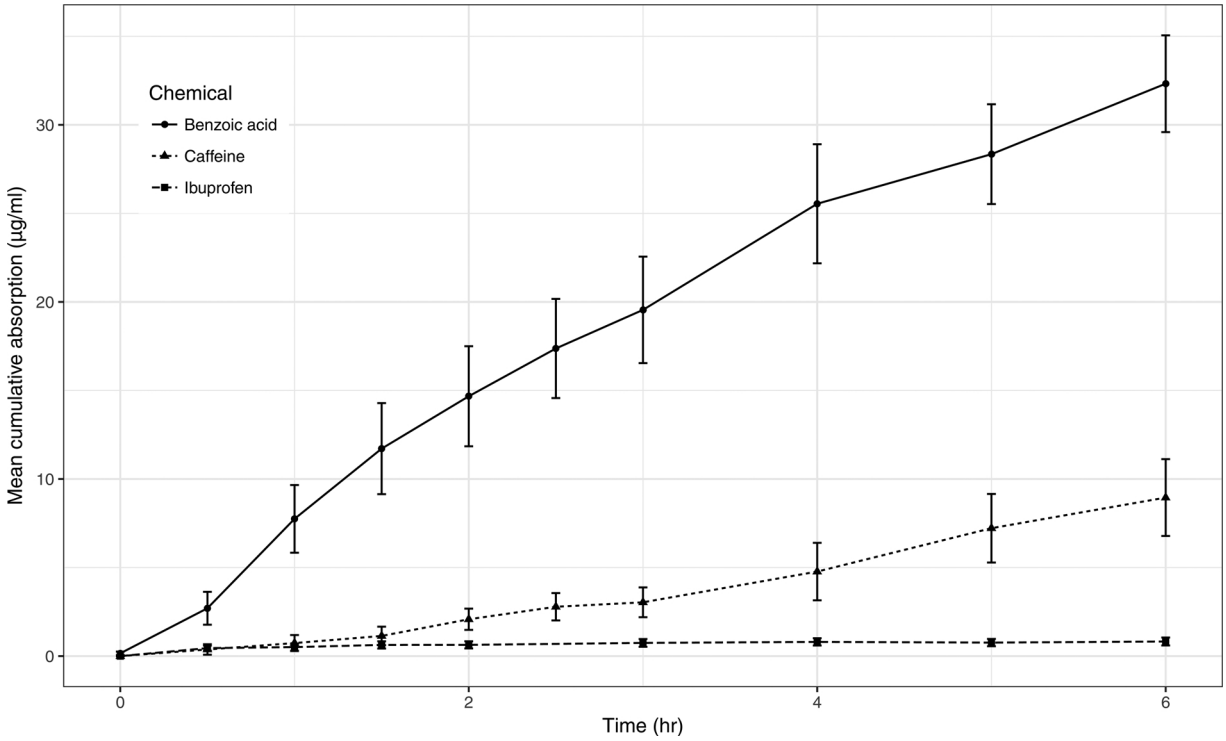

Fig. 1. Mean cumulative absorption (µg/ml) versus time (hr) for three model chemicals through dorsal *Litoria caerulea* skin. Error bars show standard error.

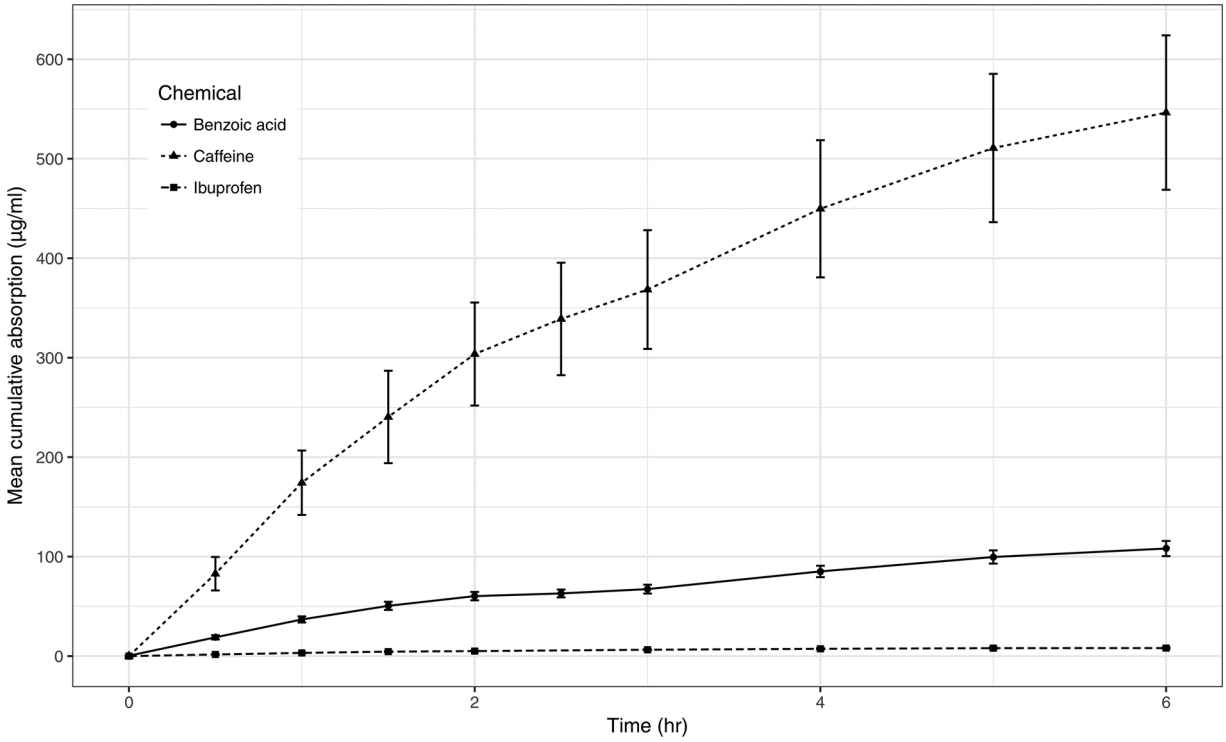

Fig. 2. Mean cumulative absorption (µg/ml) versus time (hr) for three model chemicals through ventral *Litoria caerulea* skin. Error bars show standard error.

species (Amey and Grigg, 1995; Withers et al., 1984; Wygoda, 1984, 1988). Conversely, the pelvic ventral skin is much thinner, with capillaries in this skin region being at a much higher density and closer to the skin surface (Goniakowska-Witalińska and Kubiczek, 1998). The ventral pelvic region demonstrates higher water uptake than other skin regions, presumably a function of these structural differences (Bentley and Main, 1972; Yorio and Bentley, 1977). Owing to these documented differences in thickness and cutaneous vascularization of the skin, tree frogs provide an excellent experimental animal in which to conduct transdermal pharmacokinetic studies.

As expected, ventral flux was higher than dorsal flux for all chemicals investigated, although the magnitude of this difference varied depending on the relative lipophilicity of the chemical involved. This is in agreement with the findings of Kaufmann and Dohmen (2016), who,

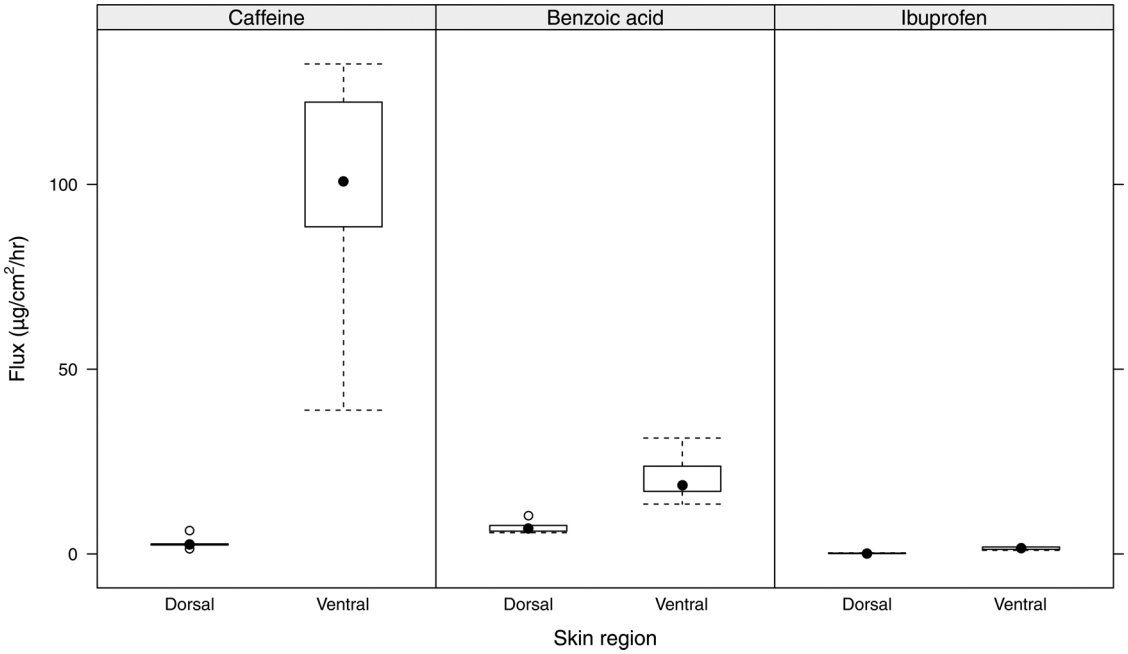

Fig. 3. Boxplots of the flux (µg/cm^2/hr) for three model drugs (caffeine, benzoic acid, and ibuprofen) through dorsal and ventral skin samples from adult *Litoria caerulea*. Chemicals are arranged (left-to-right) in order of increasing relative lipophilicity (logP).

despite previous studies showing that *Xenopus laevis* has similar whole-skin thickness across their entire skin surface, found a distinct increase in ventral flux compared to dorsal flux for both caffeine and testosterone. However, Kaufman's study was a finite-dose study and the donor solution composition changed between chemicals (ARS for caffeine and a 50% ethanol solution for testosterone), so direct comparison of their findings with the current study is not possible. While the general trends reported by Kaufmann were similar to those observed in this study, the magnitude of the difference in flux between skin regions was much lower than in the current study, with 1.5x increase in flux of caffeine (33x in the current study) and 2.3x increase for testosterone (5.5x increase for ibuprofen, similar physicochemical properties to testosterone). The larger differences in flux between skin regions in *L. caerulea* are likely due to the larger differences in skin thickness, supporting the supposition that skin thickness remains an important influence on transdermal absorption in frogs. However, it also appears that relatively small differences in skin structure in *X. laevis* do translate into quantifiable differences in transdermal absorption, and this should be investigated further.

The chemical with the highest and most variable ventral flux in this study was caffeine, the chemical with the lowest relative lipophilicity. This result may be explained by considering the functional physiology of the ventral skin in *L. caerulea* - specifically, the pelvic region. This skin region is also termed the "drinking patch", and is the primary site

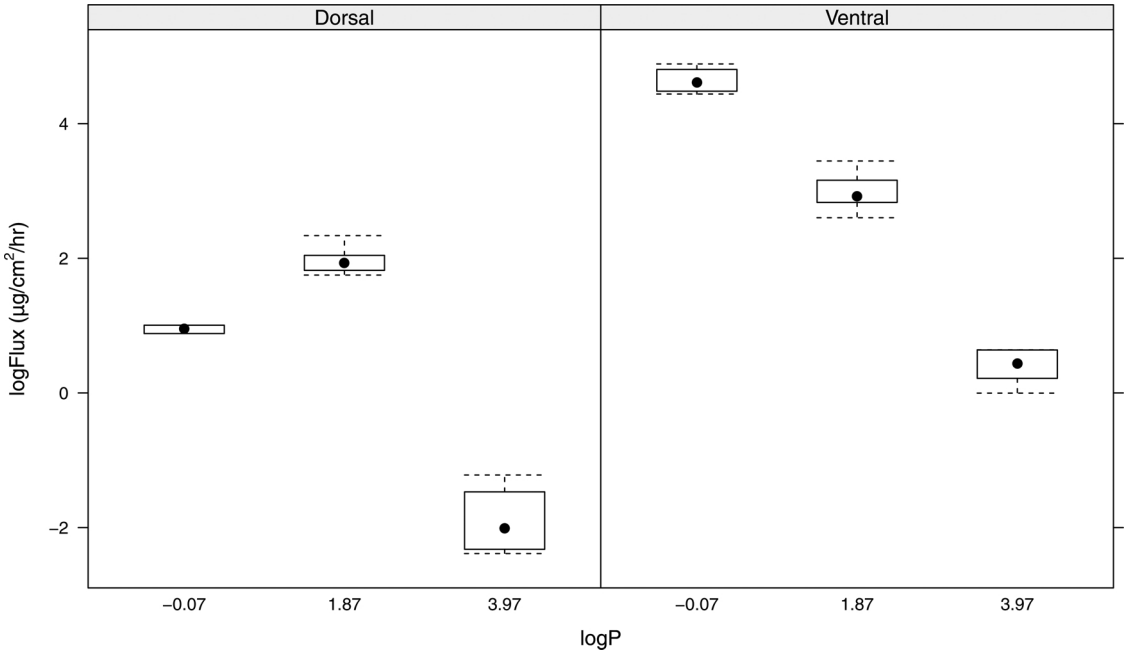

Fig. 4. Logarithm of flux (logFlux; µg/cm^2/hr) versus logarithm of partition coefficient (logP) for dorsal and ventral *Litoria caerulea* skin samples. LogP -0.07 = caffeine; logP 1.87 = benzoic acid; logP 3.97 = ibuprofen.

of rehydration in many frog species. Previous studies into the absorptive properties of this skin region in hylid frogs have demonstrated up to 20-fold higher water influx through the pelvic drinking patch compared to other skin regions (Yorio and Bentley, 1977), even in normally-hydrated animals. It is therefore not surprising that the most water-soluble chemical demonstrated the highest flux through this skin region.

While the thicker dorsal skin in *L. caerulea* is likely to be the main contributor to the reduced absorption seen for all chemicals in this study, there are other physiological differences between the dorsal and ventral surface in hylid frogs which are also likely to influence absorption. There are two additional mechanisms by which different hylid frog species are thought to retard water loss through the dorsal skin: 1) some species (for example *L. fallax* and *L. peroni*) have intraepidermal lipids found only in their dorsal skin (Amey and Grigg, 1995), which provides an additional lipid barrier to the absorption of chemicals through the dorsal skin; 2) other hylid species (including many *Phyllomedusine* sp. (Blaylock et al., 1976) and *Litoria* sp. including *L. caerulea* (Buttemer and Thomas, 2003; Young et al., 2005)) secrete a waxy, lipid-containing mucus onto the dorsal surface, which is then spread across the body to provide a barrier to evaporation. This layer of secretions may provide an additional diffusional barrier to absorption of chemicals, further impairing absorption. Finally, the dermis of *L. caerulea* contains a calcified layer between the stratum spongiosum and stratum compactum. Known alternately as the "substantia amorpha", Eberth-Kastschenko layer and lamina calcarea, its physiological purpose is debated (Mangione et al., 2011; Vickaryous and Sire, 2009), but it has been implicated in ion transport, calcium sequestration and water balance – being likened to a sponge, retaining water in the skin (Elkan, 1976). In *L. caerulea,* this layer is more continuous and abundant in the dorsal skin compared to the ventral skin (Berger et al., 2005), and while it is located mainly below the capillaries, owing to its purported role in retaining water in the dermis, it is possible that this layer may influence the transdermal absorption of chemicals through the dorsal skin. Further studies in other frog species with and without this layer will provide further insight into the relevance of this layer to transdermal kinetics.

Dermal absorption studies in mammals have regularly identified molecular size, relative lipophilicity, potential for hydrogen bonding and solubility/ionization of chemicals as factors influencing transdermal drug penetration (Magnusson et al., 2004; Naik et al., 2000; Pugh et al., 1996). In frogs, however, it is likely that only molecular weight, lipophilicity and solubility/ionization will have significant influence. However, for most chemicals of interest, molecular weight is not considered a limiting factor, as there is evidence of systemic effects in frogs following topical application of chemicals with molecular weights in excess of 500 Da (Llewelyn et al., 2016). As the model chemicals used in the current study are of comparable and relatively low molecular weight (Table 1), and infinite dosing was adopted, lipophilicity is likely to be the primary chemical-modulated influence on any differences in flux observed in this study.

An interesting finding in this study was that the relationship between flux and relative lipophilicity changed depending on the skin region being investigated. Dorsal absorption demonstrated a parabolic relationship between LogFlux and logP, whereas ventral absorption followed an inverse linear relationship. Parabolic relationships between flux and lipophilicity are quite common in transdermal penetration studies of mammals, particularly those which include data for more lipophilic chemicals (Scheuplein and Blank, 1971). It has been suggested that this relationship in mammals relates directly to the requirement that a chemical is soluble in both the lipoid stratum corneum and the relatively hydrophilic viable epidermis/dermis in order for absorption to occur. This process is favored by chemicals being slightly lipophilic, with a logP ~2.5 (Zhang et al., 2009). The thicker dorsal skin of *Litoria caerulea* and waxy secretions may explain the parabolic relationship. The fact that a linear relationship exists between logFlux and logP for ventral absorption in *L. caerulea* corresponds with Kaufmann and Dohmen (2016), but are in contrast to the findings reported by Quaranta et al. (2009). Quaranta et al. investigated the *in vitro* absorption through ventral frog (*Rana esculenta*) skin for a series of chemicals ranging from logP -3.87 to + 2.61, finding that more lipophilic substances had higher permeability than the hydrophilic substances. However, the flux was measured from the internal skin surface to the external skin surface, and chemicals investigated by Quaranta et al. were either quite hydro- or lipophilic, with no chemicals between logP −2.71 and +1.27. These methodological differences to the current study may be the source of these differing results. Regardless, further studies to investigate the relationship between relative lipophilicity and transdermal penetration of chemicals through different regions of frog skin, and in other frog species, would provide further evidence to explain these findings.

5. Conclusions

Owing to the permeable nature of frog skin, it is unsurprising that frogs are highly sensitive to xenobiotics in their immediate environment, and also that systemic therapeutics can be topically applied. However, without any true transdermal pharmacokinetic data, the extent of susceptibility to xenobiotic penetration through the skin and resultant systemic effects can only be estimated. This study represents the first infinite dose study on the transdermal pharmacokinetics for model drugs in a frog species. Establishing baseline absorption parameters for a series of model drugs through frog skin is the essential first step in the broader prediction of xenobiotic absorption through skin in frogs. Further, by quantifying the difference in absorption kinetics through different skin regions, more accurate estimations of the rate and extent of xenobiotic absorption through the skin of frogs can be made. It is anticipated that this information can also be used to predict absorption parameters for other chemicals with similar physicochemical properties, thereby informing risk analysis following topical chemical exposure or therapeutic topical dosing parameters to treat disease in frogs.

Conflict of interest

None.

Funding

This research did not receive any specific grant from funding agencies in the public, commercial, or not-for-profit sectors.

Acknowledgements

Thanks to Sherryl Robertson for advice and assistance in the laboratory, and to Rhondda Jones for help with statistical analyses.

References

Amey, A.P., Grigg, G.G., 1995. Lipid-reduced evaporative water loss in two arboreal hylid frogs. Comp. Biochem. Physiol. Part A: Physiol. 111, 283–291.
Bentley, P.J., Main, A.R., 1972. Zonal differences in permeability of the skin of some anuran amphibia. Am. J. Physiol. 223, 361–363.
Berger, L., Speare, R., Skerratt, L.F., 2005. Distribution of *Batrachochytrium dendrobatidis* and pathology in the skin of green tree frogs *Litoria caerulea* with severe chytridiomycosis. Dis. Aquat. Org. 68, 65–70.
Blaylock, L.A., Ruibal, R., Platt-Aloia, K., 1976. Skin structure and wiping behavior of phyllomedusine frogs. Copeia 1976, 283–295.
Brühl, C.A., Pieper, S., Weber, B., 2011. Amphibians at risk? Susceptibility of terrestrial amphibian life stages to pesticides. Environ. Toxicol. Chem. 30, 2465–2472.
Buttemer, W.A., Thomas, C., 2003. Influence of temperature on evaporative water loss and cutaneous resistance to water vapour diffusion in the orange-thighed frog (*Litoria xanthomera*). Aust. J. Zool. 51, 111–118.
Elkan, E., 1976. Ground substance: an anuran defense against desiccation. In: Lofts, B. (Ed.), Physiology of the Amphibia. Academic press, Inc., New York, pp. 101–110.

Fox, H., 1994. The structure of the integument. In: Heatwole, H., Barthalmus, G.T. (Eds.), Amphibian Biology. Surrey Beatty & Sons, Chipping Norton, pp. 1–32.
Goniakowska-Witalińska, L., Kubiczek, U., 1998. The structure of the skin of the tree frog (*Hyla arborea arborea* L.). Ann. Anat. 1 (80), 237–246.
Hothorn, T., Bretz, F., Westfall, P., 2008. Simultaneous inference in general parametric models. Biomet. J. 50, 346–363.
International Conference on Harmonization (ICH), 1996. Guidance for Industry: Q2B: Validation of Analytical Procedures: Methodology. ICH, Geneva.
Kaufmann, K., Dohmen, P., 2016. Adaption of a dermal in vitro method to investigate the uptake of chemicals across amphibian skin. Environ. Sci. Eur. 28.
Llewelyn, V.K., Berger, L., Glass, B.D., 2016. Percutaneous absorption of chemicals: developing an understanding for the treatment of disease in frogs. J. Vet. Pharmacol. Ther. 39, 109–121.
Magnusson, B.M., Pugh, W.J., Roberts, M.S., 2004. Simple rules for defining the potential of compounds for trandermal delivery or toxicity. Pharm. Res. 21, 1047–1054.
Mangione, S., Garcia, G., Cardozo, O., 2011. The Eberth-Katschenko layer in three species of ceratophryines anurans (Anura: Caratophrydae). Acta Zool-Stockholm 92, 21–26.
Naik, A., Kalia, Y.N., Guy, R.H., 2000. Transdermal drug delivery: overcoming the skin's barrier function. Pharm. Sci. Technol. Today 3, 318–326.
Organisation for Economic Co-operation and Development, 2004. Skin absorption: in vitro method. OECD Guidance for the Testing of Chemicals.
Organisation for Economic Co-operation and Development, 2011. Guidance Notes on Dermal Absorption, 156 ed. OECD Environment, Health and Safety Publications, Paris.
Pinheiro, J., Bates, D., DebRoy, S., Team, R.C., 2017. Nlme: linear and nonlinear mixed effects models, R Package Version 3.1-131.
Pugh, W.J., Roberts, M.S., Hadgraft, J., 1996. Epidermal permeability - penetrant structure relationships: 3. The effect of hydrogen bonding interactions and molecular size on diffusion across the stratum corneum. Int. J. Pharm. 138, 149–165.
Quaranta, A., Bellantuono, V., Cassano, G., Lippe, C., 2009. Why amphibians are more sensitive than mammals to xenobiotics. PLoS One e7699.
Core Team, R., 2016. In: Computing, R.F.f.S (Ed.), R: A Language and Environment for Statistical Computing, Vienna, Austria.
Roberts, A.A., Berger, L., Robertson, S.G., Webb, R.J., Kosch, T.A., McFadden, M., Skerratt, L.F., Glass, B.D., Motti, C.A., Brannelly, L.A., 2018. The efficacy and pharmacokinetics of terbinafine against the frog-killing fungus (Batrachochytrium dendrobatidis). Med. Mycol myy010-myy010.
Roth, J.J., 1973. Vascular supply to the ventral pelvic region of anurans as related to water balance. J. Morphol. 140, 443–460.
Scheuplein, R.J., Blank, I.H., 1971. Permeability of the skin. Physiol. Rev. 51, 702–747.
Skerratt, L.F., Berger, L., Speare, R., Cashins, S., McDonald, K.R., Phillott, A.D., Hines, H.B., Kenyon, N., 2007. Spread of chytridiomycosis has caused the rapid global decline and extinction of frogs. EcoHealth 4, 125–134.
Talbot, C.R., 1992. Regional variation and control of cutaneous gas exchange in bullfrogs. Respir. Physiol. 89, 261–272.
Toledo, R.C., Jared, C., 1993. Cutaneous adaptations to water balance in amphibians. Comp. Biochem. Physiol. Part A: Physiol. 105, 593–608.
VCCLAB, 2005. ALOGPS 2.1. Virtual Computational Chemistry Laboratory. http://www.vcclab.org/lab/alogps/.
Vickaryous, M.K., Sire, J.-Y., 2009. The integumentary skeleton of tetrapods: origin, evolution and development. J. Anat. 214, 441–464.
Withers, P.C., Hillman, S.S., Drewes, R.C., 1984. Evaporative water loss and skin lipids of anuran amphibians. J. Exp. Zool. 232, 11–17.
Wright, K.M., Whitaker, B.R., 2001. Pharmacotherapeutics. In: Wright, K.M., Whitaker, B.R. (Eds.), Amphibian Medicine and Captive Husbandry, 1st ed. Krieger Publishing Company, Malabar, FL pp. 309-332.
Wygoda, M., 1984. Low cutaneous evaporative Water loss in arboreal frogs. Physiol. Zool. 57, 329–337.
Wygoda, M., 1988. Adaptive control of Water loss resistance in an arboreal frog. Herpetologica 44, 251–257.
Yorio, T., Bentley, P.J., 1977. Asymmetrical permeability of the integument of tree frogs (*hylidae*). J. Exp. Biol. 67, 197–204.
Young, J.E., Christian, K.A., Donnellan, S., Tracy, C.R., Parry, D., 2005. Comparative analysis of cutaneous evaporative water loss in frogs demonstrated correlation with ecological habitats. Physiol. Biochem. Zool. 78, 847–856.
Zhang, Q., Grice, J.E., Li, P., Jepps, O.G., Wang, G.-J., Roberts, M.S., 2009. Skin solubility determines maximum transepidermal flux for similar size molecules. Pharm. Res. 26, 1974–1985.

Appendix 2b

Effects of skin region and relative lipophilicity on percutaneous absorption in the toad *Rhinella marina*. Llewelyn VK, Berger L, Glass BD. *Environmental Toxicology and Chemistry*, 38(2). http://dx.doi.org/10.1002/etc.4302

Environmental Toxicology and Chemistry—Volume 38, Number 2—pp. 361–367, 2019
Received: 22 May 2018 | Revised: 2 July 2018 | Accepted: 23 October 2018

Environmental Toxicology

Effects of Skin Region and Relative Lipophilicity on Percutaneous Absorption in the Toad *Rhinella marina*

Victoria K. Llewelyn,[a,*] Lee Berger,[b] and Beverley D. Glass[a]

[a]Pharmacy, College of Medicine and Dentistry, James Cook University, Townsville, Queensland, Australia
[b]One Health Research Group, College of Public Health, Medical and Veterinary Sciences, James Cook University, Townsville, Queensland, Australia

Abstract: Owing to the dynamic interaction between frog skin and the environment, xenobiotics in frog habitats are of particular concern, and knowledge of percutaneous absorption in frog skin is necessary for risk-mitigation purposes. Baseline transdermal kinetics in adult aquatic and arboreal frog species have recently been reported; however, there is little information regarding absorption kinetics in adult terrestrial species. The present study investigated the in vitro absorption kinetics of 3 model chemicals—caffeine, benzoic acid, and ibuprofen—through different skin regions in the terrestrial toad *Rhinella marina*. Caffeine flux was consistently higher than that of the other 2 chemicals ($p < 0.001$), whereas the fluxes of the moderately and highly lipophilic chemicals (benzoic acid and ibuprofen) were similar, regardless of skin region. When considering individual chemicals, caffeine demonstrated increased flux through the ventral pelvic skin compared with the ventral thoracic or dorsal skin regions. Flux did not differ between skin regions for either benzoic acid or ibuprofen. These findings have implications for management of environmental contamination in frog habitats, as many environmental xenobiotics are of moderate to high lipophilicity and would be expected to be equally absorbed from all skin surfaces in terrestrial toads. *Environ Toxicol Chem* 2019;38:361–367. © 2018 SETAC

Keywords: Absorption; Amphibians; Octanol–water partition coefficient; Toxicokinetics; Wildlife toxicology; Skin

This article includes online-only Supplemental Data.
* Address correspondence to tori.llewelyn@jcu.edu.au
Published online 29 October 2018 in Wiley Online Library (wileyonlinelibrary.com).
DOI: 10.1002/etc.4302

Appendix 3

Ethics Application A2222

8730

Project title: Development and validation of a model for transdermal drug delivery in frogs

Principal Investigator: Llewelyn, Tori

Start: 04-Sep-15 **End:** 01-Sep-18 **Approved:** 08-Sep-15

Termination Dates	Notes	Date Approved
01-Sep-18	No extensions recorded	

Research participants

1	Llewelyn, Tori	Staff	P	04-Sep-15 to 01-Sep-18
2	Glass, Beverley	Staff	S	04-Sep-15 to 01-Sep-18
3	Berger, Lee	Staff	S	04-Sep-15 to 01-Sep-18

Amendment History		Date requested
17-Aug-16	- Additional animal species and numbers (40 Litoria caerulea)	01-Aug-16
01-Jun-18	- Additional animal numbers (20 cane toads)	09-May-18

Provisos	Date	Assessed by	Assessment
September 201	04-Sep-15	Meeting	Pending
	Pending		
September 201	04-Sep-15	Meeting	Conditional Approval
	- In reference to paragraph 2 of section 13, can you please confirm if there will be any frogs euthanased considering toads will be used in this project.		
September 201	04-Sep-15	Meeting	Approved
	~		

Summary totals of all animals in the project:

Requested	Approved	Life Stage	Source	Category	Purpose
40	40	Adult	Other	Animal unconscious without recovery	Understanding of human or animal biology
60	60	Adult	Wild	Animal unconscious without recovery	Understanding of human or animal biology

Details of animals in the project:

Bufonidae

Requested	Approved	Life Stage	Source	Category	Purpose
Bufo marinus		Cane Toad			
60	60	Adult	Wild	Animal unconscious without recovery	Understanding of human or animal biology

Hylidae

Requested	Approved	Life Stage	Source	Category	Purpose
Litoria caerulea		Green Treefrog			

40	40	Adult	Other	Animal unconscious without recovery	Understanding of human or animal biology

Facilities used in the project:

Facility	Additional Information
Bush House (Building 70)	

Appendix 4a

The full dataset for the following output is available online:

Llewelyn, V. In vitro percutaneous absorption data for model chemicals in Litoria caerulea and Rhinella marina: chemicals formulated in Amphibian Ringer's solution [Internet]. James Cook University; 2019. Available from: http://dx.doi.org/10.25903/5d4a64751b5de

Statistical output from R

```
> library(nlme)
> flux.lme.LC = lme(Flux ~ Chemical*Region + Sex + Weight, random= ~1|AnimalID,  we
ights=varIdent(form = ~1|Comb),
+                   data=Frogs,control = list(opt = "optim"))
> anova(flux.lme.LC)
                numDF denDF   F-value p-value
(Intercept)         1    16  41.03324  <.0001
Chemical            2    16  73.81341  <.0001
Region              1    14 121.97780  <.0001
Sex                 1    16   0.14599  0.7074
Weight              1    16   3.28447  0.0887
Chemical:Region     2    14  43.31590  <.0001

> summary(flux.lme.LC) #weight and sex not significant. everything else is
Linear mixed-effects model fit by REML
 Data: Frogs
       AIC      BIC   logLik
  174.2568 195.2748 -72.1284

Random effects:
 Formula: ~1 | AnimalID
        (Intercept) Residual
StdDev:  0.06898584  5.96057

Variance function:
 Structure: Different standard deviations per stratum
 Formula: ~1 | Comb
 Parameter estimates:
Benzoic acid V    Ibuprofen D    Ibuprofen V Benzoic acid D     Caffeine D     Caff
eine V
  1.0000000000   0.0001198429   0.0523036445   0.3261271951   0.2976397613   5.3699
194148
Fixed effects: Flux ~ Chemical * Region + Sex + Weight
                                  Value Std.Error DF   t-value p-value
(Intercept)                    7.37656  1.316532 16  5.603024  0.0000
ChemicalCaffeine              -4.36218  1.144616 16 -3.811041  0.0015
ChemicalIbuprofen             -6.90505  1.297652 16 -5.321185  0.0001
RegionVentral                 13.07692  2.309196 14  5.662973  0.0001
SexMale                        0.66556  1.208770 16  0.550609  0.5895
```

```
Weight                            -0.01607  0.009928 16 -1.618818  0.1250
ChemicalCaffeine:RegionVentral     82.90365 12.339128 14  6.718760  0.0000
ChemicalIbuprofen:RegionVentral   -11.72025  2.312701 14 -5.067775  0.0002
 Correlation:
                                  (Intr) ChmclC ChmclI RgnVnt SexMal Weight ChC:RV
ChemicalCaffeine                  -0.611
ChemicalIbuprofen                 -0.989  0.615
RegionVentral                     -0.368  0.309  0.369
SexMale                           -0.708  0.136  0.734  0.152
Weight                            -0.172  0.036  0.029  0.030 -0.104
ChemicalCaffeine:RegionVentral     0.071 -0.096 -0.072 -0.188 -0.034 -0.001
ChemicalIbuprofen:RegionVentral    0.368 -0.309 -0.368 -0.998 -0.152 -0.030  0.187

Standardized Within-Group Residuals:
        Min          Q1         Med          Q3         Max
-1.87664352 -0.44765388 -0.01039354  0.16184468  1.89043736

Number of Observations: 38
Number of Groups: 21

> #rerun model as combination, then look at pairwise interactions
> flux2.lme.LC = lme(Flux ~ Comb, random= ~1|AnimalID,  weights=varIdent(form = ~1|
Comb),
+                    data=Frogs)
> library(multcomp)
> #Tukey's post-hoc; #mcp = multiple comparisons - all interactions compared
> compare = glht(flux2.lme.LC, linfct = mcp(Comb="Tukey"))
> summary(compare)

          Simultaneous Tests for General Linear Hypotheses

Multiple Comparisons of Means: Tukey Contrasts


Fit: lme.formula(fixed = Flux ~ Comb, data = Frogs, random = ~1 |
    AnimalID, weights = varIdent(form = ~1 | Comb))

Linear Hypotheses:
                                     Estimate Std. Error z value Pr(>|z|)
Benzoic acid V - Benzoic acid D == 0  13.0520     2.2129   5.898   <0.001 ***
Caffeine D - Benzoic acid D == 0      -4.3561     1.0722  -4.063   <0.001 ***
Caffeine V - Benzoic acid D == 0      91.7452    12.1116   7.575   <0.001 ***
Ibuprofen D - Benzoic acid D == 0     -7.2139     0.8172  -8.828   <0.001 ***
Ibuprofen V - Benzoic acid D == 0     -5.8573     0.8270  -7.082   <0.001 ***
Caffeine D - Benzoic acid V == 0     -17.4081     2.1713  -8.017   <0.001 ***
Caffeine V - Benzoic acid V == 0      78.6932    12.2579   6.420   <0.001 ***
Ibuprofen D - Benzoic acid V == 0    -20.2659     2.0574  -9.850   <0.001 ***
Ibuprofen V - Benzoic acid V == 0    -18.9093     2.0613  -9.173   <0.001 ***
Caffeine V - Caffeine D == 0          96.1013    12.1040   7.940   <0.001 ***
Ibuprofen D - Caffeine D == 0         -2.8578     0.6957  -4.108   <0.001 ***
Ibuprofen V - Caffeine D == 0         -1.5012     0.7073  -2.122    0.197
Ibuprofen D - Caffeine V == 0       -98.9591    12.0841  -8.189   <0.001 ***
```

```
Ibuprofen V - Caffeine V == 0        -97.6024    12.0848  -8.076   <0.001 ***
Ibuprofen V - Ibuprofen D == 0         1.3567     0.1273  10.659   <0.001 ***
---
Signif. codes:  0 ‘***’ 0.001 ‘**’ 0.01 ‘*’ 0.05 ‘.’ 0.1 ‘ ’ 1
(Adjusted p values reported -- single-step method)
```

Appendix 4b

The full dataset for the following output is available online:

Llewelyn, V. In vitro percutaneous absorption data for model chemicals in Litoria caerulea and Rhinella marina: chemicals formulated in Amphibian Ringer's solution [Internet]. James Cook University; 2019. Available from: http://dx.doi.org/10.25903/5d4a64751b5de

Statistical output from R

```
> library(nlme)
> Flux.RM.Var.Noweight = lme(Flux ~ Chemical*SubRegion, random= ~1|AnimalID,
+                            weights=varIdent(form = ~1|SubRegion),  data=Toads)
> anova(Flux.RM.Var.Noweight)
                   numDF denDF   F-value p-value
(Intercept)            1    47 245.17251  <.0001
Chemical               2    14 161.85460  <.0001
SubRegion              2    47   4.46993  0.0167
Chemical:SubRegion     4    47   8.21581  <.0001

> summary(Flux.RM.Var.Noweight)
Linear mixed-effects model fit by REML
 Data: Toads
       AIC      BIC    logLik
  451.6335 479.0749 -212.8168

Random effects:
 Formula: ~1 | AnimalID
        (Intercept) Residual
StdDev:    7.507291 3.843049

Variance function:
 Structure: Different standard deviations per stratum
 Formula: ~1 | SubRegion
 Parameter estimates:
       D        T        P
1.000000 2.749162 1.171809
Fixed effects: Flux ~ Chemical * SubRegion
                                Value Std.Error DF   t-value p-value
(Intercept)                  13.23395  3.084657 47  4.290252  0.0001
ChemicalCaffeine             65.52645  4.718463 14 13.887244  0.0000
ChemicalIbuprofen           -11.54251  4.741012 14 -2.434609  0.0289
SubRegionP                   -1.99051  2.176562 47 -0.914522  0.3651
SubRegionT                   -3.90412  4.453598 47 -0.876621  0.3852
ChemicalCaffeine:SubRegionP  16.61191  3.204731 47  5.183559  0.0000
ChemicalIbuprofen:SubRegionP  1.81379  3.018522 47  0.600888  0.5508
ChemicalCaffeine:SubRegionT   1.45212  6.605754 47  0.219826  0.8270
ChemicalIbuprofen:SubRegionT  3.47838  6.137972 47  0.566698  0.5736
 Correlation:
```

```
                           (Intr) ChmclC ChmclI SbRgnP SbRgnT CC:SRP CI:SRP CC:SR
T
ChemicalCaffeine           -0.654
ChemicalIbuprofen          -0.651  0.425
SubRegionP                 -0.248  0.162  0.161
SubRegionT                 -0.090  0.059  0.058  0.127
ChemicalCaffeine:SubRegionP  0.168 -0.208 -0.110 -0.679 -0.086
ChemicalIbuprofen:SubRegionP  0.179 -0.117 -0.237 -0.721 -0.092  0.490
ChemicalCaffeine:SubRegionT  0.060 -0.087 -0.039 -0.086 -0.674  0.128  0.062
ChemicalIbuprofen:SubRegionT  0.065 -0.042 -0.102 -0.092 -0.726  0.063  0.161  0.48
9

Standardized Within-Group Residuals:
        Min          Q1         Med          Q3         Max
-1.84698826 -0.32342459 -0.01191303  0.22591960  3.05038533

Number of Observations: 70
Number of Groups: 17

> #rerun model as combination, then look at pairwise interactions
> Flux.RM.lmecomb = lme(Flux ~ Comb, random= ~1|AnimalID,
+                       weights=varIdent(form = ~1|SubRegion),  data=Toads
> library(multcomp)
> #Tukey's post-hoc; #mcp = multiple comparisons - all interactions compared
> MCP.flux.RM<-glht(Flux.RM.lmecomb, linfct = mcp(Comb="Tukey"))
> summary(MCP.flux.RM)

         Simultaneous Tests for General Linear Hypotheses

Multiple Comparisons of Means: Tukey Contrasts


Fit: lme.formula(fixed = Flux ~ Comb, data = Toads, random = ~1 |
    AnimalID, weights = varIdent(form = ~1 | SubRegion))

Linear Hypotheses:
                                    Estimate Std. Error z value Pr(>|z|)
Benzoic acid P - Benzoic acid D == 0  -1.9905     2.1766  -0.915   0.9879
Benzoic acid T - Benzoic acid D == 0  -3.9041     4.4536  -0.877   0.9908
Caffeine D - Benzoic acid D == 0      65.5264     4.7185  13.887   <0.001 ***
Caffeine P - Benzoic acid D == 0      80.1478     4.9843  16.080   <0.001 ***
Caffeine T - Benzoic acid D == 0      63.0744     6.5659   9.606   <0.001 ***
Ibuprofen D - Benzoic acid D == 0    -11.5425     4.7410  -2.435   0.2125
Ibuprofen P - Benzoic acid D == 0    -11.7192     4.8383  -2.422   0.2182
Ibuprofen T - Benzoic acid D == 0    -11.9683     6.0700  -1.972   0.4897
Benzoic acid T - Benzoic acid P == 0  -1.9136     4.7022  -0.407   1.0000
Caffeine D - Benzoic acid P == 0      67.5170     4.8654  13.877   <0.001 ***
Caffeine P - Benzoic acid P == 0      82.1384     5.1236  16.032   <0.001 ***
Caffeine T - Benzoic acid P == 0      65.0650     6.6723   9.752   <0.001 ***
Ibuprofen D - Benzoic acid P == 0     -9.5520     4.8872  -1.954   0.5022
Ibuprofen P - Benzoic acid P == 0     -9.7287     4.9816  -1.953   0.5032
Ibuprofen T - Benzoic acid P == 0     -9.9777     6.1849  -1.613   0.7409
```

```
Caffeine D - Benzoic acid T == 0      69.4306     6.2958  11.028   <0.001 ***
Caffeine P - Benzoic acid T == 0      84.0520     6.4974  12.936   <0.001 ***
Caffeine T - Benzoic acid T == 0      66.9786     7.7772   8.612   <0.001 ***
Ibuprofen D - Benzoic acid T == 0     -7.6384     6.3127  -1.210   0.9348
Ibuprofen P - Benzoic acid T == 0     -7.8151     6.3861  -1.224   0.9306
Ibuprofen T - Benzoic acid T == 0     -8.0641     7.3633  -1.095   0.9631
Caffeine P - Caffeine D == 0          14.6214     2.3522   6.216   <0.001 ***
Caffeine T - Caffeine D == 0          -2.4520     4.8787  -0.503   0.9998
Ibuprofen D - Caffeine D == 0        -77.0690     5.0706 -15.199   <0.001 ***
Ibuprofen P - Caffeine D == 0        -77.2457     5.1616 -14.965   <0.001 ***
Ibuprofen T - Caffeine D == 0        -77.4947     6.3308 -12.241   <0.001 ***
Caffeine T - Caffeine P == 0         -17.0734     5.1362  -3.324   0.0186 *
Ibuprofen D - Caffeine P == 0        -91.6904     5.3188 -17.239   <0.001 ***
Ibuprofen P - Caffeine P == 0        -91.8671     5.4057 -16.994   <0.001 ***
Ibuprofen T - Caffeine P == 0        -92.1161     6.5313 -14.104   <0.001 ***
Ibuprofen D - Caffeine T == 0        -74.6170     6.8234 -10.935   <0.001 ***
Ibuprofen P - Caffeine T == 0        -74.7937     6.8913 -10.853   <0.001 ***
Ibuprofen T - Caffeine T == 0        -75.0427     7.8055  -9.614   <0.001 ***
Ibuprofen P - Ibuprofen D == 0        -0.1767     2.0914  -0.084   1.0000
Ibuprofen T - Ibuprofen D == 0        -0.4257     4.2238  -0.101   1.0000
Ibuprofen T - Ibuprofen P == 0        -0.2490     4.3240  -0.058   1.0000
---
Signif. codes:  0 ‘***’ 0.001 ‘**’ 0.01 ‘*’ 0.05 ‘.’ 0.1 ‘ ’ 1
(Adjusted p values reported -- single-step method)
```

Appendix 5

Percutaneous absorption in frog species: variability in skin may influence delivery of therapeutics. Llewelyn VK, Berger L, Glass BD. *Journal of Veterinary Pharmacology and Therapeutics*, 41(Suppl. 1). https://doi.org/10.1111/jvp.12639

Content has been removed
due to copyright restrictions

Appendix 6

Haematoxylin and Eosin (H&E) Protocol

Tissue is processed, embedded in paraffin blocks, cut into sections (5 µm thick) with a microtome, and dried (minimum 1 hour in dryer or on bench) onto Superfrost Plus adhesive microscope slides (Thermo Scientific).

Deparaffinization and rehydration

1. Place slides into a metal rack.
2. Put slides into xylene container 1 for 2 min.
3. Put slides into xylene container 2 for 2 min.
4. Put slides into 100% ethanol container 1 for 1 min
5. Put slides into 100% ethanol container 2 for 1 min.
6. Put slides into 70% ethanol container 3 for 1 min
7. Rinse in tap water bath (outside and then inside container).

H & E staining and dehydration

1. Put slides into hematoxylin for 3 min.
2. Rinse slides in tap water bath (outside and then inside container).
3. Put slides into Scott's tap water substitute for 20 sec.
4. Rinse in tap water bath (outside and then inside container).
5. Put slides into eosin for 1 min.
6. Rinse in tap water bath (outside and then inside container).
7. Put slides into ethanol container 4 for 1 min
8. Put slides into ethanol container 5 for 1 min.
9. Put slides into ethanol container 6 for 1 min
10. Put slides into xylene container 3 for 2 min.
11. Put slides into xylene container 4 for 2 min.

Mounting slides

1. Fill glass syringe with DPX
2. Put a drop of DPX on coverslip (40 mm) and add slide (facing coverslip).
3. Press any air bubbles on coverslip with toothpick.
4. Put syringe back into xylene after use.
5. Dry slides horizontally in dryer or on bench.

Appendix 7

The full dataset for the following output is available online:

Llewelyn, V. In vitro percutaneous absorption data for model chemicals in Litoria caerulea and Rhinella marina: chemicals formulated in Amphibian Ringer's solution [Internet]. James Cook University; 2019 Available from: http://dx.doi.org/10.25903/5d4a64751b5de

"Full" original model using logP (i.e., includes all other independent variables)

```
> library(nlme)
> #Full model with variability in region and species
> kp.fullmodel.logp1 = lme(Kp ~ Species*LogP*Region + Sex * Weight, random= ~1|Anim
alID,
+                          weights=(varComb(varIdent(form=~1|Species), varIdent(for
m=~1|Region))),
+                          data=Species.Model,method="ML")
> kp.fullmodel.logp1
Linear mixed-effects model fit by maximum likelihood
  Data: Species.Model
  Log-likelihood: 592.0481
  Fixed: Kp ~ Species * LogP * Region + Sex * Weight
                        (Intercept)              SpeciesRhinella marina
LogP
                       6.453438e-04                        2.418547e-03
-1.064306e-06
                            RegionV                             SexMale
Weight
                       4.629441e-03                       -1.490992e-04
7.883060e-06
        SpeciesRhinella marina:LogP      SpeciesRhinella marina:RegionV
LogP:RegionV
                      -5.971505e-05                       -4.657881e-03
-4.601539e-04
                     SexMale:Weight SpeciesRhinella marina:LogP:RegionV
                      -6.420907e-07                        2.874988e-04

Random effects:
 Formula: ~1 | AnimalID
         (Intercept)     Residual
StdDev: 0.0005656603 0.0009466111

Combination of variance functions:
 Structure: Different standard deviations per stratum
 Formula: ~1 | Species
 Parameter estimates:
Litoria caerulea  Rhinella marina
       1.0000000        0.9397479
 Structure: Different standard deviations per stratum
```

```
 Formula: ~1 | Region
 Parameter estimates:
       V        D
1.000000 0.941258
Number of Observations: 108
Number of Groups: 38
> anova(kp.fullmodel.logp1)
                   numDF denDF  F-value p-value
(Intercept)            1    66 537.1525  <.0001
Species                1    31   4.5630  0.0407
LogP                   1    31   9.0071  0.0053
Region                 1    66  25.7854  <.0001
Sex                    1    31   0.2918  0.5929
Weight                 1    31   0.2351  0.6312
Species:LogP           1    31   0.1835  0.6713
Species:Region         1    66 108.8840  <.0001
LogP:Region            1    66   5.6590  0.0203
Sex:Weight             1    31   0.0001  0.9928
Species:LogP:Region    1    66   1.4397  0.2345
> summary (kp.fullmodel.logp1)
Linear mixed-effects model fit by maximum likelihood
 Data: Species.Model
        AIC       BIC   logLik
  -1154.096 -1113.864 592.0481

Random effects:
 Formula: ~1 | AnimalID
         (Intercept)     Residual
StdDev: 0.0005656603 0.0009466111

Combination of variance functions:
 Structure: Different standard deviations per stratum
 Formula: ~1 | Species
 Parameter estimates:
Litoria caerulea  Rhinella marina
       1.0000000        0.9397479
 Structure: Different standard deviations per stratum
 Formula: ~1 | Region
 Parameter estimates:
       V        D
1.000000 0.941258
Fixed effects: Kp ~ Species * LogP * Region + Sex * Weight
                                        Value    Std.Error DF   t-value p-value
(Intercept)                          0.000645344 0.0021582559 66  0.299012  0.7659
SpeciesRhinella marina               0.002418547 0.0009695013 31  2.494630  0.0181
LogP                                -0.000001064 0.0001823466 31 -0.005837  0.9954
RegionV                              0.004629441 0.0004972603 66  9.309894  0.0000
SexMale                             -0.000149099 0.0021529784 31 -0.069253  0.9452
Weight                               0.000007883 0.0001103538 31  0.071434  0.9435
SpeciesRhinella marina:LogP         -0.000059715 0.0002408482 31 -0.247936  0.8058
SpeciesRhinella marina:RegionV      -0.004657881 0.0006102970 66 -7.632155  0.0000
LogP:RegionV                        -0.000460154 0.0001953430 66 -2.355621  0.0215
```

```
SexMale:Weight                       -0.000000642 0.0001105710 31 -0.005807  0.9954
SpeciesRhinella marina:LogP:RegionV  0.000287499 0.0002396047 66  1.199888  0.2345
 Correlation:
                                     (Intr) SpcsRm LogP   ReginV SexMal Weight SpRm:
LP SRm:RV LgP:RV SxMl:W
SpeciesRhinella marina               -0.052
LogP                                 -0.152  0.224
RegionV                              -0.156  0.225  0.432
SexMale                              -0.975  0.042  0.048  0.024
Weight                               -0.964 -0.005 -0.063  0.028  0.967
SpeciesRhinella marina:LogP           0.112 -0.589 -0.754 -0.305 -0.065  0.049
SpeciesRhinella marina:RegionV        0.127 -0.297 -0.352 -0.814 -0.021 -0.023  0.38
1
LogP:RegionV                          0.087 -0.176 -0.528 -0.754  0.010  0.001  0.38
8   0.614
SexMale:Weight                        0.962 -0.049  0.063 -0.023 -0.971 -0.998 -0.02
8   0.020 -0.003
SpeciesRhinella marina:LogP:RegionV -0.071  0.224  0.431  0.615 -0.008 -0.001 -0.49
3  -0.762 -0.815  0.003

Standardized Within-Group Residuals:
       Min         Q1        Med         Q3        Max
-2.9211758 -0.5593983 -0.0943679  0.4969300  2.7990627

Number of Observations: 108
Number of Groups: 38
```

Residual plots for the “full” original model using logP

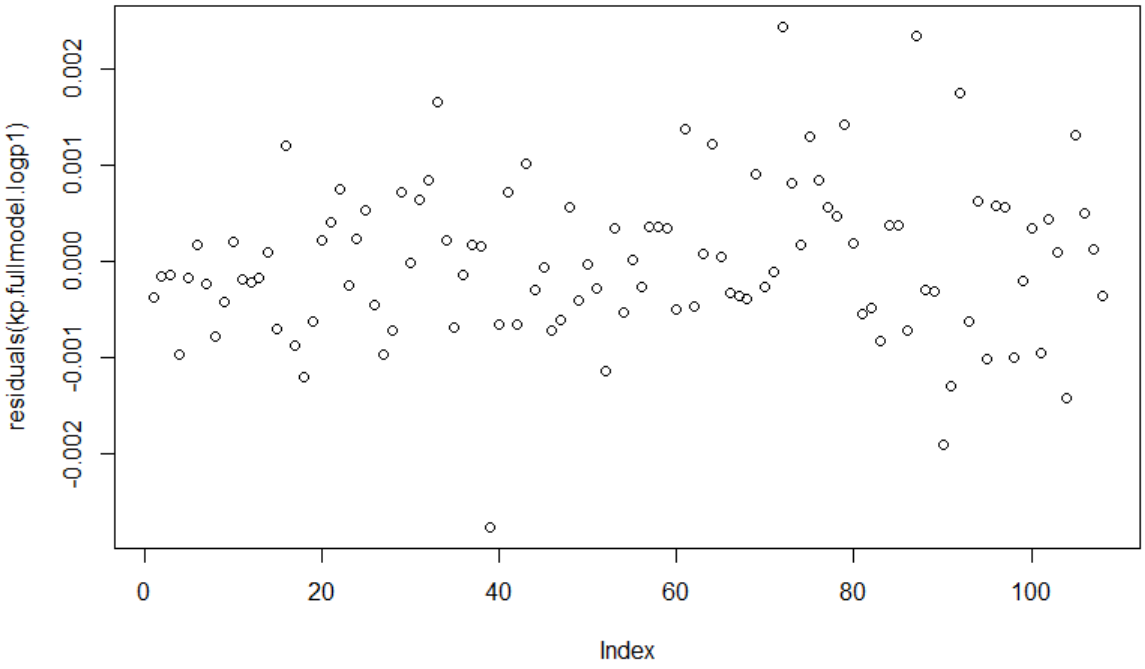

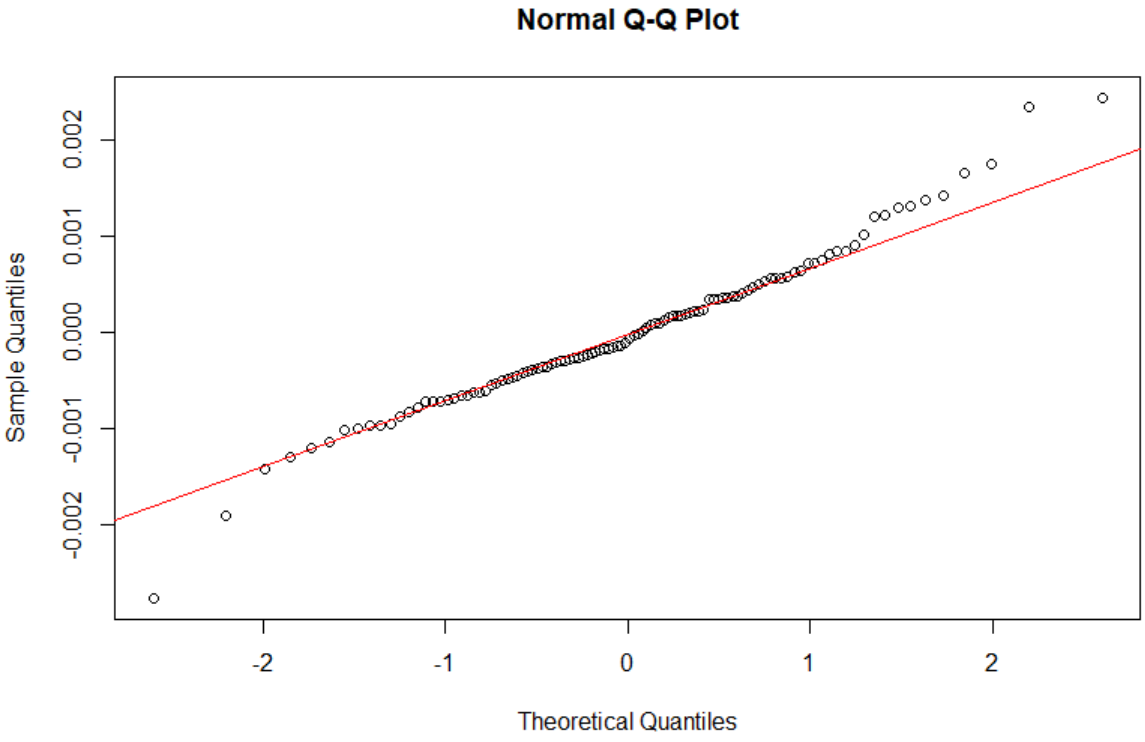

“Full” original model using MW (i.e., includes all other independent variables)

```
> #Model with variability in region and species
> kp.fullmodel.MW1 = lme(Kp ~ Species*MW*Region + Sex + Weight, random= ~1|AnimalID
,
+                       weights=(varComb(varIdent(form=~1|Species), varIdent(form=
~1|Region))),
+                       data=Species.Model,method="ML")
> kp.fullmodel.MW1
Linear mixed-effects model fit by maximum likelihood
  Data: Species.Model
  Log-likelihood: 593.1946
  Fixed: Kp ~ Species * MW * Region + Sex + Weight
                      (Intercept)            SpeciesRhinella marina
MW
                    3.986693e-03                      -9.493576e-04
-1.937285e-05
                         RegionV                           SexMale
Weight
                    3.402754e-03                      -1.572889e-04
1.096317e-05
        SpeciesRhinella marina:MW    SpeciesRhinella marina:RegionV
MW:RegionV
                    1.630833e-05                      -5.070079e-03
1.607570e-06
SpeciesRhinella marina:MW:RegionV
                    5.917367e-06

Random effects:
 Formula: ~1 | AnimalID
         (Intercept)    Residual
StdDev: 0.0004527049 0.001016588

Combination of variance functions:
 Structure: Different standard deviations per stratum
 Formula: ~1 | Species
 Parameter estimates:
Litoria caerulea  Rhinella marina
       1.0000000        0.9671466
 Structure: Different standard deviations per stratum
 Formula: ~1 | Region
 Parameter estimates:
       V        D
1.000000 0.816926
Number of Observations: 108
Number of Groups: 38
> anova(kp.fullmodel.MW1)
                  numDF denDF  F-value p-value
(Intercept)           1    66 624.4597  <.0001
Species               1    32  13.1921  0.0010
MW                    1    32   8.9435  0.0053
Region                1    66  27.3190  <.0001
```

```
Sex                   1    32   0.0714  0.7910
Weight                1    32   4.3819  0.0443
Species:MW            1    32  12.0420  0.0015
Species:Region        1    66 105.3017  <.0001
MW:Region             1    66   1.3255  0.2538
Species:MW:Region     1    66   0.3049  0.5827
> summary(kp.fullmodel.MW1)
Linear mixed-effects model fit by maximum likelihood
 Data: Species.Model
        AIC       BIC   logLik
  -1158.389 -1120.839 593.1946

Random effects:
 Formula: ~1 | AnimalID
         (Intercept)    Residual
StdDev: 0.0004527049 0.001016588

Combination of variance functions:
 Structure: Different standard deviations per stratum
 Formula: ~1 | Species
 Parameter estimates:
Litoria caerulea  Rhinella marina
       1.0000000        0.9671466
 Structure: Different standard deviations per stratum
 Formula: ~1 | Region
 Parameter estimates:
       V        D
1.000000 0.816926
Fixed effects: Kp ~ Species * MW * Region + Sex + Weight
                                       Value    Std.Error DF    t-value p-value
(Intercept)                         0.003986693 0.0014061899 66  2.8351030  0.0061
SpeciesRhinella marina             -0.000949358 0.0015912610 32 -0.5966071  0.5550
MW                                 -0.000019373 0.0000073090 32 -2.6505301  0.0124
RegionV                             0.003402754 0.0015952917 66  2.1329980  0.0366
SexMale                            -0.000157289 0.0004149180 32 -0.3790843  0.7071
Weight                              0.000010963 0.0000053954 32  2.0319370  0.0505
SpeciesRhinella marina:MW           0.000016308 0.0000088697 32  1.8386655  0.0753
SpeciesRhinella marina:RegionV     -0.005070079 0.0019079134 66 -2.6573948  0.0099
MW:RegionV                          0.000001608 0.0000089110 66  0.1804028  0.8574
SpeciesRhinella marina:MW:RegionV   0.000005917 0.0000107166 66  0.5521709  0.5827
 Correlation:
                                   (Intr) SpcsRm MW     ReginV SexMal Weight SpRm:MW
SRm:RV MW:RgV
SpeciesRhinella marina             -0.719
MW                                 -0.974  0.752
RegionV                            -0.674  0.531  0.671
SexMale                            -0.442  0.168  0.346  0.181
Weight                             -0.123 -0.265  0.045  0.043 -0.095
SpeciesRhinella marina:MW           0.803 -0.924 -0.824 -0.553 -0.285 -0.037
SpeciesRhinella marina:RegionV      0.563 -0.612 -0.561 -0.836 -0.152 -0.027  0.628
MW:RegionV                          0.647 -0.513 -0.667 -0.979 -0.174 -0.033  0.550
0.818
```

```
SpeciesRhinella marina:MW:RegionV -0.538  0.591  0.555  0.814  0.145  0.027 -0.630
-0.978 -0.832

Standardized Within-Group Residuals:
        Min          Q1         Med          Q3         Max
-1.96342631 -0.58799079 -0.09466642  0.43236472  2.59148751

Number of Observations: 108
Number of Groups: 38
```

Residual plots for the “full” original model using MW

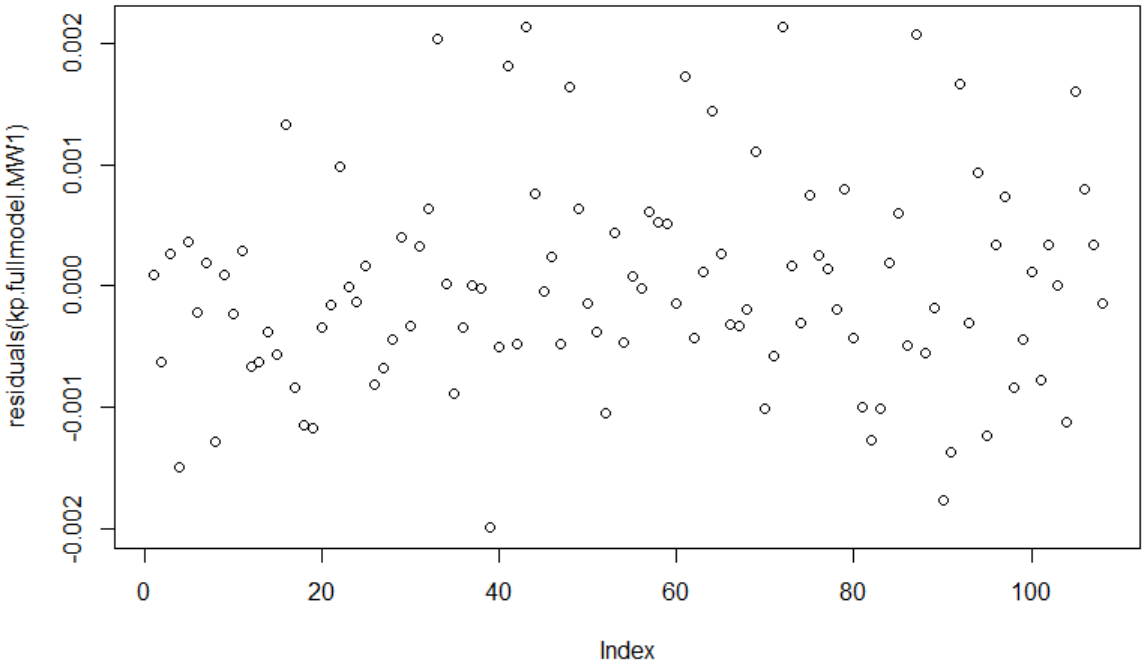

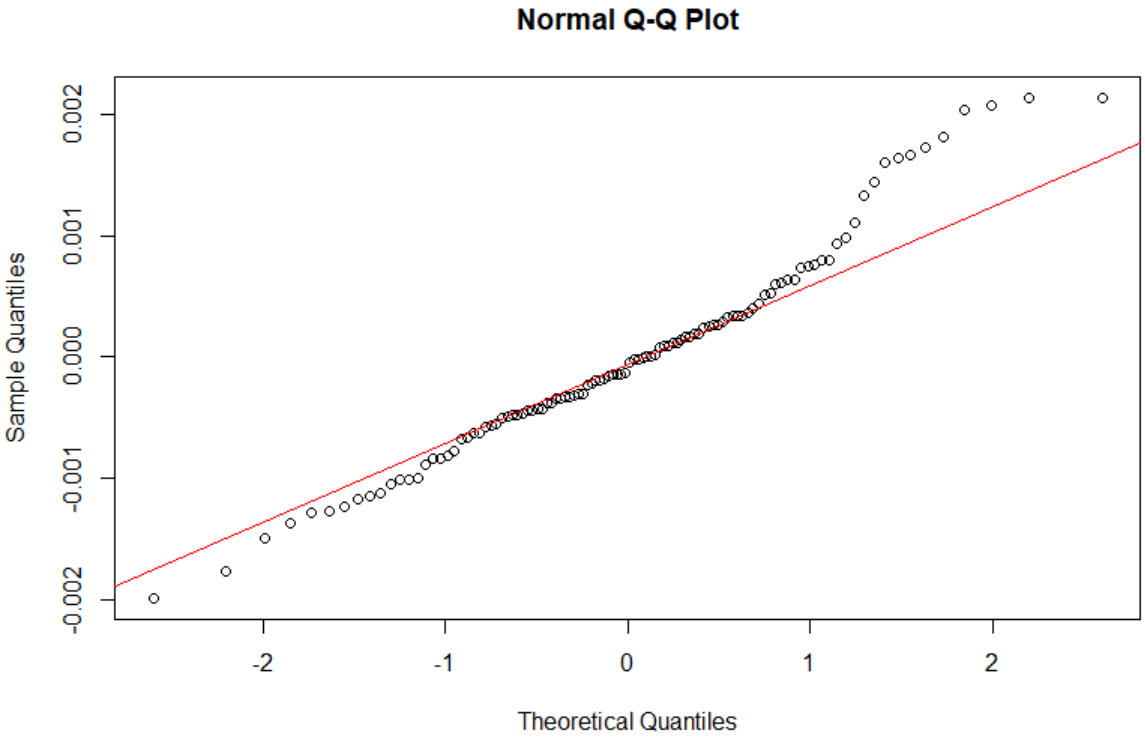

Outputs for final “top” model including logP

```
> FINAL.Kp.logP.REML<-lme(Kp ~ LogP+Region+Species*Region+LogP*Region, random= ~1|A
nimalID,
+                         data=Species.Model)
> anova(FINAL.Kp.logP.REML)
               numDF denDF  F-value p-value
(Intercept)        1    67 534.8849  <.0001
LogP               1    35   9.2672  0.0044
Region             1    67  32.7513  <.0001
Species            1    35   3.2439  0.0803
Region:Species     1    67 117.1537  <.0001
LogP:Region        1    67   6.1821  0.0154
> summary(FINAL.Kp.logP.REML)
Linear mixed-effects model fit by REML
 Data: Species.Model
        AIC       BIC   logLik
  -1072.015 -1051.015 544.0076

Random effects:
 Formula: ~1 | AnimalID
         (Intercept)     Residual
StdDev: 0.0006330886 0.0009071354

Fixed effects: Kp ~ LogP + Region + Species * Region + LogP * Region
                                      Value    Std.Error DF    t-value p-value
(Intercept)                    0.000929590 0.0003417513 67   2.720079  0.0083
LogP                          -0.000080900 0.0001061519 35  -0.762113  0.4511
RegionV                        0.004248649 0.0003732745 67  11.382105  0.0000
SpeciesRhinella marina         0.002875198 0.0003532166 35   8.140042  0.0000
RegionV:SpeciesRhinella marina -0.004085960 0.0003787796 67 -10.787170  0.0000
LogP:RegionV                   -0.000274794 0.0001105200 67  -2.486373  0.0154
 Correlation:
                               (Intr) LogP   ReginV SpcsRm RV:SRm
LogP                           -0.608
RegionV                        -0.644  0.346
SpeciesRhinella marina         -0.625  0.023  0.431
RegionV:SpeciesRhinella marina  0.440 -0.031 -0.656 -0.613
LogP:RegionV                    0.358 -0.572 -0.571 -0.030 -0.014

Standardized Within-Group Residuals:
         Min           Q1          Med           Q3          Max
-2.611806742 -0.530449848  0.004730726  0.464706263  2.692330528

Number of Observations: 108
Number of Groups: 38
```

Residual plots for the final “top” model including logP

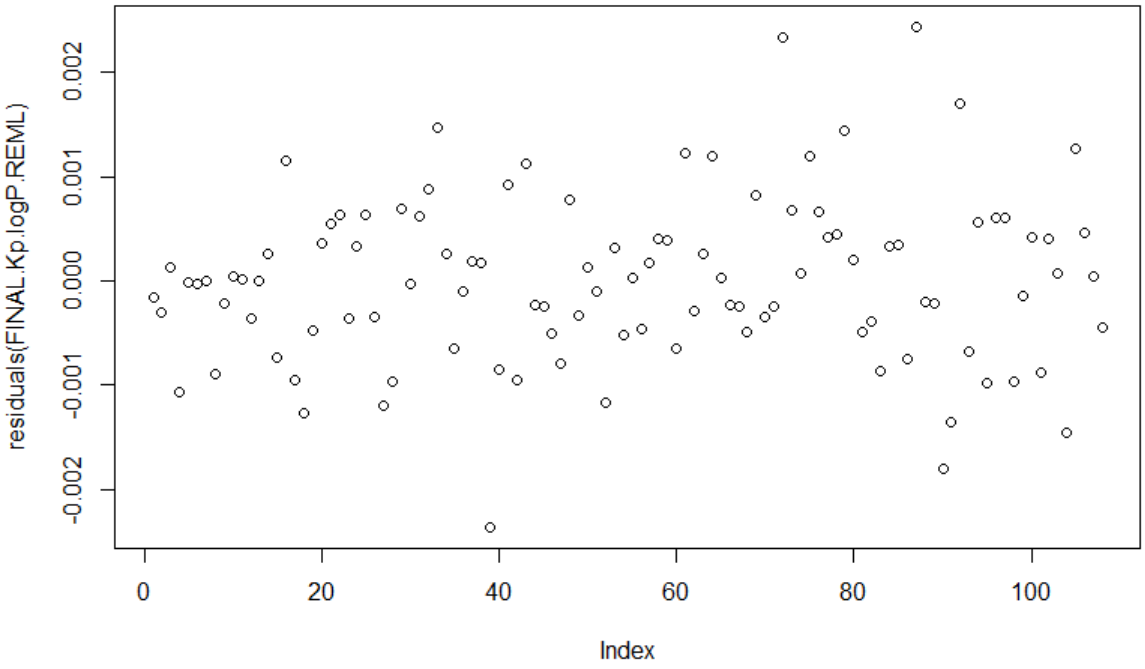

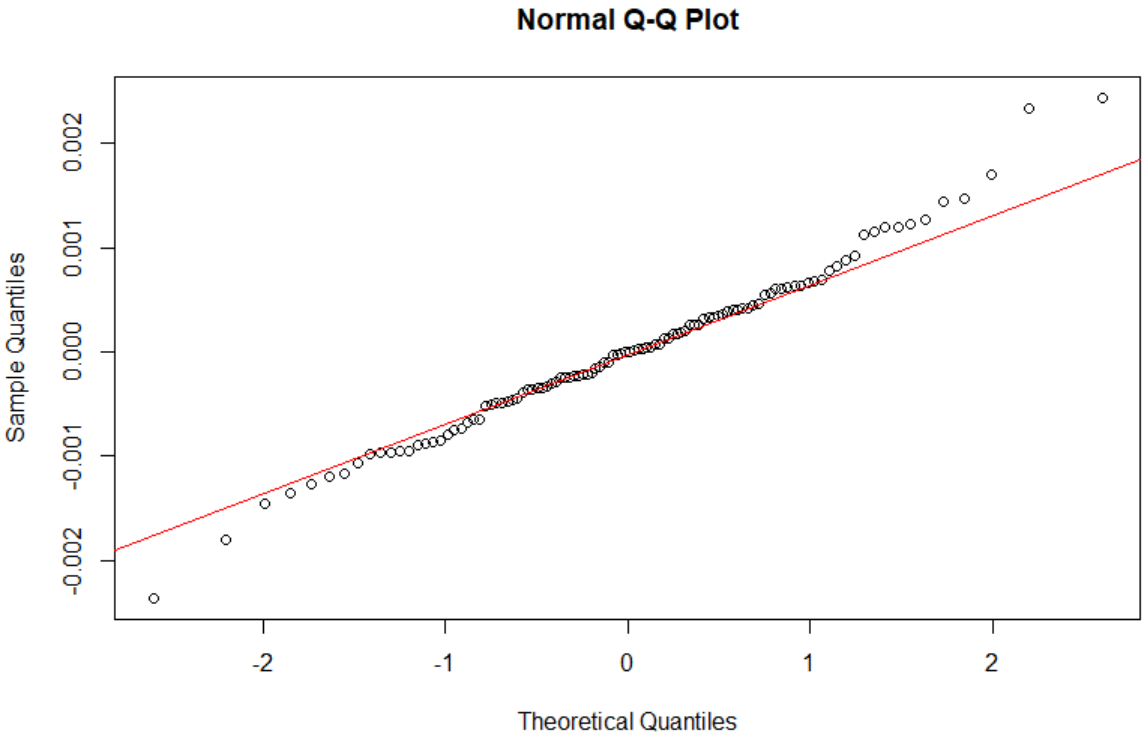

Outputs for final “top” model including MW

```
> FINAL.Kp.MW.REML<-lme(Kp ~ MW+Region + Species*MW+Species*Region, random= ~1|Anim
alID,
+                       data=Species.Model)
> anova(FINAL.Kp.MW.REML)
               numDF denDF  F-value p-value
(Intercept)        1    68 566.2082  <.0001
MW                 1    34   8.0854  0.0075
Region             1    68  30.1372  <.0001
Species            1    34   2.9145  0.0969
MW:Species         1    34  10.6851  0.0025
Region:Species     1    68 108.2521  <.0001
> summary(FINAL.Kp.MW.REML)
Linear mixed-effects model fit by REML
 Data: Species.Model
        AIC       BIC   logLik
  -1058.023 -1037.023 537.0113

Random effects:
 Formula: ~1 | AnimalID
         (Intercept)     Residual
StdDev: 0.0005864584 0.0009340284

Fixed effects: Kp ~ MW + Region + Species * MW + Species * Region
                                       Value    Std.Error DF    t-value p-value
(Intercept)                     0.003962477 0.0009851224 68   4.022320  0.0001
MW                             -0.000018087 0.0000053851 34  -3.358677  0.0019
RegionV                         0.003645649 0.0003154086 68  11.558495  0.0000
SpeciesRhinella marina         -0.000547069 0.0012870199 34  -0.425066  0.6735
MW:SpeciesRhinella marina       0.000019436 0.0000071577 34   2.715408  0.0103
RegionV:SpeciesRhinella marina -0.004052162 0.0003894651 68 -10.404427  0.0000
 Correlation:
                               (Intr) MW     ReginV SpcsRm MW:SRm
MW                             -0.961
RegionV                        -0.277  0.097
SpeciesRhinella marina         -0.765  0.736  0.212
MW:SpeciesRhinella marina       0.723 -0.752 -0.073 -0.962
RegionV:SpeciesRhinella marina  0.224 -0.079 -0.810 -0.224  0.053

Standardized Within-Group Residuals:
        Min          Q1         Med          Q3         Max
-1.84789962 -0.69100293 -0.03306582  0.42409342  2.63603755

Number of Observations: 108
Number of Groups: 38
```

Residual plots for the final “top” model including MW

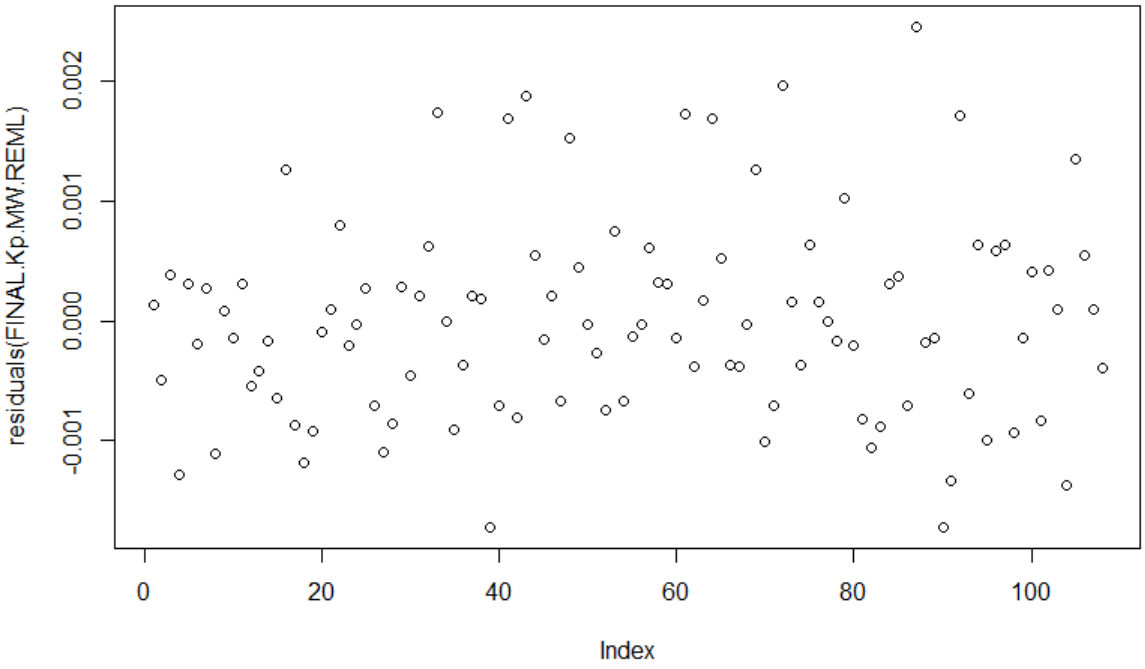

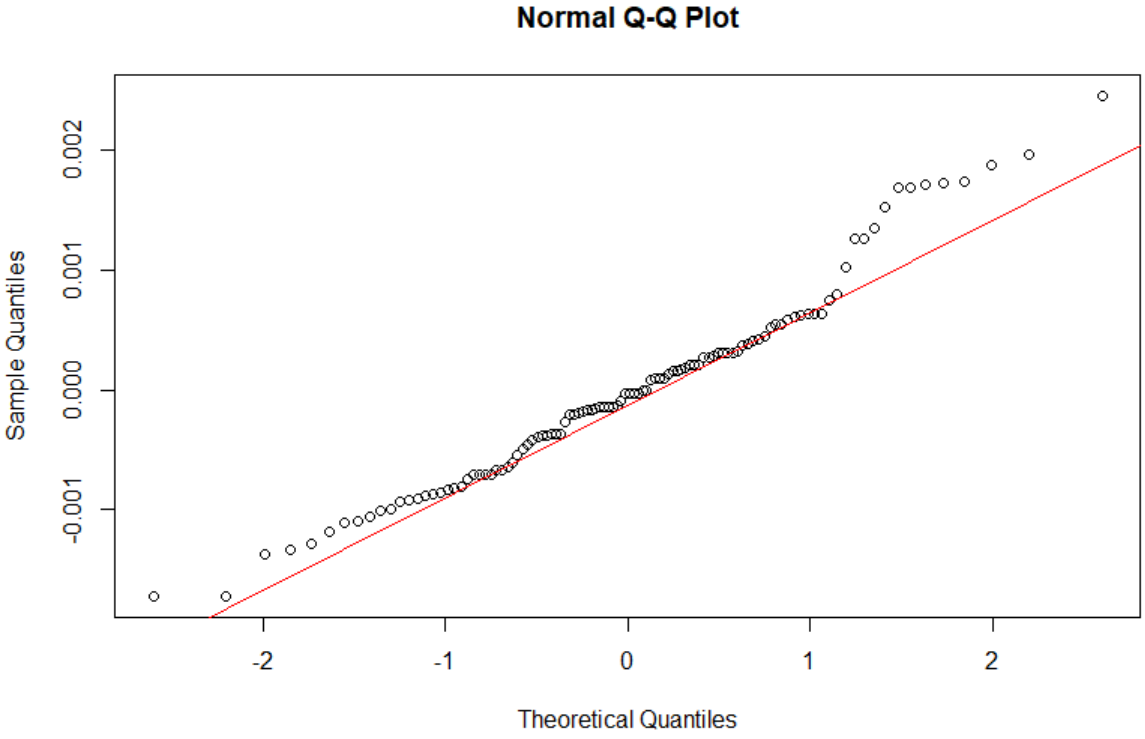

Appendix 8

Permeability of frog skin to chemicals: effect of penetration enhancers. Llewelyn VK, Berger L, Glass BD. *Heliyon*, 5(8):e02127. 2019. Available at: https://doi.org/10.1016/j.heliyon.2019.e02127 under a Creative Commons Attribution Non Commercial-No Derivatives 4.0 International (CC BY-NC-ND 4.0). Full terms at: https://creativecommons.org/licenses/by-nc-nd/4.0/

Heliyon 5 (2019) e02127

Contents lists available at ScienceDirect

Heliyon

journal homepage: www.heliyon.com

Permeability of frog skin to chemicals: effect of penetration enhancers

Victoria K. Llewelyn [a,*], Lee Berger [b], Beverley D. Glass [a]

[a] Pharmacy, College of Medicine and Dentistry, James Cook University, Townsville, 4811, Australia
[b] One Health Research Group, Melbourne Veterinary School, University of Melbourne, Werribee, 3029, Australia

ARTICLE INFO

Keywords:
Pharmaceutical science
Toxicology
Zoology

ABSTRACT

Rarely do commercial chemical products contain solely the active chemical/ingredient. It is therefore important to consider whether ingredients other than the active may: 1) alter absorption of the active chemical, or 2) be absorbed themselves, resulting in systemic effects. Frogs have highly permeable skin and are routinely exposed to commercial chemical products in the environment or therapeutically. Ethanol and propylene glycol (PG), which have known penetration-enhancing effects, are commonly included in such products. The current study has therefore investigated the *in vitro* absorption kinetics through *Rh. marina* skin of three model chemicals – caffeine, benzoic acid, and ibuprofen – formulated individually as solutions containing: 1%, 10% or 30% v/v ethanol, or 20% v/v PG. Differential scanning calorimetry and histology were used to characterise fresh frog skin, investigate the mechanism of these enhancers in frog skin, and to determine whether these enhancers significantly affected skin structure. Results showed that the extent of absorption enhancement was influenced by chemical, enhancer and skin region, and that enhancement was generally not consistent for individual enhancers or skin regions. The exception was 1% v/v ethanol, which did not significantly alter flux across the skin for any of the chemicals evaluated. Caffeine absorption was not enhanced by any of the investigated penetration enhancers, and was in fact significantly reduced by 30% v/v ethanol and PG. Ethanol caused concentration-dependant changes in skin morphology and should be avoided in concentrations ≥10% v/v. PG, however, caused minimal changes to the skin and consistently improved absorption of benzoic acid and ibuprofen through all skin regions. Owing to the significant changes in skin structure following ≥10% v/v ethanol exposure, it is recommended to avoid its use in frogs. For enhancement of penetration of moderately-to-highly lipophilic chemicals, this study has identified 20% v/v PG should to be the enhancer of choice.

1. Introduction

Penetration enhancers, substances that can partition into the skin and increase the absorption of chemicals, are commonly included in agricultural, industrial and therapeutic formulations. There is substantial evidence that these substances are able to significantly reduce the barrier function of the mammalian epidermis, resulting in greater systemic exposure to topically-administered chemicals. However, despite the common inclusion of penetration enhancers in formulations, their impact on absorption in most non-mammalian species remains unknown.

Frog skin is highly-permeable and structurally different from mammalian skin, owing to the role of frog skin in maintaining physiological homeostasis (fluid, electrolyte and acid/base balance). The stratum corneum (SC), accepted as the primary barrier to percutaneous absorption in mammals, is much thinner in frogs. While in mammals the SC is often 10–20 cell layers thick, in frogs it commonly consists of only one or two cell layers [1]. Thus, it is unsurprising that the limited comparative studies of chemical absorption in frog and mammalian skins have reported much higher absorption in frog skin [2, 3]. As absorption rates are already heightened in frogs compared to in mammals, it is likely that inclusion of a penetration enhancer in a chemical formulation will also have a heightened effect in frog skin.

Frogs are experiencing significant population declines and extinctions worldwide. While much of the decline has been attributed to disease, especially infectious chytridiomycosis, habitat change and contamination have also been identified as causative factors [4]. The dynamic interaction between frogs' skin and the immediate environment is the reason for their heightened sensitivity to environmental contaminants, and this heightened sensitivity has, in turn, led to frogs being considered indicators of the relative health of an ecosystem. They therefore represent an ideal non-mammalian candidate in which to investigate the impact of penetration enhancers on percutaneous absorption, as they are

* Corresponding author.
E-mail address: victoria.llewelyn@my.jcu.edu.au (V.K. Llewelyn).

https://doi.org/10.1016/j.heliyon.2019.e02127
Received 2 April 2019; Received in revised form 24 May 2019; Accepted 18 July 2019

likely to encounter these substances in formulations for treatment of disease and in also in the wild.

A variety of ingredients with potential penetration-enhancing effects are regularly included in commercially-available products, particularly as co-solvents (to assist in the dissolution of the active chemical). In therapeutic drug products, the most common co-solvent used is ethanol, although propylene glycol (PG), owing to its relatively lower toxicity *in vivo*, is also widely included, particularly in topical and cosmetic formulations [5]. Further, as commercially-available drug products are often inappropriate for administration directly to exotic species including frogs, clinicians are often required to compound their own formulations. Owing to their availability and favourable solubility profiles, ethanol and PG also represent the most-commonly used solvents used when compounding drug products for topical application. Ethanol also finds extensive use in agricultural and industrial formulations. In particular, the identification of ethanol as a "green" solvent has increased its use in manufacturing, inclusion in fuels, and as a solvent in agrichemicals [6]. PG is most commonly included in antifreeze for aircraft, and so can easily contaminate surrounding environments when in use [7]. While neither PG nor ethanol persist in the environment, acute impacts on wildlife when products containing these ingredients are introduced into the environment cannot be ignored.

Penetration enhancers may influence absorption by allowing higher concentrations of active chemical to be dissolved in the formulation itself, and also by altering the barrier properties of the skin – usually by inducing changes in the lipoid structure/packing of the epidermal layer. Almost all penetration enhancers act via more than one mechanism, and sometimes the primary mechanism of enhancement changes, depending on the concentration of enhancer used. Ethanol is postulated to improve absorption by: increasing chemical solubility in formulation, diffusing itself into the SC thereby improving solubility of the active chemical in the SC, and having a multitude of effects on intradermal lipids, causing lipid fluidisation, restructuring of the lipids, and at high concentrations, lipid extraction from the SC [8]. The mechanism of PG in improving percutaneous absorption is similarly debated; its effects have been attributed to: diffusion into the SC, improving solubility of the active chemical in the SC, interaction with the polar headgroups of the lipid bilayers of the skin altering the lipid packing, and alteration of protein composition in the skin [9, 10]. In order to elucidate the underlying mechanism of penetration enhancers, studies often consider the results of in vitro absorption studies alongside investigations of changes in the skin structure following exposure to the penetration enhancers. Various techniques have been used to study the effect of penetration enhancers on skin structure, including light, electron and confocal microscopy, Raman and Fourier transform infrared spectroscopy, differential scanning calorimetry (DSC) and X-ray diffractometry [11].

As penetration enhancers have different effects depending on the characteristics of the skin to which they are applied and the formulation in which they are included, it is difficult to consistently predict the impact an enhancer will have on skin structure and function. As frog skin is structurally different from mammalian skin, and penetration-enhancers likely to be included in therapeutic formulations used in frogs, and also present in frog habitats, studies are needed to investigate their effect on chemical absorption through frog skin. Further, given the vital role of frog skin in maintaining physiological homeostasis, it is also important to ensure that the integrity of the skin is not significantly altered following application of penetration enhancers.

The current study investigated the effect of the addition of ethanol or PG to an aqueous formulation containing one of three model chemicals on the absorption kinetics through frog skin. In order to further understand the underlying mechanism of penetration enhancement in frog skin, DSC and histology were used to characterise frog skin, prior to and after exposure to these penetration enhancers.

2. Material and methods

2.1. Chemicals and solutions

Model chemicals used were reagent grade caffeine, ACS reagent grade benzoic acid (both Sigma-Aldrich) and ≥98% ibuprofen (Sigma). Amphibian Ringer's solution (ARS), used in both donor and receptor solutions, was prepared according to Wright and Whitaker [12] containing: 113 mM sodium chloride, 2 mM potassium chloride, 1.35 mM calcium chloride, and 2.4 mM sodium bicarbonate. For all ibuprofen experiments, ARS was spiked with 2-hydroxypropyl-beta-cyclodextrin (HPβCD; Aldrich Chemistry) 2.75 mg/ml to ensure adequate solubilization. Donor solutions (Table 1) comprised a saturated ("infinite dose") solution of each of the model chemicals in either: (a) 1% v/v ethanol, (b) 10% v/v ethanol (ibuprofen only), (c) 30% v/v ethanol, or (d) 20% v/v PG, all prepared in ARS ± HPβCD. As the study included prolonged exposure, the penetration enhancers chosen, and concentrations used, were selected due to their inclusion in commercially-available drug products, at amounts reported to be safe in frogs. 10% v/v ethanol was included as a mid-range concentration in the ibuprofen studies, after preliminary studies showed almost no influence of 1% v/v ethanol and extremely high absorption from 30% v/v ethanol. To ensure solubilisation of the chemicals in the receptor solution, all receptor solutions comprised ARS spiked with 2-hydroxypropyl-beta-cyclodextrin (HPβCD; Aldrich Chemistry): 2.75 mg/ml HPβCD was used for the caffeine and ibuprofen experiments, and 5.75 mg/ml HPβCD for benzoic acid experiments. Euthanasia of animals was carried out by bathing in a solution of 0.2% w/v ethyl 3-aminobenzoate methanesulfonate solution (MS-222; Aldrich Chemistry), buffered to pH 7.3 with sodium bicarbonate.

Methanol and acetonitrile used were high-performance liquid chromatography (HPLC) grade (Fisher Chemicals, Trinidad and Thermo

Table 1
LogP of each model chemical, and the composition, saturation solubility data and sampling times for each donor solution used in the absorption kinetics/diffusion cell experiments *values from [17].

Model drug	LogP	Donor solution composition (% v/v)			Saturated solubility (g/L)	Sampling times (hr)
		ARS	Ethanol	PG		
Benzoic acid	1.87	100%	–	–	3.972*	0, 0.5, 1, 1.5, 2, 2.5, 3, 4, 5, 6
Benzoic acid		99%	1%	–	5.240	0, 0.5, 1, 1.5, 2, 2.5, 3, 4, 5
Benzoic acid		70%	30%	–	12.101	0, 0.5, 1, 1.5, 2, 2.5, 3, 4, 5
Benzoic acid		80%	–	20%	2.619	0, 0.5, 1, 1.5, 2, 2.5, 3, 4, 5
Caffeine	-0.07	100%	–	–	20.298*	0, 0.5, 1, 1.5, 2, 2.5, 3, 4, 5, 6
Caffeine		99%	1%	–	19.238	0, 0.5, 1, 1.5, 2, 2.5, 3, 4
Caffeine		70%	30%	–	20.046	0, 0.5, 1, 1.5, 2, 2.5, 3, 4, 5
Caffeine		80%	–	20%	17.947	0, 0.5, 1, 1.5, 2, 2.5, 3, 4, 5
Ibuprofen	3.97	100%	–	–	0.490*	0, 0.5, 1, 1.5, 2, 2.5, 3, 4, 5, 6
Ibuprofen		99%	1%	–	0.243	0, 0.5, 1, 1.5, 2, 2.5, 3, 4, 5, 6
Ibuprofen		90%	10%	–	0.810	0, 0.5, 1, 1.5, 2, 2.5, 3, 4, 5
Ibuprofen		70%	30%	–	1.338	0, 0.5, 1, 1.5, 2, 2.5, 3, 4, 5, 6
Ibuprofen		80%	–	20%	0.262	0, 0.5, 1, 1.5, 2, 2.5, 3, 4

Fisher Scientific, Australia), formic acid was analytical grade (Thermo Fisher Scientific, Australia) and water used for HPLC was ultrapure (Milli-Q Integral, Millipore Australia). All solutions were freshly prepared.

2.1.1. Determining saturation solubility of donor solutions

The saturation solubility of each chemical in each penetration enhancer solution was determined by placing an excess of chemical into 5–100 mL of penetration enhancer solution. The resultant mixture was then sonicated at room temperature for 24 hr before centrifuging at 12,000 RCF for 15 minutes. Supernatant was removed, diluted appropriately with ARS + HPβCD, and analysed using previously-validated HPLC methods [13].

2.2. Study animals

Adult male *Rhinella marina* (cane toads), wild-caught in the Townsville region (Australia) were used in this study. The cane toad has a wide distribution, being a native species in Central and South America, and also having been introduced several nations in the Asia-Pacific region [14]. Extensive biological and ecological research exists for this species, including baseline kinetics of skin absorption. Cane toads are also generally not adversely affected by chytridiomycosis infection (only metamorphs and subadults succumb to the disease [15]), and so present a suitable model for design and trial of therapeutic treatments for this infection. This species, therefore, represents an appropriate model species when investigating the impact of penetration enhancers on the skin of frogs. Thirty-four toads, ranging from 54.5 – 128.65 g body weight (mean = 89.74 g) were randomly allocated to one of the penetration enhancer/chemical treatments. Twenty-five toads were used for the in vitro penetration enhancer experiments, and the remaining toads provided skin samples both for histological analysis (light microscopy) and DSC experiments. Toads were handled carefully in order to minimize potential damage to the skin. Euthanasia was carried out within 24 hr of collection. Full-thickness skin samples were excised immediately after euthanasia. For all studies, each toad provided five skin samples from a combination of the following skin regions: dorsal bilaterally from the central dorsal truncal midline, ventral pelvic bilaterally along the pelvic truncal midline, ventral thoracic bilaterally from the central ventral truncal midline. All studies were completed in accordance with Animal Ethics approval A2222 from James Cook University, Australia.

2.3. Diffusion cell experiments

The effect of penetration enhancers on the absorption of model chemicals in static Franz diffusion cells (Permegear, USA) was investigated. Each diffusion cell consisted of a 1 ml donor chamber with a 9 mm orifice, and a 5 ml receptor chamber. The donor chamber was filled with a saturated solution of one of the model chemicals (benzoic acid, caffeine, or ibuprofen) in ARS (± HPβCD) + penetration enhancer, as outlined in section 2.1. Receptor solution (ARS + HPβCD) was magnetically stirred and allowed to equilibrate in the diffusion cell for 30 minutes prior to skin mounting. Prior to mounting, each skin sample was rinsed in ARS and microscopically inspected for signs of damage. Samples were mounted on diffusion cells with the external skin surface facing the donor chamber. Samples with signs of damage were not used in the study.

After mounting skin samples on the diffusion cell, 1 ml of donor solution was applied to the donor chamber, and the chamber was occluded by application of laboratory film (Parafilm M™, Pecheney Plastics Packaging, Chicago) to the external donor chamber orifice. 1 ml samples were then collected from the receptor chamber until steady-state was achieved for at least four sampling points, as indicated in preliminary studies (data not included). Samples were collected from the center of the diffusion cell, by inserting a 200mm long stainless-steel needle via the sidearm and withdrawing the sample from directly above the stir bar into a glass syringe. Samples were collected at t = 0, 0.5, 1, 1.5, 2, 2.5, 3 and 4 hr for caffeine in 1% v/v ethanol. All other caffeine experiments followed the same schedule with an additional sample taken at t = 5 hr. All benzoic acid samples were taken at t = 0, 0.5, 1, 1.5, 2, 3, 4 and 5 hr. Ibuprofen samples were withdrawn at t = 0, 0.5, 1, 1.5, 2, 3, and 4 hr when dissolved in 20% v/v PG, with an additional sample withdrawn at t = 5 hr for the 10% v/v ethanol-containing samples, and two additional samples (t = 5 and t = 6 hr) for ibuprofen in 1% v/v or 30% v/v ethanol (Table 1). Immediately following sample collection, fresh receptor solution was added to the receptor chamber using a clean needle and glass syringe, the chamber inverted to ensure no air bubbles were present, and the chamber then returned to its holder. This allowed replenishment of lost receptor chamber volume from sample collection, while also ensuring that fresh receptor solution was mixed into the remaining donor chamber solution. Collected samples were analyzed for the chemical content using previously-described HPLC methods [13].

2.3.1. High-performance liquid chromatography (HPLC)

The HPLC system comprised a Shimadzu Nexera-i LC-2040C 3D equipped with a photodiode-array detector. Post-run analysis was performed using Labsolutions 5.82 (Shimadzu). All HPLC methods have been validated and previously described [13]. As the penetration enhancers used in this study could potentially interfere with the analysis, specificity was investigated. Blank samples containing 100% penetration enhancer, samples of individual penetration enhancers spiked with known quantities of each of the chemicals, and samples run in unspiked ARS were injected onto the column to ensure no interference with the chemical peak occurred. All methods remained specific for the determination of the respective chemicals and no interference was detected, thus specificity was assured. HPLC methods were therefore used as previously reported. Calibrations were performed daily ($r^2 > 0.999$), and all samples measured in triplicate.

2.3.2. Data analysis and statistics

Data were examined and analyzed using R [16]. Previously-collected data involving percutaneous absorption of model chemicals from ARS [17] were included in data analyses to determine any differences in absorption due to the penetration enhancers.

Cumulative absorption versus time plots were produced for each sample, and any curves with significant deviation suggestive of skin damage were excluded. Consequently, results from four samples were excluded from further analysis.

Flux (mcg/cm^2/hr; J_{ss}) was determined for each sample from the steady-state slope of the cumulative absorption versus time plot. Steady state was identified as the slope taken from at least four consecutive sampling points, after initial equilibration had occurred. In the case of 30% ethanol, where a distinct lag phase was noted, we ensured that the first sampling timepoint for calculation of the linear portion of the curve was no less than 2.3 x lag time (as per [18]). Permeability coefficient (K_p) was calculated by dividing flux by the concentration of chemical in the donor solution ($K_p = J_{ss}/C_v$). Concentration of drug in the donor solution (C_v) was the saturation solubility of each chemical in the penetration enhancer as determined in stage 1 of this study (sections 2.1.1 and 3.1; Table 1). In addition to data collected in this study, K_p was calculated from previously-collected data involving percutaneous absorption of the model chemicals from ARS [17].

The effect of the penetration enhancer and skin region on chemical flux through the skin was determined for each individual chemical by fitting a series of linear mixed-effects models using the nlme package [19]. Each model used penetration enhancer as the fixed factor, included the individual animal as a random effect, and allowed for heteroskedasticity in the data.

Enhancement ratio (ER) was calculated for each drug/penetration enhancer formulation, as the ratio of K_p of each drug in penetration

enhancer divided by its K_p in ARS (i.e., ER = K_{pPE}/K_{pARS}). This allowed comparison of relative effect of each penetration enhancer to each other and ARS, for a specific skin region and model chemical. ERs reported are the mean ratios from at least four replicates.

2.4. Differential scanning calorimetry (DSC)

The thermal behavior of dorsal and ventral frog skin was investigated using differential scanning calorimetry (DSC; Mettler Toledo DSC822^e with STARe version 14.00). Full-thickness skin samples were used in the study, either freshly-excised or skin that had been exposed to ARS or penetration enhancer solutions for 6 hr. Skin was prepared and mounted on diffusion cells as described in sections 2.2 and 2.4. Donor solutions were as outlined in section 2.1, however model chemicals were not included in any solutions. The donor solutions thus comprised of: (a) ARS, (b) 1% v/v ethanol, (c) 10% v/v ethanol, (d) 30% v/v ethanol, or (e) 20% v/v PG, all prepared in ARS. The receptor solution for all studies was ARS to maintain viability of the inner skin surface. Following the 6-hr exposure time, skin samples were removed from the diffusion cells, rinsed with ARS, and blot-dried. Exposed skin was then excised from surrounding (non-exposed) tissue, cut into pieces weighing approximately 20 mg, and sealed in 40 mcl aluminium crucibles. Baseline samples of freshly-excised frog skin were used in the investigation of the ramp rate on DSC output. Heating rates of 1 °C, 5 °C and 10 °C/min were investigated, with optimal balance between resolution, sensitivity, and reproducibility seen with the 5 °C/min heating rate. Thus, all samples were analysed over the temperature range 30–150 °C, with a heating rate of 5 °C/min under nitrogen flow. Transition data represent the average of at least three skin samples.

2.5. Histology

Ventral and dorsal skin samples, either fresh or following exposure to ARS or penetration enhancers as part of the DSC experiments, were preserved in 4% phosphate-buffered formaldehyde. Preserved skin was then dehydrated and processed for histology using standard methods to produce 5 mcm sections on slides stained with haematoxylin and eosin.

3. Results

3.1. Saturation solubility studies

Table 1 presents the solubility data for each chemical in each of the penetration enhancer solutions. Increasing concentrations of ethanol increased the solubility of both benzoic acid and ibuprofen, with solubility increasing 3-fold for benzoic acid in 30% v/v ethanol, and 2-fold for ibuprofen. 20% v/v PG decreased the solubility of all chemicals investigated (Table 1).

3.2. Diffusion cell studies - absorption kinetics

3.2.1. Cumulative absorption versus time for each model chemical

The cumulative absorption of model chemicals from the different penetration enhancers changed markedly depending on the skin region and model chemical applied. Of note, 30% v/v ethanol demonstrated a distinct lag phase in absorption profile through all skin regions and for all chemicals, with negligible absorption occurring in the first 30 minutes of the experiments. The lag phase was most obvious in the benzoic acid experiments. Following this lag phase, however, absorption rapidly increased. This lag phase was absent for other enhancers. Discussion of results will therefore focus on absorption following resolution of the lag phase.

3.2.1.1. Caffeine. The addition of 1% v/v ethanol consistently showed greater absorption compared to ARS alone for all skin regions, whereas the relative effect of PG and 30% v/v ethanol differed depending on the skin region (Fig. 1). In dorsal skin, the inclusion of 30% v/v ethanol slightly reduced absorption compared to ARS alone, whereas PG reduced absorption by approximately half.

Ventrally, absorption of caffeine was essentially unchanged for PG compared to ARS, through both the thoracic and pelvic skin regions. In 30% v/v ethanol, caffeine absorption was similar to both ARS and PG through thoracic skin, however the absorption profile changed in the later sampling times in pelvic skin. Specifically, pelvic absorption of caffeine was similar between PG, ARS and 30% v/v ethanol over the first 3 hr, however absorption rate of caffeine from 30% v/v ethanol was lower from t = 3 hr, with the final total cumulative amount absorbed ~30% lower than that from PG.

3.2.1.2. Benzoic acid. The addition of any of the investigated penetration enhancers resulted in greater absorption than in ARS alone, in all skin regions. In contrast to caffeine, 30% v/v ethanol consistently resulted in the most rapid uptake of benzoic acid through all skin regions. There was also very little difference in absorption profiles between skin regions, with 30% v/v ethanol consistently having the highest absorption, followed by PG, and then 1% v/v ethanol (Fig. 2). Notably, in dorsal skin the improvement in absorption compared to ARS alone were similar for PG and 1% v/v ethanol, whereas in ventral skin the difference between these enhancers was more prominent, with PG resulting in markedly higher absorption.

3.2.1.3. Ibuprofen. The cumulative absorption versus time curves for

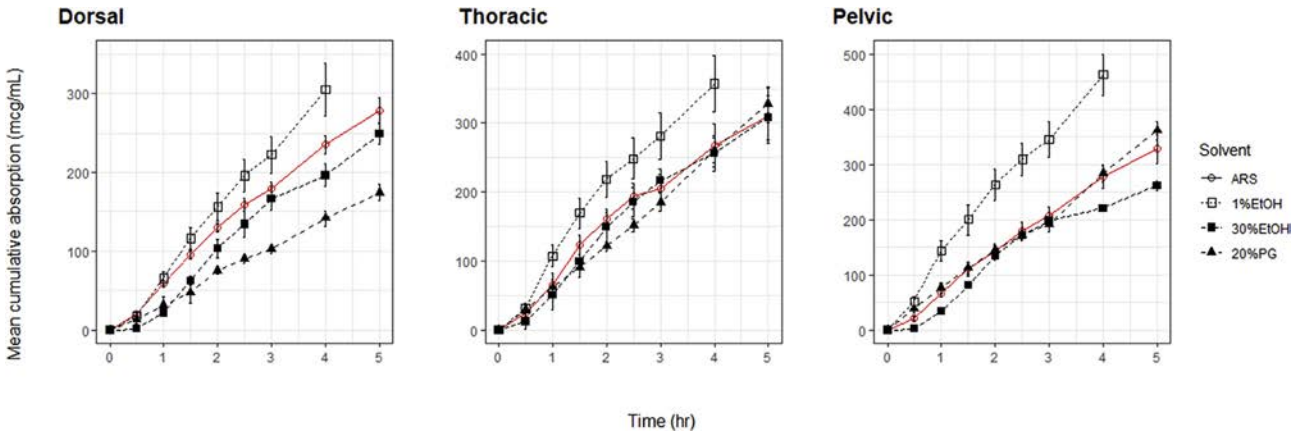

Fig. 1. Cumulative absorption versus time curves for absorption of caffeine for the various penetration enhancers through dorsal, ventral thoracic and ventral pelvic *Rh. marina* skin. Error bars show standard error. ARS data from [17].

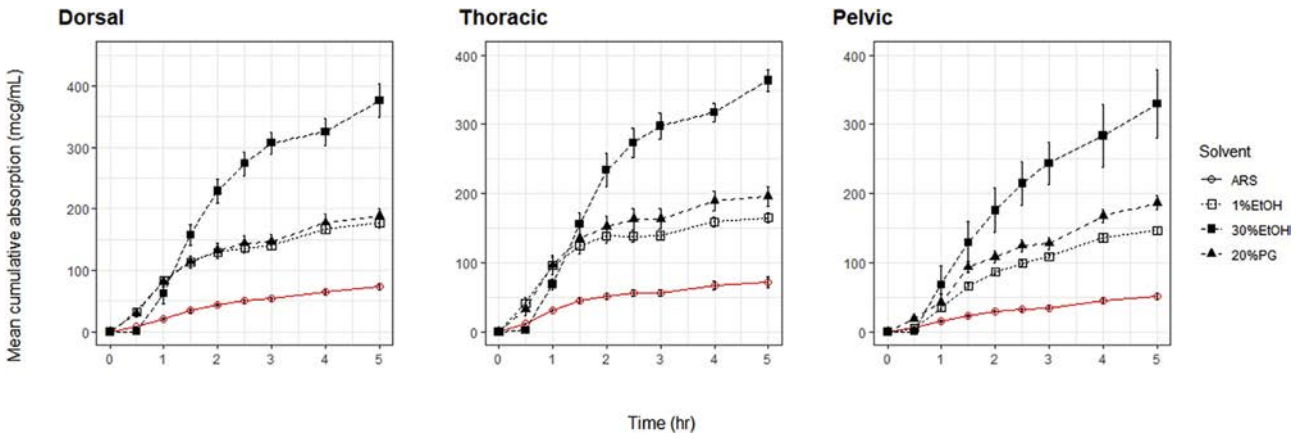

Fig. 2. Cumulative absorption versus time curves for absorption of benzoic acid for the various penetration enhancers through dorsal, ventral thoracic and ventral pelvic *Rh. marina* skin. Error bars show standard error. ARS data from [17].

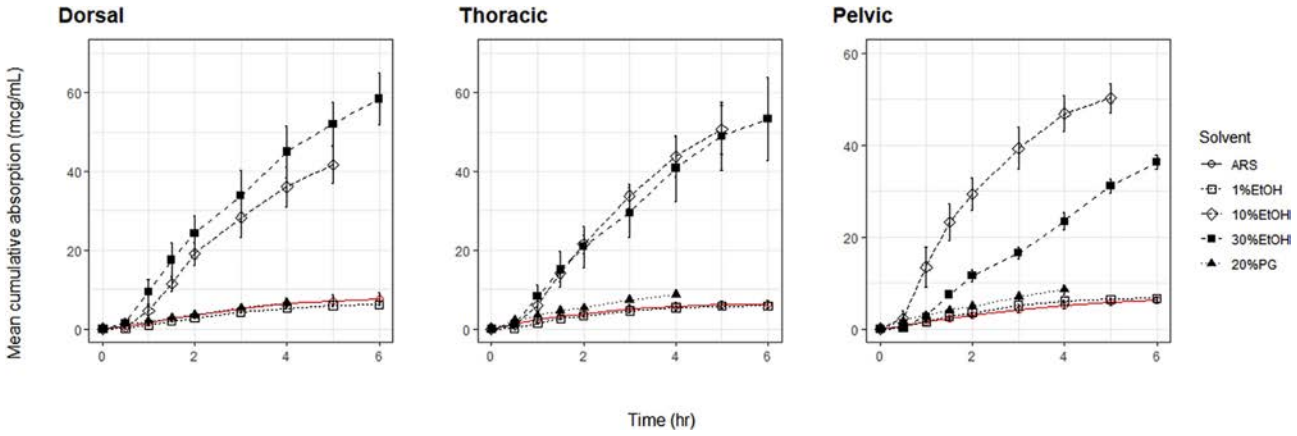

Fig. 3. Cumulative absorption versus time curves for absorption of ibuprofen for the various penetration enhancers through dorsal, ventral thoracic and ventral pelvic *Rh. marina* skin. Error bars show standard error. ARS data from [17].

ibuprofen through dorsal skin showed a much higher absorption of ibuprofen from 10% and 30% v/v ethanol compared to 1% v/v ethanol, PG and ARS (Fig. 3), with highest absorption from 30% v/v ethanol. Absorption of ibuprofen from PG, 1% v/v ethanol, and ARS in dorsal skin was similar.

The absorption trends in the ventral skin (both thoracic and pelvic) were different from dorsal absorption. While absorption remained low from both PG and 1% v/v ethanol, PG does appear to improve absorption marginally compared to 1% v/v ethanol and ARS, especially through thoracic skin.

Although thoracic absorption was highest for 10% and 30% v/v ethanol, no discernible difference was noted between these enhancers. Of interest is the observation that although the absorption characteristics of ibuprofen from the lower ethanol concentrations and PG remain relatively constant for both ventral skin regions, absorption changes significantly between these regions for the 30% v/v ethanol, with pelvic absorption being much lower than thoracic absorption.

3.2.2. *Influence of penetration enhancers on the flux of model chemicals*

1% v/v ethanol did not significantly influence flux for any of the chemicals, and the ability of the other enhancers to significantly affect flux was inconsistent between chemicals and skin regions.

Of interest, 30% v/v ethanol and PG produced significant reductions in flux of caffeine (Table 2), with PG significantly reducing flux through the dorsal skin ($t = -4.387$, $df = 8$, $p = 0.0023$), and 30% v/v ethanol reducing flux through both dorsal ($t = -2.909$, $df = 8$, $p = 0.0196$) and ventral pelvic skin ($t = -5.223$, $df = 8$, $p = 0.0008$). Thoracic application of 30% v/v ethanol reduced caffeine flux substantially, however this failed to reach significance ($t = -2.097$, $df = 9$, $p = 0.0655$).

For benzoic acid and ibuprofen (Tables 3 and 4), 30% v/v ethanol increased flux significantly for both chemicals through all skin regions. PG had variable effects, significantly improving flux of benzoic acid through the dorsal and thoracic skin regions and marginally improving flux through the pelvic skin ($t = 2.063$, $df = 10$, $p = 0.0661$). Its ability to improve flux of ibuprofen was only significant following thoracic

Table 2
Flux and permeability coefficients for caffeine from a saturated solution of different penetration enhancers through dorsal, ventral thoracic and ventral pelvic *Rh. marina* skin. J_{ss} and K_p reported as mean ± standard error. N = 4. *indicates solvent flux values that are significantly different ($p < 0.05$) to ARS flux values reported in [17].

Solvent	Dorsal		Thoracic		Pelvic	
	J_{ss} (mcg/cm^2/hr)	K_p (cm/hr) × 10^{-3}	J_{ss} (mcg/cm^2/hr)	K_p (cm/hr) × 10^{-3}	J_{ss} (mcg/cm^2/hr)	K_p (cm/hr) × 10^{-3}
1% ethanol	72.747 ± 7.632	3.781 ± 0.793	68.939 ± 7.670	3.584 ± 0.797	102.391 ± 7.108	5.322 ± 0.739
30% ethanol	47.871 ± 2.388*	2.547 ± 0.254	52.286 ± 5.294	2.786 ± 0.561	40.627 ± 4.325*	2.162 ± 0.460
20% PG	33.650 ± 2.643*	1.903 ± 0.299	69.622 ± 6.353	3.937 ± 0.718	73.625 ± 6.097	4.163 ± 0.689

Table 3
Flux and permeability coefficients for benzoic acid from a saturated solution of different penetration enhancers through dorsal, ventral thoracic and ventral pelvic *Rh. marina* skin. J_{ss} and K_p reported as mean ± standard error. N = 4. *indicates solvent flux values that are significantly different ($p < 0.05$) to ARS flux values reported in [17].

Solvent	Dorsal		Thoracic		Pelvic	
	J_{ss} (mcg/cm^2/hr)	K_p (cm/hr) × 10^{-3}	J_{ss} (mcg/cm^2/hr)	K_p (cm/hr) × 10^{-3}	J_{ss} (mcg/cm^2/hr)	K_p (cm/hr) × 10^{-3}
1% ethanol	17.759 ± 2.155	4.416 ± 0.536	11.910 ± 2.420	2.961 ± 0.602	19.800 ± 2.463	4.924 ± 0.612
30% ethanol	37.841 ± 4.669*	3.127 ± 0.386	33.981 ± 5.051*	2.808 ± 0.417	44.994 ± 8.686*	3.718 ± 0.718
20% PG	21.221 ± 1.447*	9.891 ± 0.675	17.086 ± 0.980*	7.964 ± 0.457	27.187 ± 1.856	12.672 ± 0.865

Table 4
Flux and permeability coefficients for ibuprofen from a saturated solution of different penetration enhancers through dorsal, ventral thoracic and ventral pelvic *Rh. marina* skin. J_{ss} and K_p reported as mean ± standard error. N = 4 except for dorsal PG where N = 3. *indicates solvent flux values that are significantly different ($p < 0.05$) to ARS flux values reported in [17].

Solvent	Dorsal		Thoracic		Pelvic	
	J_{ss} (mcg/cm^2/hr)	K_p (cm/hr) × 10^{-3}	J_{ss} (mcg/cm^2/hr)	K_p (cm/hr) × 10^{-3}	J_{ss} (mcg/cm^2/hr)	K_p (cm/hr) × 10^{-3}
1% ethanol	1.406 ± 0.061	5.791 ± 0.501	1.303 ± 0.142	5.365 ± 1.167	1.504 ± 0.071	6.196 ± 0.582
10% ethanol	8.346 ± 0.760*	10.306 ± 1.876	10.841 ± 1.832*	13.387 ± 4.524	8.314 ± 0.779*	10.266 ± 1.925
30% ethanol	9.887 ± 0.527*	7.389 ± 0.788	9.711 ± 1.506*	7.258 ± 2.251	6.573 ± 0.212*	4.913 ± 0.316
20% PG	1.557 ± 0.076	6.069 ± 0.514	1.787 ± 0.083*	6.964 ± 0.649	1.883 ± 0.252	7.339 ± 1.967

application (t = 2.222, df = 11, p = 0.0482). Finally, and interestingly, while both 10% and 30% v/v ethanol significantly improved flux of ibuprofen, the effect was greater for the lower (10% v/v) ethanol concentration, following both thoracic and pelvic application.

3.2.3. Enhancement ratio – comparing the effects of penetration enhancers

Direct comparison of the magnitude of enhancement for each penetration enhancer can be made by considering the enhancement ratio (ER) for a specified chemical and skin region (Fig. 4).

As expected from the flux and K_p data, none of the enhancers were effective in improving the penetration of caffeine, and in some cases, a significant reduction in caffeine penetration was observed.

The effects of ethanol were varied, and dependent upon the concentration applied. 1% v/v ethanol only improved permeability for ibuprofen, with a 2-fold increase for ventral application and 1.7-fold increase following dorsal application. 30% v/v ethanol effectively increased permeability of ibuprofen through all skin regions, although the effect was lower in ventral pelvic skin compared to dorsal or thoracic application (ER = 1.5 for ventral skin, 2.16 and 2.68 for dorsal and thoracic skin, respectively). 30% v/v ethanol was not an effective enhancer for benzoic acid, in all cases having an ER < 1.2, nor for caffeine (all ER < 0.75). Interestingly, 10% v/v ethanol was the most effective enhancer for ibuprofen, with at least a 3-fold increase in absorption (dorsal), extending to a 5-fold increase following thoracic application.

PG generally improved absorption, except for caffeine, which did not change appreciably following ventral application (ER = 1.04 and 0.90 for thoracic and pelvic application, respectively), and was reduced by almost 50% through dorsal skin (ER = 0.49). Dorsal and ventral absorption was enhanced by PG for both benzoic acid and ibuprofen, with a 2.5- to 3.95-fold increase for benzoic acid and 1.8- to 2.6-fold increase for ibuprofen, depending on the skin region. Ventral applications showed the largest increases, with ER ranging from 2.28 – 3.95.

3.3. Differential scanning calorimetry (DSC)

Three endothermic transitions were observed in fresh dorsal *Rh. marina* skin samples ($T2_{frog}$, $T3_{frog}$, $T4_{frog}$; Fig. 5) while only two transitions were noted in fresh ventral skin ($T2_{frog}$ and $T4_{frog}$; Fig. 6). The transition temperature for $T2_{frog}$ was consistent between skin regions (62.8 ± 0.4 °C), whereas the transition temperature of $T4_{frog}$ was higher in dorsal skin (124.3 °C versus 116.4 °C). $T3_{frog}$ occurring at 79.7 °C in fresh dorsal skin.

Following exposure to ARS or penetration enhancers, changes in all three transitions were noted in both dorsal and ventral skin. In dorsal skin samples (Fig. 5), $T2_{frog}$ transition temperature was unaffected by

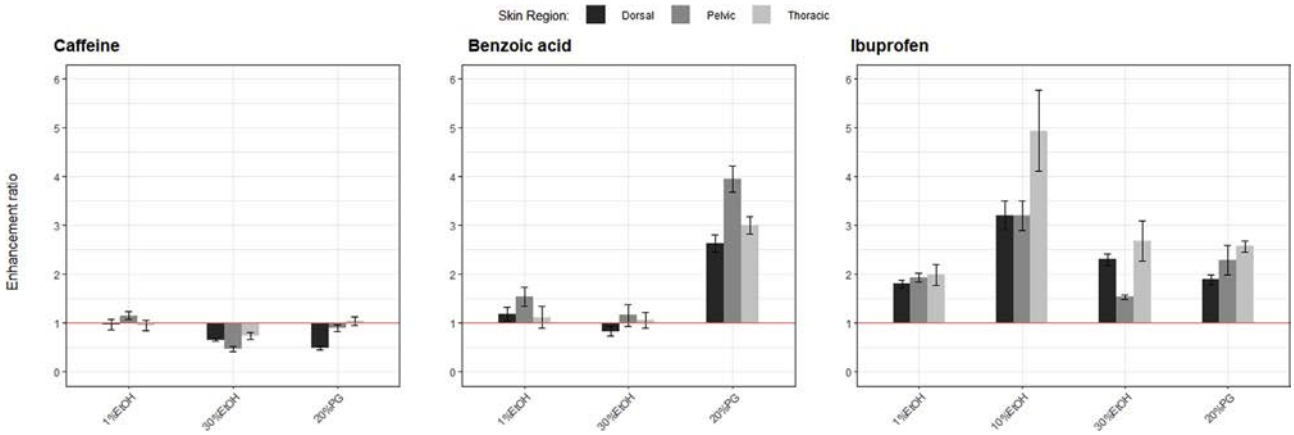

Fig. 4. Effect of ethanol and PG on the penetration of caffeine, benzoic acid, and ibuprofen. Red line indicates ER = 1 (i.e., no change in penetration compared to ARS); error bars are standard error.

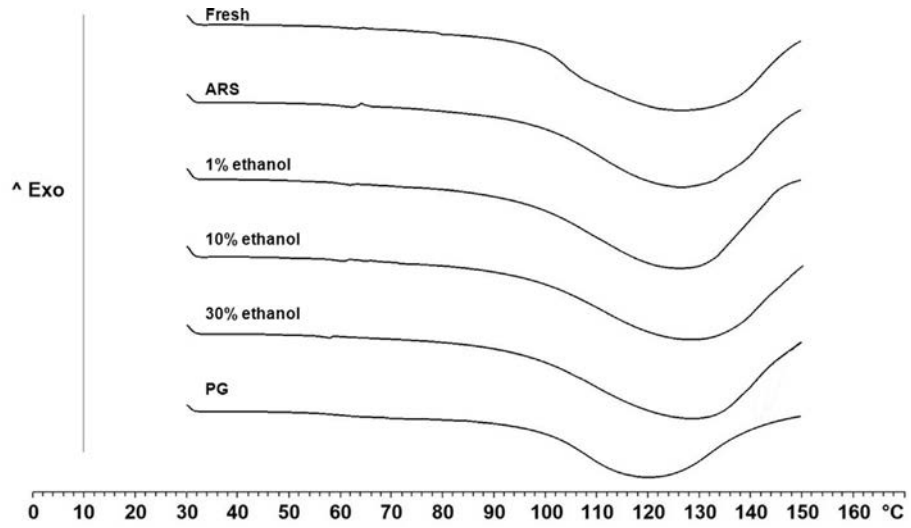

Fig. 5. Representative DSC thermoanalytical curves of dorsal full-thickness Rh. marina skin. From top: fresh skin; skin exposed to: ARS; 1% v/v ethanol; 10% v/v ethanol; 30% v/v ethanol; 20% v/v PG.

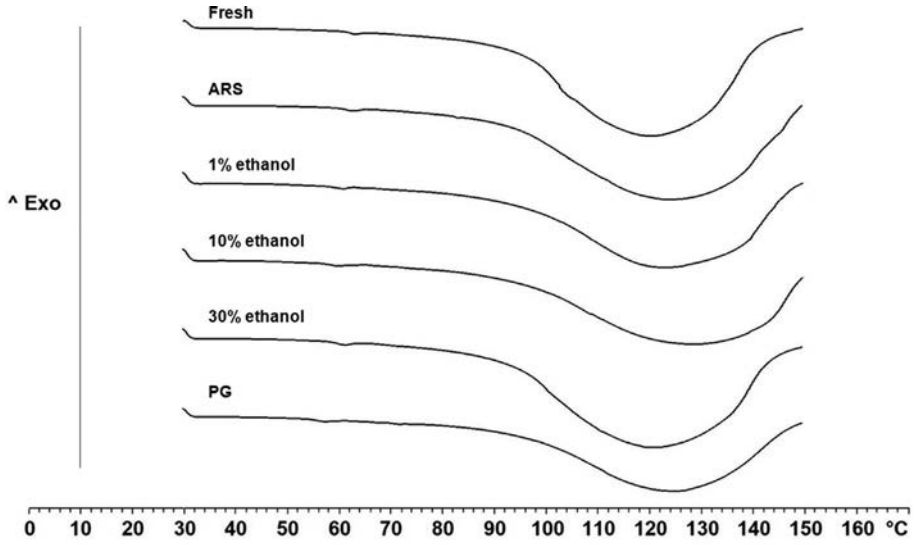

Fig. 6. Representative DSC thermoanalytical curves of ventral pelvic full-thickness Rh. marina skin. From top: fresh skin; skin exposed to: ARS; 1% v/v ethanol; 10% v/v ethanol; 30% v/v ethanol; 20% v/v PG.

ARS, PG or 1% v/v ethanol. As ethanol concentration increased, there was a sequential decrease in transition temperature, with a marked difference in transition temperature, compared to fresh skin, noted for both 10% and 30% v/v ethanol (60.6 °C and 60.0 °C, respectively). Notably, although the transition temperature for ARS-exposed skin did not change, the absence of $T3_{frog}$ was noted, with a corresponding increase in the enthalpy of $T2_{frog}$. A similar phenomenon was observed for the 30% v/v ethanol-exposed skin, where both $T2_{frog}$ and $T3_{frog}$ were present, however the enthalpy of $T2_{frog}$ was increased with a corresponding decrease in the enthalpy of $T3_{frog}$. The opposite trend was observed for PG; although transition temperature of $T2_{frog}$ was essentially unchanged, the enthalpy of the transition decreased and an increase in $T3_{frog}$ enthalpy was noted. $T4_{frog}$ transition temperature was essentially unchanged for most exposed skin; the exceptions were ARS and PG-exposed samples, which showed decreases in transition temperatures (122.6 °C for ARS, and 120.1 °C for PG). Enthalpy of these transitions remained essentially unchanged.

In ventral skin (Fig. 6), the $T2_{frog}$ transition temperature was unaffected by ARS, however the enthalpy of the transition doubled in size compared to fresh skin. For ethanol-exposed skin, decreases in transition temperature were noted for all concentrations, although in contrast to dorsal skin, 10% v/v ethanol had the lowest transition temperature compared to fresh skin (60.3 °C), followed by 30% v/v ethanol and then 1% v/v ethanol. The enthalpy of transition increased by ~50% for all ethanol exposures. Of note, in comparison to dorsal skin where PG did not affect transition temperature of $T2_{frog}$, in ventral skin PG recorded the greatest reduction in transition temperature, compared to fresh skin (57.7 °C). Interestingly, while $T3_{frog}$ was absent in fresh ventral skin, it did appear in all PG-exposed ventral skin, but at a lower temperature than that seen in dorsal skin (72.4 °C). The effects of exposure on $T4_{frog}$ were different from those observed in dorsal skin, with increases in transition temperature and peak broadening noted for all skin exposures. The magnitude of these temperature increases ranged from 119.4 °C for the 30% v/v ethanol concentration to 123.2 °C for ARS-exposed skin. All of the increases in transition temperature were accompanied with a reduction in enthalpy, except for 1% v/v ethanol, which was essentially unchanged.

3.4. Histology

Changes suggestive of disruption to skin integrity and function were noted for all skin samples exposed to all penetration enhancers. The most severe changes were noticeable with ethanol exposures, with changes observable in both epidermal and dermal skin layers. Epidermal changes, including pale nuclei and loss of nuclear and cellular outlines, were most obvious in dorsal skin following exposure to ethanol (Fig. 7), and the severity of these effects increased with increasing ethanol concentrations. PG-exposed skin was noted for swelling/expansion of ventral epidermal keratinocytes resulting in a thickened epidermis (Fig. 8). None of these effects were observed in fresh or ARS-exposed skin samples, indicating they were not associated with the delay between sample collection and preservation, nor with specific ARS-induced changes in the skin.

The most obvious impact of both ethanol and PG on the skin were the effects on the dermis, with marked separation of dermal fibrocytes by oedematous spaces and expansion of melanocytes observed in both dorsal and ventral skin (Fig. 9). The severity of these changes increased with higher concentrations of ethanol, being particularly noticeable in dorsal skin exposed to 30% v/v ethanol. In ventral skin samples, this appeared to reach maximal effect with exposure to 10% v/v ethanol; no further deterioration of the dermis was observed in ventral skin exposed to 30% v/v ethanol. Skin exposed to PG showed similar separation effects, however the severity was similar to that seen following exposure to 1% v/v ethanol.

4. Discussion

4.1. Summary of key findings

While the SC provides the primary barrier to absorption in mammals, this layer is often only 1–2 cell layers thick in frogs, contributing to the heightened permeability of frog skin. As the SC in frogs provides only a modest barrier to absorption, any changes to it, or other skin regions induced by exposure to penetration enhancers is likely to significantly impact absorption through, and regulatory function of, the skin. The DSC and histology findings reported herein found that exposure to penetration enhancers resulted in significant changes to the skin structure, especially in the case of ethanol. 30% v/v ethanol caused loss of cellular outlines in the keratinised cells of the epidermis, leading to coalescence of this layer, and severe changes to the dermis. Even 10% v/v ethanol appeared to induce significant changes in the dermis, and so ethanol in concentrations $\geq$10% v/v should be avoided, as these stark anatomical changes may negatively affect the animal's ability to maintain physiological homeostasis. A minimal effect on the skin was seen following dorsal application of 1% v/v ethanol, however, this concentration of ethanol was ineffective in enhancing penetration for all chemicals, so its value in a therapeutic formulation would primarily be as a co-solvent, enabling reduction in dosing volumes and not enhancement of absorption kinetics.

The best solvent for absorption of a hydrophilic chemical was ARS alone, as none of the enhancers improved penetration of caffeine. 30% v/v ethanol and PG effectively reduced caffeine absorption (30% v/v ethanol following both dorsal and ventral application, PG only following dorsal application). Ergo sequitur, from an environmental toxicology perspective, hydrophilic chemicals used as overhead sprays would be best formulated with PG to reduce absorption of these chemicals in frog skin. Despite the reduction in absorption of hydrophilic chemicals from both dorsal and ventral skin regions due to 30% v/v ethanol, this cannot be recommended, as the histology results suggest that prolonged skin contact with such formulations adversely affect the skin structure in frogs, increasing the absorption of most other chemicals in the environment, and may also negatively affect the frog's ability to maintain physiological homeostasis.

PG was the most consistently-effective enhancer for moderately and highly lipophilic chemicals (all skin regions), while causing the least observable skin changes. As the majority of therapeutic chemicals are of moderate to high lipophilicity, PG represents the safest and most effective option for penetration enhancement for a wide range of therapeutic chemicals in frogs.

4.2. In vitro studies – absorption kinetics

As these experiments included saturated solutions of each chemical, flux results that differ significantly from the use of ARS alone suggest modification of the skin barrier by the penetration enhancers [20]. It is unsurprising that higher concentrations of ethanol improved flux for benzoic acid and ibuprofen in the current study, considering the obvious changes in frog skin structure observed (Fig. 9). Of note is the finding that 10% v/v ethanol was more effective in improving ibuprofen flux than 30% v/v ethanol for ibuprofen. Similar results were observed in human epidermis in a study by Watkinson et al. [21], who reported that flux of ibuprofen from binary ethanol/water solutions increased rapidly up to a 50/50 v/v mixture, thereafter remaining relatively steady up to 75/25 v/v, before decreasing significantly in 100% ethanol. The authors

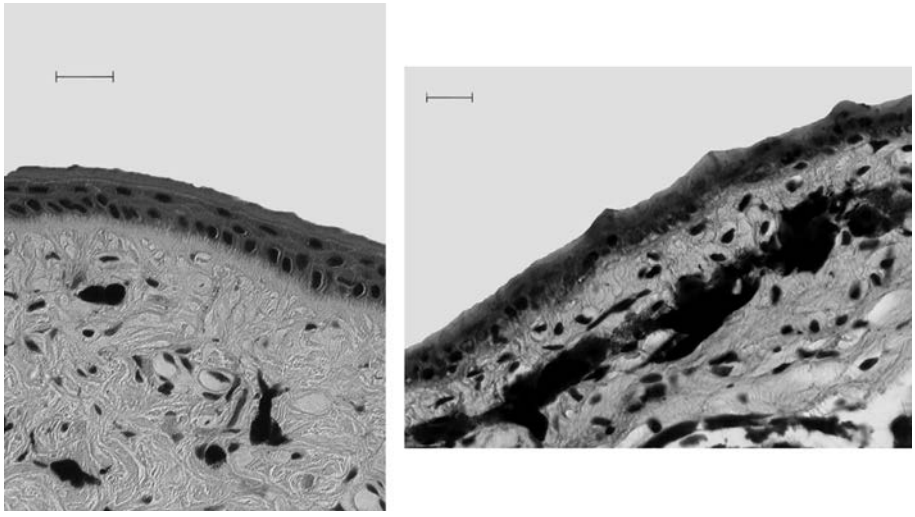

Fig. 7. Histological sections of dorsal skin in *Rh. marina* showing effect of ethanol exposure on epidermal structure. Left: fresh *Rh. marina* skin. Right: skin exposed to 30% v/v ethanol for 6 hr. Note loss of cellular outlines in epidermis. Scale bar = 20 mcm.

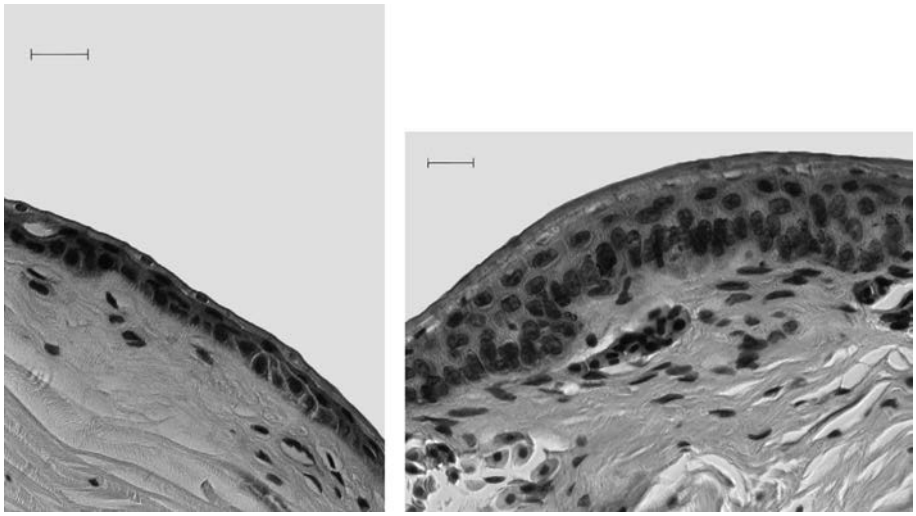

Fig. 8. Histological sections of ventral skin in *Rh. marina* showing effect of PG exposure on epidermal structure. Left: fresh *Rh. marina* skin. Right: skin exposed to 20% v/v PG for 6 hr. Note swelling of keratinocytes compared to control. Scale bar = 20 mcm.

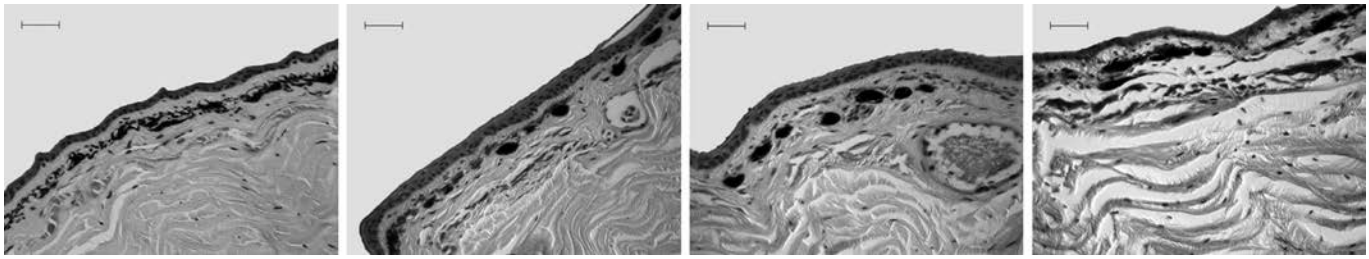

Fig. 9. Effect of ethanol exposure on dorsal skin from *Rh. marina*. Ethanol concentrations increasing from left. Left-to-right: fresh skin, 1% v/v ethanol, 10% v/v ethanol, 30% v/v ethanol. Note separation of dermal fibrocytes by oedematous spaces. Scale bar = 50 mcm.

postulated that this effect could be due to dehydration of the SC at higher ethanol concentrations. However, as can be seen from the histological sections of frog skin (Fig. 7), it is likely the reduction in flux demonstrated with the higher ethanol concentration is due to the homogenization of the SC, creating a solid, relatively lipophilic barrier to absorption. It is likely, given the lipophilic nature of ibuprofen, that it may partition from the dosing solution into the SC/epidermal layer, however the epidermal restructuring caused by the ethanol may cause ibuprofen to be less likely to partition further into the more hydrophilic dermis. Further studies, including fixed-dose applications with full mass balance to determine skin ibuprofen content may provide clarification of this hypothesis. Regardless, the use of ethanol in formulations for application to frog skin cannot be recommended at these higher concentrations, as such changes to the skin structure is likely to have serious implications for the animal's ability to maintain homeostasis.

In mammalian skin studies, a lag phase for absorption is regularly observed, as an applied chemical must diffuse from the donor, across the thick SC and the remaining skin barrier before it reaches the receptor. However, as frog skin is much thinner than mammalian skin, lag times have not previously been reported when measuring transdermal absorption from simple aqueous solutions [13, 17, 22]. A lag phase was, however, noted in the current study when chemicals were formulated in 30% ethanol. In mammals, coformulation with ethanol has different effects on the lag phase depending on the ethanol concentration, due to the concentration-dependant effects of ethanol on the skin. Typically, ethanol at lower concentrations causes fluidisation of the skin membrane, and this is associated with decreased lag time and improved absorption. Conversely, at higher concentrations ethanol is known to extract skin lipids; this is typically observed as a significantly increased lag time followed by rapid flux [8, 23]. In mammals, the first mechanism (membrane fluidisation, decreased lag time and increased permeability) is dominant for ethanol concentrations up to ~60% [21, 24], with lag times increasing higher ethanol concentrations. In reptiles, no lag phase was reported in shed snake skin when an aminophylline gel was formulated with the penetration enhancers lauric acid, sodium taurooglycocholate (a surfactant), or PG, however a lag time was reported when formulated in 60% ethanol [25]. It is therefore not surprising that a lag time was observed with the higher ethanol concentration in the current study, but not with the lower concentrations. We predict that the underlying mechanism is the same in both animal classes, simply that the thinner nature of frog skin means that lower ethanol concentrations are needed for these effects to be observed. Indeed, significant changes to the keratinized cells of the epidermis were noted in skin samples exposed to 30% ethanol (Fig. 7).

PG was the most consistently-effective enhancer for benzoic acid and ibuprofen, although the magnitude of improvement changed depending on the skin region of application. It was the most effective penetration enhancer for benzoic acid, and while not able to enhance penetration as much as ethanol for ibuprofen solutions, induced less severe changes in the skin, and so provides a safer alternative for penetration-enhancement. These results contribute to the contradictory reports in the literature as to the effectiveness of PG as a penetration enhancer on its own [26]. In mammals, often the effect of PG on absorption kinetics is negligible when formulated alone, with enhancement only occurring when used in combination with another known enhancer, such as fatty acids. It is possible that the effectiveness of PG demonstrated in the current study is due to the thinner barrier provided by frog epidermis, and that modulating effects of PG are insufficient to significantly alter the barrier properties of the thicker SC in mammals. The findings in the current study reinforce the caution required by clinicians when using

formulations (containing penetration-enhancing ingredients) designed for use in mammals in frogs, as although these formulations may be reported to not influence absorption in mammals, different effects may be observed in frogs [27].

Finally, penetration enhancers investigated in the current study had different effects on absorption, depending on both the chemical being applied to the skin and the skin region. As skin region influenced the absorption kinetics from the different solvents, the application site needs to be considered together with the formulation composition when developing therapeutics for use in frogs. This finding is of interest, as a previous study by this research group in *Rh. marina* found that the flux of benzoic acid and ibuprofen did not significantly change between skin regions [17] when formulated in ARS alone.

4.3. DSC and histology

This study is the first to characterise full-thickness frog skin, including the effect of penetration enhancers, using DSC. Previous studies have reported findings in a variety of mammalian skins (for review, see Babita et al. [28]), and snake skin has also been reported [3]. Most studies in mammals identify three or four main transitions common to all investigated skin types ($T1_{mammal}$-$T4_{mammal}$), occurring at ~40 °C ($T1_{mammal}$; sometimes absent in studies), 70–75 °C ($T2_{mammal}$), 80–85 °C ($T3_{mammal}$) and 105 °C ($T4_{mammal}$) [28]. T2-T4 were evident in fresh dorsal frog skin, and T2 and T4 in ventral frog skin, however T1 was not observed in either skin region. This may be due to the starting temperature in the current experiment being necessarily high owing to the ambient laboratory conditions, preventing observation of the transition. In addition, $T2_{frog}$ and $T3_{frog}$ were found to be 10–15 °C lower than reported in mammalian SC, so it is possible that this first transition may also have occurred at a reduced temperature, below the temperature range investigated in the current study.

$T2_{mammal}$ and $T3_{mammal}$ have been attributed to intracellular lipids changes, and lipid-protein complex changes, respectively, whereas $T4_{mammal}$ is associated with protein denaturation. It is interesting that the lipid-associated transitions in frog skin occur at lower temperatures, and the protein denaturation at higher temperatures, than seen in mammalian skin. Differences in lipid-associated transitions between species are likely due to differences in constituent skin lipids and their arrangement in the epidermis. In particular, lower phospholipid content of the skin has been reported to correlate with reduced transition temperatures, and ceramides with increased transition temperatures [28]. While the exact lipid composition of *Rh. marina* skin has not been reported, the lipid composition of epidermis in a group of frogs from *Cyclorana* spp. reported 0.86% phospholipid content and a complete absence of ceramides [29]. Comparatively, human SC is reported to contain 3–5% phospholipids and 27% ceramides, depending on the skin region investigated [30]. Additionally, more permeable skins typically exhibit looser packing of the epidermal lipids and as frog skin is highly permeable, it is likely this also contributed to the lower transition temperatures observed for $T2_{frog}$ and $T3_{frog}$ in the current study.

An interesting finding in the current study was the observation that for dorsal skin samples, exposure to ARS or 30% v/v ethanol resulted in a reduction in enthalpy of $T3_{frog}$ with a corresponding increase in the enthalpy of $T2_{frog}$. This has been reported previously in porcine skin [31], whereby heating of the skin resulted in a loss of T3 and an increase in the enthalpy of T2 equivalent in size to that of T3. Of note in the current study was the opposite finding in PG-exposed dorsal skin – where $T3_{frog}$ increased in enthalpy, with a corresponding decrease in enthalpy of $T2_{frog}$. Studies utilizing different methodologies to investigate changes in frog skin following PG-exposure will assist in explaining this phenomenon.

$T4_{mammal}$, in contrast, is associated with the hydration status of skin; it is absent in dehydrated skin and skin with a total water content of <15%, and the temperature of this transition declines continuously with increasing hydration of the skin [28]. Further, it has been suggested that higher transition temperatures of $T4_{mammal}$ with broad peaks indicates dehydration of the membrane. As the pelvic ventral patch in frogs is physiologically designed to optimize water uptake, it is perhaps unsurprising that the transition temperature was lower for fresh ventral skin samples than for the dorsal samples. Similarly, this may also explain the reduction in $T4_{frog}$ temperature following exposure of dorsal skin to ARS (which would be expected to increase hydration of the skin), and the increases in $T4_{frog}$ with accompanying broadening of the peak, for all ventral skin exposures, as presumably fresh ventral skin would already be optimally-hydrated.

For penetration enhancer-exposed skin samples, the thermal analysis curves for dorsal skin exposed to ARS or 1% v/v ethanol were essentially the same, corresponding with the in vitro absorption studies and histology, which suggested that 1% v/v ethanol only marginally affects skin structure and absorption kinetics. Of note, considering the in vitro absorption results for PG in the current study, is the DSC and histology results for PG-exposed skin samples, which showed a reduction in transition temperature for $T2_{frog}$ in both dorsal and ventral skin. These findings concur with those of Brinkmann and Müller-Goymann [9], who found a similar reduction in transition temperature for T2 when investigating the impact of PG pretreatment on human skin. Following x-ray diffraction studies on the pre-exposed skin, the authors concluded that PG integrates into the hydrophilic regions of the SC lipid bilayer, causing expansion to this region and thus disturbing the lipid organization. This conclusion also agrees with the histology findings in the current study, which showed distinct swelling of the epidermal layers of the frog skin following PG exposure.

An ideal chemical penetration enhancer should enhance penetration, without permanently disrupting the skin structure. However, the histology results for ethanol demonstrated significant changes in both the epidermal and dermal skin layers. At higher concentrations, ethanol is reported to extract lipids from the SC in mammals [8]; in the current study higher ethanol concentrations altered the cellular outlines of the epidermal keratinocytes, causing coalescence of the keratinocytes. These effects have numerous safety implications: lipid extraction can create pores in the SC, allowing unimpeded passage of chemicals into the dermis and supratherapeutic (and potentially toxic) drug levels, whereas disruption of the keratinocyte outlines and coalescence of the keratinocytes may result in the formation of a relatively impervious barrier, which may either impede drug absorption (resulting in sub-therapeutic effects) or could provide a depot for sustained drug release. Such damage to the skin is irreversible and would remain until new epidermal turnover is complete. Additionally, such skin damage in a frog would be likely to substantially impact on the ability of the frog to maintain physiological homeostasis, leading to impaired fluid and electrolyte balance. While skin changes, including expansion of the epidermal keratinocytes, were noted in PG-exposed skin, these changes are likely to be more readily reversible than those identified in ethanol-exposed skin.

4.4. General discussion

While the focus of this study has been on the impact of penetration enhancers on model chemical absorption, the ability of the enhancers themselves to be absorbed must be considered. Ethanol and PG rapidly penetrate mammalian skin; indeed, the initial rapid increase in absorption noted with benzoic acid and ibuprofen when formulated in ethanol in the current study is likely due to initial solvent drag. These results emphasise the need for the clinician and the environmental toxicologist to consider the impact formulation of chemical(s) with penetration enhancers may have on systemic absorption of the chemical, while also considering that the enhancers themselves are also likely to be absorbed, having local or systemic effects including potential toxicity. Krause et al. [32] reported on toxicity resulting in death of a group of red-eyed tree frogs (*Agalychnis calidryas*) following topical application of ivermectin diluted in PG. Necropsy results showed supra-therapeutic levels of both the ivermectin and PG, and the authors concluded that toxicity was likely

caused by incomplete mixing of the solution. Ivermectin is a large molecule with a logP (estimated) of 5.83 [33]. In the current study, ibuprofen, the most lipophilic chemical investigated, showed a 1.8–2.6-fold increase in penetration following formulation in 20% v/v PG. It is therefore likely that the penetration-enhancing effects of the PG contributed to the toxicity reported by Krause et al. [32]. Similarly, toxicology researchers have highlighted that the inclusion of surfactants in the herbicide glyphosate contributes to the toxicity of these formulations to amphibians [34]. Howe et al. [35] investigated individually the toxicity of neat glyphosate, the surfactant used in some glyphosate formulations, and five commercial glyphosate formulations in four frog species. Acute toxicity was highest with the surfactant alone, and lowest with the neat glyphosate. However, this and other studies have been primarily concerned with the toxicity caused by the surfactant itself, and have not considered that the surfactant is also likely increasing the absorption of the glyphosate in the formulation, contributing to the toxicological profile. While the current study did not investigate surfactant action on percutaneous absorption in frogs, surfactants are known penetration-enhancers and should be expected to influence absorption of both the chemical and the enhancer itself. Thus, both the contribution of penetration enhancers to altered absorption and the individual toxicity of the enhancers themselves must be considered when formulating chemicals which may be administered to frogs (whether intentionally, for therapeutic purposes, or inadvertently following exposure in their habitat). Studies that investigate other penetration enhancers that are commonly included in agricultural and industrial chemical formulations would therefore provide valuable data regarding risk assessment and management when using these products in frog habitats.

5. Conclusions

The penetration enhancers investigated in this study are the most common agents used in commercial and compounded therapeutic liquid formulations administered to frogs, and are also often included in agrichemicals and other industrial products and so are likely to be present in frog habitats. The results herein provide information on the absorption-enhancing effects of these agents when included in formulations, and can be used to guide dose/application site adjustment when used in frogs. In particular, the use of ethanol in concentrations over 10% v/v cannot be recommended, despite demonstrated penetration-enhancing effects, owing to the severe skin changes caused by ethanol at these concentrations. 1% v/v ethanol may find use in formulations as a co-solvent, with minimal impact on both absorption kinetics and skin morphology. PG can enhance percutaneous absorption of moderately and highly-lipophilic chemicals, with minimal impact on the skin, and so should be considered when penetration enhancement of these chemicals through frog skin is required. Finally, hydrophilic chemicals may have significantly reduced absorption when included in formulations containing PG or higher concentrations of ethanol, particularly when administered to the ventral skin surface, and so these enhancers should be avoided unless reduced absorption is desired, for example in retarding absorption of hydrophilic environmental contaminants.

Declarations

Author contribution statement

Victoria K Llewelyn: Conceived and designed the experiments; Performed the experiments; Analyzed and interpreted the data; Contributed reagents, materials, analysis tools or data; Wrote the paper.

Lee Berger: Conceived and designed the experiments; Analyzed and interpreted the data; Wrote the paper.

Beverley D Glass: Conceived and designed the experiments; Contributed reagents, materials, analysis tools or data; Wrote the paper.

Funding statement

This research did not receive any specific grant from funding agencies in the public, commercial, or not-for-profit sectors.

Competing interest statement

The authors declare no conflict of interest.

Additional information

No additional information is available for this paper.

Acknowledgements

We thank Sieara Claytor and Rebecca Webb for assistance with preparation of histological sections, and Sherryl Robertson for assistance with DSC.

References

[1] P. Helmer, D. Whiteside, Amphibian anatomy and physiology, in: B. O'Malley (Ed.), Clinical Anatomy and Physiology of Exotic Species, Elsevier Saunders, Edinburgh, 2005, pp. 3–14.
[2] A. Quaranta, V. Bellantuono, G. Cassano, C. Lippe, Why amphibians are more sensitive than mammals to xenobiotics, PLoS ONE [Internet] 4 (11) (2009), e7699.
[3] S.Y. Lin, S.J. Hou, T.H.S. Hsu, F.L. Yeh, Comparisons of different animal skins with human skin in drug percutaneous penetration studies, Methods Find. Exp. Clin. Pharmacol. 14 (8) (1992) 645–654.
[4] D.B. Wake, V.T. Vredenburg, Are we in the midst of the sixth mass extinction? A view from the world of amphibians, Proc. Natl. Acad. Sci. U. S. A 105 (Suppl. 1) (2008) 11466–11473.
[5] European Medicines Agency Committee for Human Medicinal Products, Propylene Glycol Used as an Excipient, 2017, 9 October 2017. Contract No.: EMA/CHMP/334655/2013.
[6] C. Capello, U. Fischer, K. Hungerbühler, What is a green solvent? A comprehensive framework for the environmental assessment of solvents, Green Chem. 9 (9) (2007) 927–934.
[7] M.S. Switzenbaum, S. Veltman, D. Mericas, B. Wagoner, T. Schoenberg, Best management practices for airport deicing stormwater, Chemosphere 43 (8) (2001) 1051–1062.
[8] M.E. Lane, Skin penetration enhancers, Int. J. Pharm. 447 (2013) 12–21.
[9] I. Brinkmann, C.C. Müller-Goymann, An attempt to clarify the influence of glycerol, propylene glycol, isopropyl myristate and a combination of propylene glycol and isopropyl myristate on human stratum corneum, Pharmazie 60 (3) (2005) 215–220.
[10] N. Dragicevic, J.P. Atkinson, H.I. Maibach, Chemical penetration enhancers: classification and mode of action, in: N. Dragicevic, H.I. Maibach (Eds.), Percutaneous Penetration Enhancers Chemical Methods in Penetration Enhancement: Modification of the Stratum Corneum, Springer, Berlin, 2015, pp. 11–28.
[11] L. Roussel, R. Abdayem, E. Gilbert, F. Pirot, M. Haftek, Influence of excipients on two elements of the stratum corneum barrier: intercellular lipids and epidermal tight junctions, in: N. Dragicevic, H.I. Maibach (Eds.), Percutaneous Penetration Enhancers Chemical Methods in Penetration Enhancement: Drug Manipulation Strategies and Vehicle Effects, Springer Berlin Heidelberg, Berlin, Heidelberg, 2015, pp. 69–90.
[12] K.M. Wright, B.R. Whitaker, Pharmacotherapeutics, in: K.M. Wright, B.R. Whitaker (Eds.), Amphibian Medicine and Captive Husbandry, first ed., Krieger Publishing Company, Malabar, FL, 2001, pp. 309–332.
[13] V.K. Llewelyn, L. Berger, B.D. Glass, Regional variation in percutaneous absorption in the tree frog *Litoria caerulea*, Environ. Toxicol. Pharmacol. 60 (2018) 5–11.
[14] S. Easteal, The history of introductions of *Bufo marina* (Amphibia: Anura); a natural experiment in evolution, Biol. J. Linn. Soc. 16 (1981) 93–113.
[15] L.A. Brannelly, G. Martin, J. Llewelyn, L.F. Skerratt, L. Berger, Age- and size-dependent resistance to chytridiomycosis in the invasive cane toad *Rhinella marina*, Dis. Aquat. Org. 131 (2) (2018) 107–120.
[16] R Core Team, in: Computing RFfS (Ed.), R: A Language and Environment for Statistical Computing, 2016. Vienna, Austria.
[17] V.K. Llewelyn, L. Berger, B.D. Glass, Effects of skin region and relative lipophilicity on percutaneous absorption in the toad *Rhinella marina*, Environ. Toxicol. Chem. 38 (2) (2019) 361–367.
[18] J. Kielhorn, S. Melching-Kollmuss, I. Mangelsdorf, Dermal Absorption, World Health Organisation, Contract No, 2006, p. 235.
[19] J. Pinheiro, D. Bates, S. DebRoy, D. Sarkar, R.C. Team, nlme: Linear and Nonlinear Mixed Effects Models, R package version 31-131, 2017, https://CRAN.R-project.org/package=nlme.
[20] M.S. Roberts, S.E. Cross, M.A. Pellett, Skin transport, in: K.A. Walters (Ed.), Dermatological and Transdermal Formulations. Drugs and the Pharmaceutical Sciences, CRC Press, New York, 2002, pp. 89–195.

[21] R.M. Watkinson, C. Herkenne, R.H. Guy, J. Hadgraft, G. Oliveira, M.E. Lane, Influence of ethanol on the solubility, ionization and permeation characteristics of ibuprofen in silicone and human skin, Skin Pharmacol. Physiol. 22 (2009) 15–21.
[22] K. Kaufmann, P. Dohmen, Adaption of a dermal in vitro method to investigate the uptake of chemicals across amphibian skin, Environ. Sci. Eur. 28 (10) (2016).
[23] D.W. Osborne, J. Musakhanian, Skin penetration and permeation properties of Transcutol®— neat or diluted mixtures, AAPS PharmSciTech 19 (8) (2018) 3512–3533.
[24] G.C. Ceschel, P. Maffei, S. Lombardi Borgia, Correlation between the transdermal permeation of ketoprofen and its solubility in mixtures of a ph 6.5 phosphate buffer and various solvents, Drug Deliv. 9 (1) (2002) 39–45.
[25] M. Kouchak, S. Handali, Effects of various penetration enhancers on penetration of aminophylline through shed snake skin, Jundishapur J. Nat. Pharm. Prod. 9 (1) (2014) 24–29.
[26] H. Trommer, R.H.H. Neubert, Overcoming the stratum corneum: the modulation of skin penetration, Skin Pharmacol. Physiol. 19 (2006) 106–121.
[27] V.K. Llewelyn, L. Berger, B.D. Glass, Percutaneous absorption of chemicals: developing an understanding for the treatment of disease in frogs, J. Vet. Pharmacol. Ther. 39 (2) (2016) 109–121.
[28] K. Babita, V. Kiumar, V. Rana, S. Jain, A.K. Tiwary, Thermotropic and spectroscopic behaviour of the skin: relationship with percutaneous permeation enhancement, Curr. Drug Deliv. 3 (2006) 95–113.
[29] L.M. Sadowski-Fugitt, C.R. Tracy, K.A. Christian, J.B. Williams, Cocoon and epidermis of Australian *Cyclorana* frogs differ in composition of lipid classes that affect water loss, Physiol. Biochem. Zool. 85 (1) (2012) 40–50.
[30] M.A. Lampe, A.L. Burlingame, J. Whitney, M.L. Williams, B.E. Brown, E. Roitman, et al., Human stratum corneum lipids: characterization and regional variations, JLR (J. Lipid Res.) 24 (1983) 120–130.
[31] M.L. Francoeur, G.M. Golden, R.O. Potts, Oleic acid: its effects on stratum corneum in relation to (trans)dermal drug delivery, Pharm. Res. 7 (6) (1990) 621–627.
[32] Fatal ivermectin toxicity in a collection of frogs, in: K. Krause, D. Reaville, S. Weldy (Eds.), Annual Conference of the Association of Reptilian and Amphibian Veterinarians, 2012. Oakland, California.
[33] ALOGPS 2.1 [Internet], Virtual Computational Chemistry Laboratory, 2005. Available from: http://www.vcclab.org.
[34] N. Wagner, W. Reichenbecher, H. Teichmann, B. Tappeser, S. Lötters, Questions concerning the potential impact of glyphosate-based herbicides on amphibians, Environ. Toxicol. Chem. 32 (8) (2013) 1688–1700.
[35] C.M. Howe, M. Berrill, B.D. Pauli, C.C. Helbing, K. Werry, N. Veldhoen, Toxicity of glyphosate-based pesticides to four North American frog species, Environ. Toxicol. Chem. 23 (8) (2004) 1928–1938.

Appendix 9

The full dataset for the following output is available online:

Llewelyn, V. In vitro percutaneous absorption data for model chemicals in Rhinella marina: chemicals formulated in penetration enhancers ethanol or propylene glycol [Internet]. James Cook University; 2019. Available from: http://dx.doi.org/10.25903/5d4a6ff6bae14

Effect of each solvent/penetration enhancer on chemical flux through skin regions of *Rh. marina*

Caffeine

```
> Flux.lmevar.Caff.D<-lme(Flux ~ Solvent_AEP, random= ~1|AnimalID,
+                         weights=varIdent(form = ~1|Solvent_AEP),  data=Caffeine,
subset=SubRegion=="D" )
> Flux.lmevar.Caff.P<-lme(Flux ~ Solvent_AEP, random= ~1|AnimalID,
+                         weights=varIdent(form = ~1|Solvent_AEP),  data=Caffeine,
subset=SubRegion=="P" )
> Flux.lmevar.Caff.T<-lme(Flux ~ Solvent_AEP, random= ~1|AnimalID,
+                         weights=varIdent(form = ~1|Solvent_AEP),  data=Caffeine,
subset=SubRegion=="T" )
> summary(Flux.lmevar.Caff.D)
Linear mixed-effects model fit by REML
 Data: Caffeine
  Subset: SubRegion == "D"
       AIC      BIC   logLik
  149.9184 157.9317 -65.9592

Random effects:
 Formula: ~1 | AnimalID
        (Intercept) Residual
StdDev:    12.07514  5.16598

Variance function:
 Structure: Different standard deviations per stratum
 Formula: ~1 | Solvent_AEP
 Parameter estimates:
      ARS    1%EtOH     20%PG   30%EtOH
1.0000000 0.9173140 0.3865329 1.0984811
Fixed effects: Flux ~ Solvent_AEP
                       Value Std.Error DF   t-value p-value
(Intercept)         78.76040  5.641854 10 13.960022  0.0000
Solvent_AEP1%EtOH   -2.12213  9.306627  8 -0.228024  0.8253
Solvent_AEP30%EtOH -30.88940 10.620056  8 -2.908591  0.0196
Solvent_AEP20%PG   -45.11065 10.282596  8 -4.387088  0.0023
 Correlation:
                   (Intr) S_AEP1 S_AEP3
Solvent_AEP1%EtOH  -0.606
Solvent_AEP30%EtOH -0.531  0.322
```

```
Solvent_AEP20%PG   -0.549  0.333  0.291

Standardized Within-Group Residuals:
       Min         Q1        Med         Q3        Max
-1.3004467 -0.6456382  0.1412724  0.4155518  1.2082223

Number of Observations: 22                         Number of Groups: 12
> summary(Flux.lmevar.Caff.P)
Linear mixed-effects model fit by REML
 Data: Caffeine
  Subset: SubRegion == "P"
       AIC      BIC    logLik
  125.9971 131.0817 -53.99857

Random effects:
 Formula: ~1 | AnimalID
        (Intercept) Residual
StdDev:     8.83948 14.82838

Variance function:
 Structure: Different standard deviations per stratum
 Formula: ~1 | Solvent_AEP
 Parameter estimates:
      ARS    1%EtOH     20%PG   30%EtOH
1.0000000 0.9139616 0.4201879 0.4513543
Fixed effects: Flux ~ Solvent_AEP
                       Value Std.Error DF   t-value p-value
(Intercept)         93.38180  7.720326  8 12.095577  0.0000
Solvent_AEP1%EtOH    9.00945 12.024545  8  0.749255  0.4752
Solvent_AEP30%EtOH -51.63932  9.886744  8 -5.223086  0.0008
Solvent_AEP20%PG   -19.75705 10.410431  8 -1.897813  0.0943
 Correlation:
                   (Intr) S_AEP1 S_AEP3
Solvent_AEP1%EtOH  -0.642
Solvent_AEP30%EtOH -0.781  0.501
Solvent_AEP20%PG   -0.742  0.476  0.579

Standardized Within-Group Residuals:
        Min          Q1         Med          Q3         Max
-1.31764174 -0.63284660  0.08853887  0.55859577  1.24830817

Number of Observations: 17                         Number of Groups: 12
> summary(Flux.lmevar.Caff.T)
Linear mixed-effects model fit by REML
 Data: Caffeine
  Subset: SubRegion == "T"
       AIC     BIC    logLik
  131.3804 136.465 -56.69021

Random effects:
 Formula: ~1 | AnimalID
        (Intercept) Residual
```

```
StdDev:    8.410165 23.25553

Variance function:
 Structure: Different standard deviations per stratum
 Formula: ~1 | Solvent_AEP
 Parameter estimates:
      ARS    1%EtOH   30%EtOH     20%PG
1.0000000 0.6666661 0.2531574 0.4562934
Fixed effects: Flux ~ Solvent_AEP
                       Value Std.Error DF   t-value p-value
(Intercept)         76.30840  11.05939  9  6.899874  0.0001
Solvent_AEP1%EtOH   -7.14167  14.42299  9 -0.495159  0.6324
Solvent_AEP30%EtOH -26.12513  12.46105  9 -2.096542  0.0655
Solvent_AEP20%PG    -9.00317  13.79775  9 -0.652510  0.5304
 Correlation:
                   (Intr) S_AEP1 S_AEP3
Solvent_AEP1%EtOH  -0.767
Solvent_AEP30%EtOH -0.888  0.681
Solvent_AEP20%PG   -0.802  0.615  0.711

Standardized Within-Group Residuals:
       Min         Q1        Med         Q3        Max
-1.0468358 -0.5304755 -0.1694430  0.6623816  1.4857819

Number of Observations: 17                         Number of Groups: 13
```

Benzoic acid

```
> Flux.lmevar.BA.D<-lme(Flux ~ Solvent_AEP, random= ~1|AnimalID,
+                       weights=varIdent(form = ~1|Solvent_AEP),  data=Benzoic, sub
set=SubRegion=="D" )
> Flux.lmevar.BA.P<-lme(Flux ~ Solvent_AEP, random= ~1|AnimalID,
+                       weights=varIdent(form = ~1|Solvent_AEP),  data=Benzoic, sub
set=SubRegion=="P" )
> Flux.lmevar.BA.T<-lme(Flux ~ Solvent_AEP, random= ~1|AnimalID,
+                       weights=varIdent(form = ~1|Solvent_AEP),  data=Benzoic, sub
set=SubRegion=="T" )
>
> summary(Flux.lmevar.BA.D)
Linear mixed-effects model fit by REML
 Data: Benzoic
  Subset: SubRegion == "D"
       AIC      BIC    logLik
  155.9388 165.7582 -68.96942

Random effects:
 Formula: ~1 | AnimalID
         (Intercept) Residual
StdDev: 0.0001918135 10.44035

Variance function:
 Structure: Different standard deviations per stratum
 Formula: ~1 | Solvent_AEP
 Parameter estimates:
  30%EtOH       ARS     20%PG    1%EtOH
1.0000000 0.4007939 0.3099703 0.4127594
Fixed effects: Flux ~ Solvent_AEP
                      Value Std.Error DF   t-value p-value
(Intercept)        13.186767  1.207940 12 10.916741  0.0000
Solvent_AEP1%EtOH   4.572483  2.470171 10  1.851080  0.0939
Solvent_AEP30%EtOH 24.654633  4.822788 12  5.112113  0.0003
Solvent_AEP20%PG    8.034433  1.885129 10  4.262006  0.0017
 Correlation:
                   (Intr) S_AEP1 S_AEP3
Solvent_AEP1%EtOH  -0.489
Solvent_AEP30%EtOH -0.250  0.122
Solvent_AEP20%PG   -0.641  0.313  0.160

Standardized Within-Group Residuals:
        Min          Q1         Med          Q3         Max
-1.61337505 -0.52560121 -0.08597754  0.54557820  1.96711157

Number of Observations: 26                         Number of Groups: 14
> summary(Flux.lmevar.BA.P)
Linear mixed-effects model fit by REML
 Data: Benzoic
  Subset: SubRegion == "P"
       AIC      BIC    logLik
  120.5325 127.4858 -51.26625
```

```
Random effects:
 Formula: ~1 | AnimalID
        (Intercept)  Residual
StdDev:    9.837391 0.2871837

Variance function:
 Structure: Different standard deviations per stratum
 Formula: ~1 | Solvent_AEP
 Parameter estimates:
    30%EtOH         ARS       20%PG      1%EtOH
 1.00000000 15.14832158  0.07879043 15.24155427
Fixed effects: Flux ~ Solvent_AEP
                      Value Std.Error DF  t-value p-value
(Intercept)        11.44188  4.327502 10 2.643991  0.0246
Solvent_AEP1%EtOH   8.35812  8.479636 10 0.985670  0.3475
Solvent_AEP30%EtOH 35.86098  7.142008 10 5.021134  0.0005
Solvent_AEP20%PG   14.72813  7.140414 10 2.062643  0.0661
 Correlation:
                   (Intr) S_AEP1 S_AEP3
Solvent_AEP1%EtOH  -0.510
Solvent_AEP30%EtOH -0.606  0.309
Solvent_AEP20%PG   -0.606  0.309  0.367

Standardized Within-Group Residuals:
         Min           Q1          Med           Q3          Max
-1.103524477 -0.271632890 -0.007941986  0.246247981  1.166407427

Number of Observations: 20                         Number of Groups: 14
> summary(Flux.lmevar.BA.T)
Linear mixed-effects model fit by REML
 Data: Benzoic
  Subset: SubRegion == "T"
       AIC      BIC    logLik
  104.6356 110.3871 -43.31781

Random effects:
 Formula: ~1 | AnimalID
         (Intercept) Residual
StdDev: 0.0001223139 10.10224

Variance function:
 Structure: Different standard deviations per stratum
 Formula: ~1 | Solvent_AEP
 Parameter estimates:
  30%EtOH       ARS    1%EtOH     20%PG
1.0000000 0.3849066 0.4791254 0.1939737
Fixed effects: Flux ~ Solvent_AEP
                      Value Std.Error DF  t-value p-value
(Intercept)         9.282648  1.587441 10 5.847557  0.0002
Solvent_AEP1%EtOH   2.626852  2.894296 10 0.907596  0.3854
Solvent_AEP30%EtOH 24.698352  5.294694 10 4.664737  0.0009
```

```
Solvent_AEP20%PG    7.803352  1.865461 10 4.183068  0.0019
 Correlation:
                   (Intr) S_AEP1 S_AEP3
Solvent_AEP1%EtOH  -0.548
Solvent_AEP30%EtOH -0.300  0.164
Solvent_AEP20%PG   -0.851  0.467  0.255

Standardized Within-Group Residuals:
       Min         Q1        Med         Q3        Max
-1.1466764 -0.6088527 -0.4057272  0.9260478  1.4662389

Number of Observations: 18                        Number of Groups: 14
```

Ibuprofen

```
> Flux.lmevar.IBU.D<-lme(Flux ~ Solvent_AEP, random= ~1|AnimalID,
+                        weights=varIdent(form = ~1|Solvent_AEP),  data=Ibuprofen,
subset=SubRegion=="D" )
> Flux.lmevar.IBU.P<-lme(Flux ~ Solvent_AEP, random= ~1|AnimalID,
+                        weights=varIdent(form = ~1|Solvent_AEP),  data=Ibuprofen,
subset=SubRegion=="P" )
> Flux.lmevar.IBU.T<-lme(Flux ~ Solvent_AEP, random= ~1|AnimalID,
+                        weights=varIdent(form = ~1|Solvent_AEP),  data=Ibuprofen,
subset=SubRegion=="T" )
> summary(Flux.lmevar.IBU.D)
Linear mixed-effects model fit by REML
 Data: Ibuprofen
  Subset: SubRegion == "D"
       AIC      BIC    logLik
  62.73729 73.12612 -20.36865

Random effects:
 Formula: ~1 | AnimalID
        (Intercept)  Residual
StdDev:     0.11435 0.8743373

Variance function:
 Structure: Different standard deviations per stratum
 Formula: ~1 | Solvent_AEP
 Parameter estimates:
       ARS      20%PG     1%EtOH    10%EtOH    30%EtOH
1.00000000 0.07509324 0.09509059 1.73217371 1.20761201
Fixed effects: Flux ~ Solvent_AEP
                                Value Std.Error DF   t-value p-value
(Intercept)                     1.617669 0.2961124 10  5.463024  0.0003
Solvent_AEP1%EtOH        -0.211644 0.3097558 10 -0.683261  0.5100
Solvent_AEP10%EtOH       6.727623 0.8160956 10  8.243670  0.0000
Solvent_AEP30%EtOH       8.269656 0.6106805 10 13.541705  0.0000
Solvent_AEP20%PG         -0.060436 0.3057419 10 -0.197669  0.8473
 Correlation:
                  (Intr) S_AEP1% S_AEP10 S_AEP3
Solvent_AEP1%EtOH  -0.956
Solvent_AEP10%EtOH -0.363  0.347
Solvent_AEP30%EtOH -0.485  0.464   0.176
Solvent_AEP20%PG   -0.969  0.926   0.351   0.470

Standardized Within-Group Residuals:
        Min          Q1         Med          Q3         Max
-1.39967087 -0.74443024 -0.02331409  0.54971140  1.53934832

Number of Observations: 24                        Number of Groups: 15
> summary(Flux.lmevar.IBU.P)
Linear mixed-effects model fit by REML
 Data: Ibuprofen
  Subset: SubRegion == "P"
```

```
       AIC      BIC    logLik
  51.49586 61.88469 -14.74793

Random effects:
 Formula: ~1 | AnimalID
        (Intercept)  Residual
StdDev:   0.3221138 0.2160701

Variance function:
 Structure: Different standard deviations per stratum
 Formula: ~1 | Solvent_AEP
 Parameter estimates:
      ARS     20%PG    1%EtOH   10%EtOH   30%EtOH
1.0000000 0.9092215 0.8416991 6.9672101 2.0966330
Fixed effects: Flux ~ Solvent_AEP
                       Value Std.Error DF   t-value p-value
(Intercept)         1.524111 0.1646274 10  9.257942  0.0000
Solvent_AEP1%EtOH  -0.035828 0.2659220  9 -0.134733  0.8958
Solvent_AEP10%EtOH  6.790089 0.8034566  9  8.451096  0.0000
Solvent_AEP30%EtOH  5.048964 0.3609537  9 13.987845  0.0000
Solvent_AEP20%PG    0.359064 0.2977071  9  1.206098  0.2585
 Correlation:
                   (Intr) S_AEP1% S_AEP10 S_AEP3
Solvent_AEP1%EtOH  -0.619
Solvent_AEP10%EtOH -0.205  0.127
Solvent_AEP30%EtOH -0.456  0.282   0.093
Solvent_AEP20%PG   -0.553  0.342   0.113   0.252

Standardized Within-Group Residuals:
        Min          Q1         Med          Q3         Max
-1.44599520 -0.58533008  0.06110081  0.51679879  1.53193773

Number of Observations: 24                         Number of Groups: 14
> summary(Flux.lmevar.IBU.T)
Linear mixed-effects model fit by REML
 Data: Ibuprofen
  Subset: SubRegion == "T"
       AIC      BIC    logLik
  63.86729 73.66138 -20.93365

Random effects:
 Formula: ~1 | AnimalID
        (Intercept)  Residual
StdDev:   0.2187443 0.3636876

Variance function:
 Structure: Different standard deviations per stratum
 Formula: ~1 | Solvent_AEP
 Parameter estimates:
       ARS      20%PG     1%EtOH    30%EtOH    10%EtOH
 1.0000000  0.2060039  0.5261867  8.3941580 10.0777959
Fixed effects: Flux ~ Solvent_AEP
```

```
                      Value Std.Error DF   t-value p-value
(Intercept)         1.267943 0.1709909 11  7.415263  0.0000
Solvent_AEP1%EtOH  -0.017556 0.2345075  7 -0.074863  0.9424
Solvent_AEP10%EtOH  9.573307 1.8470325 11  5.183075  0.0003
Solvent_AEP30%EtOH  8.492711 1.5394331  7  5.516778  0.0009
Solvent_AEP20%PG    0.518957 0.2335931 11  2.221629  0.0482
 Correlation:
                   (Intr) S_AEP1% S_AEP10 S_AEP3
Solvent_AEP1%EtOH  -0.729
Solvent_AEP10%EtOH -0.093  0.068
Solvent_AEP30%EtOH -0.111  0.101   0.010
Solvent_AEP20%PG   -0.732  0.534   0.068   0.081

Standardized Within-Group Residuals:
       Min         Q1        Med         Q3        Max
-1.3511102 -0.6075111 -0.1884745  0.6733754  1.4408225

Number of Observations: 23                        Number of Groups: 14
```

Appendix 10

This administrative form has been removed

Appendix 11

The full dataset for the following output is available online:

Llewelyn, V. In vivo percutaneous absorption data for model chemicals in Rhinella marina: chemicals formulated in Amphibian Ringer's Solution [Internet]. James Cook University; 2019. Available from: http://dx.doi.org/10.25903/5d4d00bb0d310

Outputs for final models presented in Chapter 6

F.logP-4

```
> library(nlme)
> #output from model F.logP-4 (aka: FINAL.logFlux.logP.toads.REML)
> FINAL.logFlux.logP.toads.REML<- lme(log_Flux ~ LogP+SubRegion, random= ~1|AnimalI
D,
+                                     weights=(varComb(varIdent(form=~1|LogP), varI
dent(form=~1|SubRegion))),data = Toads2)
> anova(FINAL.logFlux.logP.toads.REML)
            numDF denDF   F-value p-value
(Intercept)     1    51 1884.3548  <.0001
LogP            1    15  854.9776  <.0001
SubRegion       2    51    7.0879  0.0019
> summary(FINAL.logFlux.logP.toads.REML)
Linear mixed-effects model fit by REML
 Data: Toads2
       AIC       BIC   logLik
  -63.74114 -41.84459 41.87057

Random effects:
 Formula: ~1 | AnimalID
        (Intercept)  Residual
StdDev:  0.08936226 0.0591831

Combination of variance functions:
 Structure: Different standard deviations per stratum
 Formula: ~1 | LogP
 Parameter estimates:
   -0.07     3.97     1.87
1.000000 1.796639 2.715468
 Structure: Different standard deviations per stratum
 Formula: ~1 | SubRegion
 Parameter estimates:
        D         T         P
1.0000000 1.1532757 0.6257147
Fixed effects: log_Flux ~ LogP + SubRegion
                 Value  Std.Error DF   t-value p-value
(Intercept)  1.8694438 0.03905495 51  47.86702  0.0000
LogP        -0.4387055 0.01498165 15 -29.28286  0.0000
SubRegionP   0.0457535 0.02039950 51   2.24287  0.0293
```

```
SubRegionT  -0.0520023 0.02886960 51  -1.80128  0.0776
 Correlation:
           (Intr) LogP   SbRgnP
LogP       -0.698
SubRegionP -0.295 -0.035
SubRegionT -0.206 -0.020  0.420

Standardized Within-Group Residuals:
        Min          Q1         Med          Q3         Max
-2.18301709 -0.63963516 -0.02403287  0.48222467  2.40459557

Number of Observations: 70
Number of Groups: 17
```

K.logP-28

```
> #output from model K.logP-28 (aka: FINAL.Kp.logP.toads.REML)
> FINAL.Kp.logP.toads.REML<- lme(Kp ~ LogP+SubRegion*LogP, random= ~1|AnimalID,
+                                weights=varIdent(form = ~1|LogP), data=Toads2)
> anova(FINAL.Kp.logP.toads.REML)
               numDF denDF  F-value p-value
(Intercept)        1    49 320.7262  <.0001
LogP               1    15   4.5402  0.0501
SubRegion          2    49   3.9739  0.0252
LogP:SubRegion     2    49   2.4331  0.0983
> summary(FINAL.Kp.logP.toads.REML)
Linear mixed-effects model fit by REML
 Data: Toads2
        AIC       BIC   logLik
  -669.7746 -648.1857 344.8873

Random effects:
 Formula: ~1 | AnimalID
         (Intercept)     Residual
StdDev: 0.0006787011 0.0005524073

Variance function:
 Structure: Different standard deviations per stratum
 Formula: ~1 | LogP
 Parameter estimates:
   -0.07     3.97     1.87
1.000000 1.356728 1.947443
Fixed effects: Kp ~ LogP + SubRegion * LogP
                       Value    Std.Error DF   t-value p-value
(Intercept)      0.003817961 0.0003151274 49 12.115611  0.0000
LogP            -0.000125426 0.0001302955 15 -0.962631  0.3510
SubRegionP       0.000563473 0.0002851678 49  1.975936  0.0538
SubRegionT      -0.000219394 0.0002860581 49 -0.766957  0.4468
LogP:SubRegionP -0.000247375 0.0001178327 49 -2.099376  0.0410
LogP:SubRegionT -0.000176897 0.0001206114 49 -1.466668  0.1489
 Correlation:
               (Intr) LogP   SbRgnP SbRgnT LP:SRP
```

```
LogP            -0.722
SubRegionP      -0.313  0.206
SubRegionT      -0.303  0.205  0.335
LogP:SubRegionP  0.213 -0.372 -0.664 -0.227
LogP:SubRegionT  0.207 -0.364 -0.223 -0.650  0.403

Standardized Within-Group Residuals:
        Min          Q1         Med          Q3         Max
-1.63992904 -0.70704994 -0.06134259  0.42101135  2.55551508

Number of Observations: 70
Number of Groups: 17
```

Appendix 12

The full dataset for the following output is available online:

Llewelyn, V. In vivo percutaneous absorption data for model chemicals in Rhinella marina: chemicals formulated in Amphibian Ringer's Solution [Internet]. James Cook University; 2019. Available from: http://dx.doi.org/10.25903/5d4d00bb0d310

Statistical output from R

```
> library(nlme)
> #create df for in vitro predictions
> INVITRO_chloramphenicol_predict<-predict_chloramphenicol
>
> #predict logflux from FINAL.logFlux.logP.toads.REML
> FINAL.logFlux.logP.toads.REML<- lme(log_Flux ~ LogP+SubRegion, random= ~1|AnimalI
D,
+                                     weights=(varComb(varIdent(form=~1|LogP), varI
dent(form=~1|SubRegion))),data = Toads2)
>
> InvitroModel.logflux<-FINAL.logFlux.logP.toads.REML
>
> INVITRO_chloramphenicol_predict$logflux<-predict(InvitroModel.logflux, predict_ch
loramphenicol,level=0)
>
> #convert logflux to flux
> INVITRO_chloramphenicol_predict$flux<-10^(INVITRO_chloramphenicol_predict$logflux
)
>
> INVITRO_chloramphenicol_predict
# A tibble: 12 x 6
    LogP    MW SubRegion Weight logflux  flux
   <dbl> <dbl> <chr>      <dbl>   <dbl> <dbl>
 1  1.14  323. D            100  1.37   23.4
 2  1.14  323. T            100  1.32   20.8
 3  1.14  323. P            100  1.42   26.0
 4 -0.07  194. P            100  1.95   88.3
 5 -0.07  194. T            100  1.85   70.5
 6 -0.07  194. D            100  1.90   79.5
 7  1.87  122. P            100  1.09   12.4
 8  1.87  122. T            100  0.997   9.93
 9  1.87  122. D            100  1.05   11.2
10  3.97  206. P            100  0.174   1.49
11  3.97  206. T            100  0.0758  1.19
12  3.97  206. D            100  0.128   1.34
>
> #predict Kp from FINAL.Kp.logP.toads.REML
> FINAL.Kp.logP.toads.REML<- lme(Kp ~ LogP+SubRegion*LogP, random= ~1|AnimalID,
+                                weights=varIdent(form = ~1|LogP), data=Toads2)
```

```
>
> InvitroModel.Kp.logP<-FINAL.Kp.logP.toads.REML
>
> INVITRO_chloramphenicol_predict$Kp.logP<-predict(InvitroModel.Kp.logP, predict_ch
loramphenicol,level=0)
>
> #add columns for Kp x 10^-3
> INVITRO_chloramphenicol_predict$Kp.logPx1000<-1000*(INVITRO_chloramphenicol_predi
ct$Kp.logP)
>
> INVITRO_chloramphenicol_predict
# A tibble: 12 x 8
    LogP    MW SubRegion Weight logflux  flux Kp.logP Kp.logPx1000
   <dbl> <dbl> <chr>      <dbl>   <dbl> <dbl>   <dbl>        <dbl>
 1  1.14  323. D            100  1.37   23.4  0.00367         3.67
 2  1.14  323. T            100  1.32   20.8  0.00325         3.25
 3  1.14  323. P            100  1.42   26.0  0.00396         3.96
 4 -0.07  194. P            100  1.95   88.3  0.00441         4.41
 5 -0.07  194. T            100  1.85   70.5  0.00362         3.62
 6 -0.07  194. D            100  1.90   79.5  0.00383         3.83
 7  1.87  122. P            100  1.09   12.4  0.00368         3.68
 8  1.87  122. T            100  0.997   9.93 0.00303         3.03
 9  1.87  122. D            100  1.05   11.2  0.00358         3.58
10  3.97  206. P            100  0.174   1.49 0.00290         2.90
11  3.97  206. T            100  0.0758  1.19 0.00240         2.40
12  3.97  206. D            100  0.128   1.34 0.00332         3.32
```

Appendix 13

The full dataset for the following output is available online:

Llewelyn, V. In vivo percutaneous absorption data for chloramphenicol, formulated in 20% propylene glycol, in Rhinella marina [Internet]. James Cook University; 2019. Available from:

http://dx.doi.org/10.25903/5d4a733601e97

Statistical output from R

```
> library(PKNCA)
> #import Chloramphenicol_PKNCA
> my.conc<-PKNCAconc(Chloramphenicol_PKNCA,Conc~Time|Subject)
> d.dose<-subset(Chloramphenicol_PKNCA,Chloramphenicol_PKNCA$Time==0,
+                c("Dose","Time","Subject"))
> my.dose<-PKNCAdose(d.dose,Dose~Time|Subject)
> my.data.automatic<-PKNCAdata(my.conc,my.dose)
> my.results.automatic<-pk.nca(my.data.automatic)
> my.results.automatic
$result
   start end Subject            PPTESTCD      PPORRES exclude
1      0  24    Real             auclast 306.01912190    <NA>
2      0 Inf    Real                cmax  17.09350218    <NA>
3      0 Inf    Real                tmax   2.00000000    <NA>
4      0 Inf    Real               tlast  24.00000000    <NA>
5      0 Inf    Real           clast.obs  10.48256727    <NA>
6      0 Inf    Real            lambda.z   0.03711407    <NA>
7      0 Inf    Real           r.squared   0.95047093    <NA>
8      0 Inf    Real       adj.r.squared   0.90094186    <NA>
9      0 Inf    Real lambda.z.time.first  12.00000000    <NA>
10     0 Inf    Real   lambda.z.n.points   3.00000000    <NA>
11     0 Inf    Real          clast.pred  10.17938758    <NA>
12     0 Inf    Real           half.life  18.67613014    <NA>
13     0 Inf    Real          span.ratio   0.64253140    <NA>
14     0 Inf    Real          aucinf.obs 588.46099865    <NA>

$data
Formula for concentration:
 Conc ~ Time | Subject
With 2 subjects defined in the 'Subject' column.
Nominal time column is not specified.

First 6 rows of concentration data:
 Subject   Weight     Dose Time      Conc exclude volume duration
    Real 104.0585 62.75117 0.00  0.000000    <NA>     NA        0
    Real 104.0585 62.75117 0.25  4.398044    <NA>     NA        0
    Real 104.0585 62.75117 0.50  6.839657    <NA>     NA        0
    Real 104.0585 62.75117 1.00  8.009947    <NA>     NA        0
    Real 104.0585 62.75117 1.50 11.261014    <NA>     NA        0
```

```
    Real 104.0585 62.75117 2.00 17.093502    <NA>     NA        0
Formula for dosing:
 Dose ~ Time | Subject
Nominal time column is not specified.

Data for dosing:
     Dose Time Subject exclude         route duration
 62.75117    0    Real    <NA> extravascular        0

With 4 rows of AUC specifications.
Options changed from default are:
$adj.r.squared.factor
[1] 1e-04
$max.missing
[1] 0.5
$auc.method
[1] "lin up/log down"
$conc.na
[1] "drop"
$conc.blq
$conc.blq$first
[1] "keep"
$conc.blq$middle
[1] "drop"
$conc.blq$last
[1] "keep"
$first.tmax
[1] TRUE
$allow.tmax.in.half.life
[1] FALSE
$min.hl.points
[1] 3
$min.span.ratio
[1] 2
$max.aucinf.pext
[1] 20
$min.hl.r.squared
[1] 0.9
$tau.choices
[1] NA
$single.dose.aucs
  start end auclast aucall aumclast aumcall aucint.last aucint.last.dose aucint.all
aucint.all.dose auclast.dn aucall.dn
1     0  24    TRUE  FALSE    FALSE   FALSE       FALSE            FALSE      FALSE
FALSE      FALSE     FALSE
2     0 Inf   FALSE  FALSE    FALSE   FALSE       FALSE            FALSE      FALSE
FALSE      FALSE     FALSE
  aumclast.dn aumcall.dn  cmax  cmin  tmax tlast tfirst clast.obs cl.last cl.all
f mrt.last mrt.iv.last vss.last vss.iv.last
1       FALSE      FALSE FALSE FALSE FALSE FALSE  FALSE     FALSE   FALSE  FALSE FA
LSE    FALSE       FALSE    FALSE       FALSE
```

```
2       FALSE      FALSE  TRUE FALSE  TRUE FALSE  FALSE     FALSE   FALSE  FALSE FA
LSE    FALSE       FALSE    FALSE       FALSE
    cav ctrough   ptr  tlag deg.fluc swing  ceoi    ae clr.last clr.obs clr.pred
fe half.life r.squared adj.r.squared
1 FALSE   FALSE FALSE FALSE    FALSE FALSE FALSE FALSE    FALSE   FALSE    FALSE FA
LSE     FALSE     FALSE         FALSE
2 FALSE   FALSE FALSE FALSE    FALSE FALSE FALSE FALSE    FALSE   FALSE    FALSE FA
LSE      TRUE     FALSE         FALSE
  lambda.z lambda.z.time.first lambda.z.n.points clast.pred span.ratio cmax.dn cmin
.dn clast.obs.dn clast.pred.dn cav.dn
1    FALSE               FALSE             FALSE      FALSE      FALSE   FALSE   FA
LSE        FALSE         FALSE  FALSE
2    FALSE               FALSE             FALSE      FALSE      FALSE   FALSE   FA
LSE        FALSE         FALSE  FALSE
  ctrough.dn thalf.eff.last thalf.eff.iv.last kel.last kel.iv.last aucinf.obs aucin
f.pred aumcinf.obs aumcinf.pred
1      FALSE          FALSE             FALSE    FALSE       FALSE      FALSE
FALSE       FALSE        FALSE
2      FALSE          FALSE             FALSE    FALSE       FALSE       TRUE
FALSE       FALSE        FALSE
  aucint.inf.obs aucint.inf.obs.dose aucint.inf.pred aucint.inf.pred.dose aucinf.ob
s.dn aucinf.pred.dn aumcinf.obs.dn
1          FALSE               FALSE           FALSE                FALSE         F
ALSE          FALSE          FALSE
2          FALSE               FALSE           FALSE                FALSE         F
ALSE          FALSE          FALSE
  aumcinf.pred.dn aucpext.obs aucpext.pred cl.obs cl.pred mrt.obs mrt.pred mrt.iv.o
bs mrt.iv.pred mrt.md.obs mrt.md.pred vz.obs
1           FALSE       FALSE        FALSE  FALSE   FALSE   FALSE    FALSE      FAL
SE       FALSE      FALSE       FALSE  FALSE
2           FALSE       FALSE        FALSE  FALSE   FALSE   FALSE    FALSE      FAL
SE       FALSE      FALSE       FALSE  FALSE
  vz.pred vss.obs vss.pred vss.iv.obs vss.iv.pred vss.md.obs vss.md.pred vd.obs vd.
pred thalf.eff.obs thalf.eff.pred
1   FALSE   FALSE    FALSE      FALSE       FALSE      FALSE       FALSE  FALSE   F
ALSE         FALSE          FALSE
2   FALSE   FALSE    FALSE      FALSE       FALSE      FALSE       FALSE  FALSE   F
ALSE         FALSE          FALSE
  thalf.eff.iv.obs thalf.eff.iv.pred kel.obs kel.pred kel.iv.obs kel.iv.pred
1            FALSE             FALSE   FALSE    FALSE      FALSE       FALSE
2            FALSE             FALSE   FALSE    FALSE      FALSE       FALSE

$exclude
[1] "exclude"
attr(,"class")
[1] "PKNCAresults" "list"
attr(,"provenance")
Provenance hash eb7c97c6f6f4d33606144212ff706a04 generated on 2019-06-26 11:51:29 w
ith R version 3.5.2 (2018-12-20).
```